FINAL DESIGN REPORT

BRAYTON HEAT EXCHANGER UNIT DEVELOPMENT PROGRAM (ALTERNATE DESIGN)

by

J. D. Duncan, J. C. Gibson, R. F. Graves, C. J. Morse, and C. E. Richard

AIRESEARCH MANUFACTURING COMPANY
Los Angeles, California

prepared for

NATIONAL AERONAUTICS AND SPACE ADMINISTRATION

August 2, 1973

CONTRACT NAS 3-13454

NASA Lewis Research Center
Cleveland, Ohio
P. T. Kerwin, Project Manager

NASA CR-121269
AiResearch 73-9461

FINAL DESIGN REPORT

BRAYTON HEAT EXCHANGER UNIT DEVELOPMENT PROGRAM (ALTERNATE DESIGN)

by

J. D. Duncan, J. C. Gibson, R. F. Graves, C. J. Morse, and C. E. Richard

AIRESEARCH MANUFACTURING COMPANY
Los Angeles, California

prepared for

NATIONAL AERONAUTICS AND SPACE ADMINISTRATION

August 2, 1973

CONTRACT NAS 3-13454

NASA Lewis Research Center
Cleveland, Ohio
P. T. Kerwin, Project Manager

FOREWORD

The program described in this report was conducted by AiResearch Manufacturing Company, a division of The Garrett Corporation, under NASA contract NAS3-13454. This program was performed under the management of P. T. Kerwin, Project Manager, Power Systems Division, NASA-Lewis Research Center.

CONTENTS

ILLUSTRATIONS

ILLUSTRATIONS (Continued)

ILLUSTRATIONS (Continued)

TABLES

ABSTRACT

A Brayton Heat Exchanger Unit Alternate Design (BHXU-Alternate) consisting of a recuperator, a heat sink heat exchanger, and a gas ducting system, was designed and fabricated. The design was formulated to provide a high performance unit suitable for use in a long-life Brayton-cycle powerplant. Emphasis was on double containment against external leakage and leakage of the organic coolant into the gas stream.

A parametric analysis and design study was performed to establish the optimum component configurations to achieve low weight and size and high reliability, while meeting the requirements of high effectiveness and low pressure drop. Layout studies and detailed mechanical and structural design were performed to obtain a flight-type packaging arrangement, including the close-coupled integration of the BHXU-Alternate with the Brayton Rotating Unit (BRU).

Fabrication development was undertaken and units were manufactured with satisfactory structural integrity and leaktight containment. Evaluation testing was not conducted on the BHXU-Alternate heat exchanger system.

SECTION 1

SUMMARY

AiResearch has designed a Brayton Heat Exchanger Unit Alternate Design (BHXU-Alternate) consisting of a gas-to-gas recuperator, a gas-to-liquid heat sink heat exchanger, and a gas ducting system that interconnects with other Brayton components to form the Brayton power conversion loop.

This BHXU-Alternate is selected to operate in a power system with a rated output of 10 kw_e. The design objective for the BHXU-Alternate is an effectiveness of 0.95 for both the recuperator and heat sink exchanger, a total gas fractional pressure drop through the unit of 0.045, and an operating lifetime capability of 5 years in a space environment. The unit is designed to employ a gaseous helium-xenon mixture with a molecular weight of 83.8 as the primary working fluid. The liquid coolant in the heat sink exchanger is Dow Corning 200 fluid with a viscosity grade of 2.0 centistokes at 25°C.

A parametric analysis and design study was conducted to establish the most favorable heat exchanger configurations with respect to weight, size, and reliability. Layout studies were performed involving component matching and design tradeoffs to obtain an optimum integral unit. Utilizing these studies in combination with detailed mechanical and structural analyses, a compact, flight-type arrangement was evolved for integration with the Brayton Rotating Unit, the gas management system, and the Brayton heat source.

Fabrication development was undertaken with emphasis on leaktight containment. One unit was manufactured and it demonstrated satisfactory structural integrity and containment.

The BHXU-Alternate is illustrated in Figure 1-1. In Figure 1-1(a), the system recuperator is shown after final assembly. The finned tube waste heat exchanger is shown in Figure 1-1(b) just prior to its braze operation. In Figure 1-1(c) the completed BHXU-Alternate assembly is shown with its interconnecting ducting and bellows. The unit as shown in Figure 1-1(c) was delivered to NASA Lewis in July of 1973.

The heat exchanger and system weights and overall dimensions are summarized below.

Item	Weight, lb (kg)	Dimension, in. (cm)
Recuperator	348 (157.9)	322 x 27.0 x 20.8 (81.8 x 68.6 x 52.8)
Heat sink heat exchanger	147 (66.7)	31.9 x 12.6 x 8.0 (81.0 x 320.0 x 20.3)
Ducting, transition sections, and manifolds	98 (44.5)	--
Heat exchanger and duct assembly	593 (269.1)	61.6 x 60.3 x 22.3 (156.5 x 153.0 x 56.6)

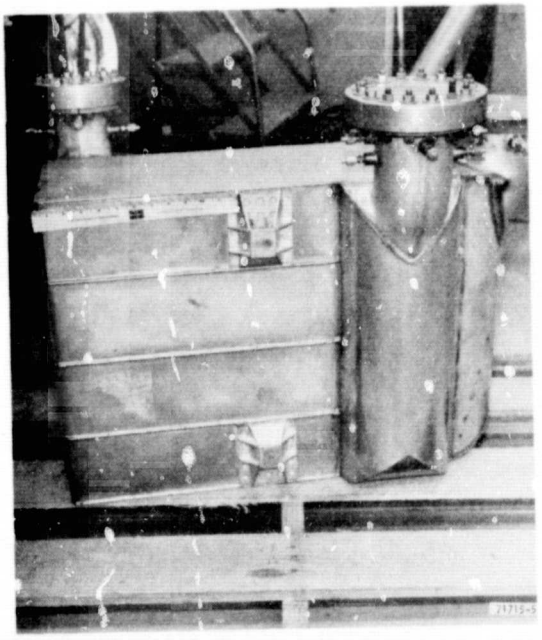

a. RECUPERATOR

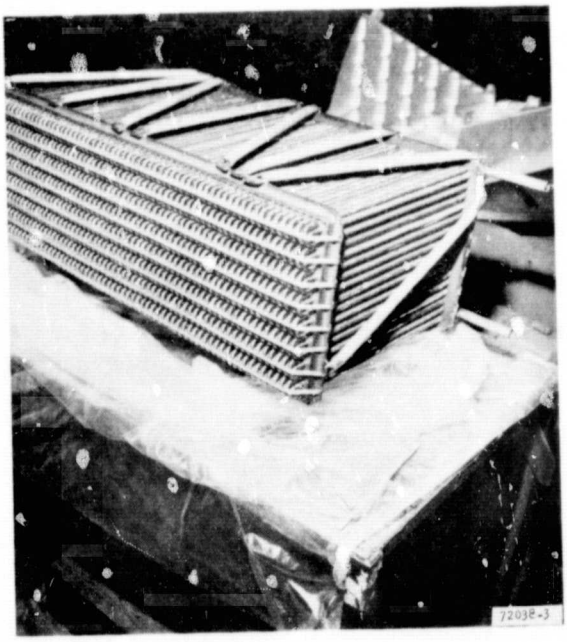

b. HEAT SINK HEAT EXCHANGER

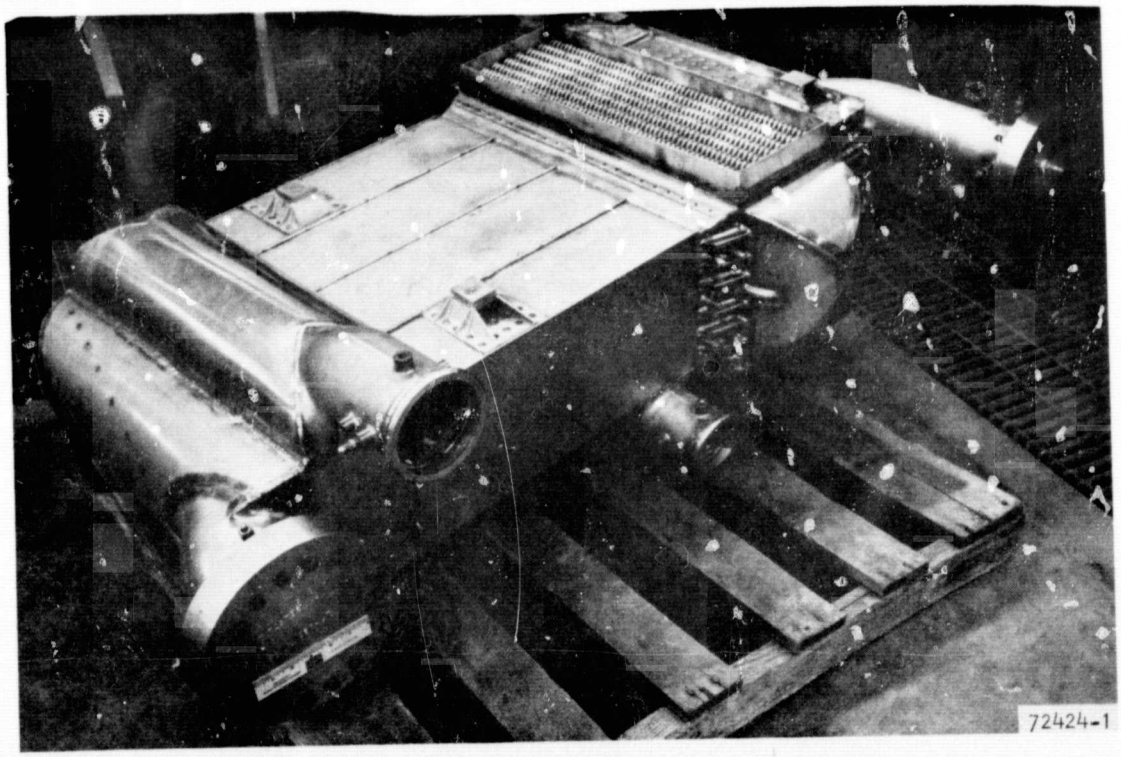

c. COMPLETED ASSEMBLY

F-18318

Figure 1-1. BHXU-Alternate

SECTION 2

INTRODUCTION

NASA is currently engaged in the development of closed Brayton cycle system technology for generation of electric power in space. The system presently under consideration was chosen to investigate the means of producing power in the range of 2 to 10 kw_e for long durations of time. Such a system is potentially applicable to supplying the power for a manned orbiting space station or base. For extended missions, radioisotope energy sources have been considered and were found to be suitable candidates to deliver the required thermal powers.*

The concept selected for the Brayton power conversion equipment incorporates a single-shaft Brayton Rotating Unit (BRU), consisting of a turbine, a compressor, and an alternator, coupled to a Brayton Heat Exchanger Unit-Alternate design (BHXU-Alternate). The BHXU-Alternate consists of a gas-to-gas recuperator, a gas-to-liquid heat sink exchanger and the ducting that connects the heat exchangers with the BRU. The recuperator transfers heat from the low-pressure turbine exhaust gas to the high-pressure gas leaving the compressor. The heat sink heat exchanger transfers heat from the low-pressure gas leaving the recuperator to the liquid coolant in the radiator loop for ultimate rejection as waste heat from the cycle.

The program described here includes the design and fabrication of the BHXU-Alternate prior to delivery of the unit to NASA for system integration and testing. Cycle conditions on which the design of the BHXU-Alternate is based are summarized in Table 2-1. These design goals were established by NASA in conjunction with a systems analysis performed to identify operating conditions that result in high overall conversion efficiency.

The preliminary thermal and structural designs were performed under NASA Contract NAS3-10607 and are reported in Topical Report, "Design Study, Alternate Brayton Heat Exchanger Unit Brayton Cycle System," AiResearch Report 69-5194.

The BHXU-Alternate system is the second-generation hardware system to the BHXU-Engine B system. The final design report of the Engine B system is presented in NASA CR-120816. The improved features of the BHXU-Alternate system with respect to the BHXU-Engine B system are summarized on the next page.

*McKhann, G.G., "Preliminary Design of a Pu-238 Isotope Brayton Cycle Power System for MORL," Vol I - Technical Summary, Report No. SM-48832 (NASA CR-68809), Douglas Aircraft Co., Inc., September 1965.

Item	BHXU-A	BHXU-Engine B
Recuperator size	Increased over Engine B to obtain heat transfer performance (test data of Engine B)	--
Brazing alloy	Gold alloy (AMS 4784)	Nickel base alloy (AMS 4778)
Modularized	Yes	No
Seal plates (double containment)	Yes	No
Material	Hastelloy X	347 stainless steel
End configuration	Rectangular	Triangular
Heat sink heat exchanger	Finned-tube	Plate-fin

The size of the BHXU-Alternate recuperator was increased by 16 percent based on the results of the performance test of the BHXU-Engine B heat exchanger system. The end configuration of the recuperator was changed from triangular to rectangular for system packaging and fabrication purposes. The BHXU-Alternate recuperator was fabricated from Hastelloy X material and brazed with gold based brazing alloys (Palniro series) instead of 347 stainless steel and AMS 4778 brazing alloy. These changes were required because of a higher pressure requirement and also to obtain an assembly with higher as-brazed ductility than the 347 stainless steel and AMS 4778 brazing alloy combination. The BHXU-Alternate recuperator was modularized with each module evaluated prior to assembling the modules into the full-size recuperator configuration. The recuperator was designed to provide double containment on all brazed joints to prevent external gas leakage.

The heat sink heat exchanger was designed as a helical-wound finned-tube core with U-tubes connecting the tubes into a continuous liquid flow path. This design was selected over the plate-fin design of the Engine B system to eliminate liquid-to-gas leak paths.

The final thermal and structural design of the BHXU-Alternate is described in Section 3. Also included in Section 3 is a summary of the design and off-design performance of the unit under conditions specified by NASA. Fabrication is discussed in Section 4. Detailed technical discussions of several aspects of the design are included as appendixes.

TABLE 2-1

BHXU-ALTERNATE DESIGN CONDITIONS

Working fluid (gas)	Xe-He mixture Molecular weight 83.8
Liquid coolant	Dow Corning 200 fluid (2 centistokes at 25°C)
Recuperator hot side	
Gas flow rate, lb/sec	1.28
Inlet temperature, °R	1701
Inlet pressure, psia	24.1*
Recuperator cold side	
Gas flow rate, lb/sec	1.267
Inlet temperature, °R	738
Inlet pressure, psia	43.1*
Recuperator effectiveness	0.95
Heat sink heat exchanger	
Gas exit temperature, °R	540
Effectiveness	0.95
Capacity-rate ratio $\left(\frac{\text{hot side}}{\text{cold side}}\right)$	0.87
Maximum liquid pressure drop, psi	25
Overall BHXU-Alternate gas pressure drop, percent	4.5

*Structurally, the recuperator hot side is designed to withstand 30.5 psia and the cold side 56.0 psia.

SECTION 3

DESIGN STUDY

THERMAL ANALYSIS

Heat Exchanger Core Designs

Because of the high pressures, the recuperator material was changed from stainless to Hastelloy X. At the same time the number of low-pressure side passages was increased from 70 to 71. The net effect of these two changes on recuperator thermal performance was calculated and found to be negligible. Predicted effectiveness of the recuperator remains at 0.95.

For structural reasons the heat sink heat exchanger tube outside diameters in the first three and last three tube rows were increased from 0.156 in. (0.397 cm) to 0.18 in. (0.457 cm). The same increase was applied to the three tubes at each end of each remaining tube row; thus 534 out of the 2016 tubes were affected by this change. The effect on thermal performance is twofold: a decrease in heat exchanger UA due to a reduction in total outside heat transfer area, and a tendency toward gas flow maldistribution due to the reduced flow area near the core sides. It was found that the heat transfer area effect yielded 1.5 percent reduction in UA and the maldistribution effect was virtually negligible (less than one percent in equivalent UA). Since these effects are well within the UA margin originally allotted to this unit, the predicted effectiveness of the heat sink heat exchanger remains at 0.95.

Original sizing of the heat sink heat exchanger core was based on heat transfer and friction factor design data for a slanted-flap turbulator inserted in the tubes. Isothermal pressure drop tests were run on a single-flap turbulator, a double-flap turbulator (constructed by placing two single-flap turbulators back-to-back within the tubes), and a slanted-flap turbulator. These tests showed that the single-flap turbulator had a lower friction factor than either the double-flap or slanted-flap turbulator and therefore (by inference) would yield poorer heat transfer conductance than either of these other two designs. The double-flap and slanted-flap turbulators had approximately equal friction factors at the heat exchanger design Reynolds number, but these friction factors were substantially below the design curve.

Heat transfer tests were run on the double-flap and slanted-flap turbulators. These tests showed quite similar heat transfer performance (similar j curves) for the two designs, with the back-to-back j-curve higher by about ten percent. Furthermore, the j-factor for the back-to-back configuration was approximately equal to that obtained from the original slanted-flap design curve. On this basis, either the slanted-flap or double-flap turbulator was deemed suitable for the heat sink heat exchanger, with the double-flap configuration slightly preferred. Based on this slight preference from a performance standpoint, as well as easier fabricability, the double-flap configuration was selected.

Manifold Designs

Manifold designs were calculated following the usual sizing procedure to obtain uniform core flow distribution. The recuperator high-pressure manifolds are arranged in a U-flow configuration (the gas enters and exits from the same sides of the heat exchanger) and therefore are designed for constant area in the flow direction. The calculated manifold flow area ratio yielding uniform flow is 2.37 (outlet manifold area to inlet manifold area). The areas used are those of the BHXU manifolds, i.e., 8.9 sq in. (57.4 sq cm) for the high-pressure inlet manifold and 21.1 sq in. (136 sq cm) for the high-pressure outlet manifold. On the low-pressure side, uniform static pressure is required at the recuperator low-pressure inlet face to match the uniform pressure of the outlet plenum. This can be obtained with a linear manifold flow area taper from full radius area at the inlet to ten percent of full radius area at the end of the manifold. Due to structural requirements of the manifold, a liner is used inside a full radius manifold to provide approximately the required taper. The heat source heat exchanger low-pressure gas outlet manifold is a full radius manifold to minimize the stresses imposed on the heat exchanger by the manifold.

Thermal Performance

The performance of the BHXU-Alternate was calculated for the off-design conditions listed in Table 3-1. Design and off-design performance are summarized in Table 3-2. A breakdown of the gas system pressure drop at design conditions is given in Table 3-3.

Transient Analyses

1. Tie Rods

An important transient involves the temperature difference between the transition section tie rods and the heat sink exchanger tubes during startup. An excessive temperature difference between these components could cause buckling of the heat exchanger tubes. Temperature calculations were made for two tie rod diameters, 0.100 in. and 0.150 in., and two values of the initial radiator temperature, 0° and $-100^{\circ}F$. The following system conditions were assumed:

(a) The system is initially at $0^{\circ}F$.

(b) At startup the low-pressure recuperator inlet temperature steps to $1701^{\circ}R$ and remains constant thereafter.

(c) The heat sink heat exchanger gas outlet temperature is initially equal to the radiator temperature and increases linearly during the transient at a rate of $0.1^{\circ}F/sec$.

(d) The recuperator high-pressure inlet temperature is $200^{\circ}F$ above the heat sink heat exchanger gas outlet temperature.

(e) The upstream heat sink exchanger (i.e., the heat exchanger closer to the transition section) is inactive.

TABLE 3-1

OFF-DESIGN CONDITIONS

	Gas Flow Rate, lb/sec	Hot Side		Cold Side	
		Recuperator Inlet Temperature, ^{o}F	Recuperator Inlet Pressure, psia	Recuperator Inlet Temperature, ^{o}F	Recuperator Inlet Pressure, psia
Case I	0.38	1709	6.86	740	12.8
Case II	0.55	1705	9.95	739	18.5
Case III	0.76	1701	13.9	733	25.6
Case IV	1.0	1701	18.1	738	33.7
Case V	1.5	1701	27.2	738	50.5
Case VI	2.5	1701	45.3	738	84.25
Case VII	2.72	1647	50	740	92
Case VIII	3.8	1400	72	810	125
Case IX	7.23	1220	124	768	222

TABLE 3-2

BHXU-ALTERNATE PERFORMANCE

Condition	Effectiveness		Pressure Drop	
	Recuperator*	HSHX**	Gas, percent	Liquid, psi
Design	0.950	0.950	3.87	8.1
I	0.971	0.979	9.17	1.1
II	0.967	0.972	7.03	2.0
III	0.962	0.965	5.60	3.4
IV	0.956	0.958	4.76	5.4
V	0.944	0.945	3.74	10.6
VI	0.923	0.925	2.92	24.7
VII	0.921	0.922	2.71	28.4
VIII	0.906	0.914	2.27	48.6
IX	0.867	0.869	2.07	148.0

*Based on capacity-rate ratio = 0.99

**Based on capacity-rate ratio = 0.87

TABLE 3-3

BHXU ALTERNATE GAS PRESSURE DROPS

	Pressure Drop, Percent	
Recuperator core		
High pressure side	0.541	
Low pressure side	1.158	1.699
Recuperator end sections		
High pressure inlet	0.216	
High pressure outlet	0.239	
Low pressure inlet	0.094	
Low pressure outlet	0.068	0.617
Heat sink exchanger		0.560
Manifolds		
High pressure inlet	0.096	
High pressure outlet	0.068	
Low pressure inlet	0.199	
Low pressure outlet	0.019	0.382
Ducts		
High pressure inlet	0.164	
High pressure outlet	0.009	
Low pressure inlet	0.278	
Low pressure outlet	0.158	0.610
Total BHXU		3.870

Calculation of the time constants for the tie rods, recuperator, and heat sink heat exchanger (nonactive) tubes yielded the following values: 28 sec and 52 sec respectively for the 0.100-in. and 0.150-in. tie rods, 15 sec for the recuperator, and 4 sec for the heat exchanger tubes. Because of the relatively low value for the tube time constant, the simplifying assumption was made that the tube time constant is zero. The tube temperature therefore is taken to be equal to the gas inlet temperature to the heat sink exchanger throughout the transient.

Figure 3-1 shows the results of a stepwise calculation of system temperatures vs time, based on a tie rod diameter of 0.150-in. and an initial radiator temperature of $0^{\circ}F$. The recuperator low-pressure outlet temperature rises rapidly at first, due to the temperature step at the low pressure inlet. Following this initial rise, it continues to increase slowly due to the gradual increase in compressor outlet temperature. The maximum difference of $177^{\circ}F$ between tube temperature and tie rod temperature occurs during the initial rapid transient, at a time of approximately 27 sec.

Figure 3-2 shows the difference between tube and tie rod temperatures as a function of time for the three cases studied. It can be seen that a reduction in tie rod diameter from 0.150 in. to 0.100 in. causes a reduction in maximum temperature difference from 177° to $144^{\circ}F$. Also, the lower initial radiator temperature of $-100^{\circ}F$ results in a lesser maximum temperature difference between tubes and tie rods, because of the reduced initial compressor outlet temperature for this condition.

2. Brackets

A calculation was made of the maximum temperature differential experienced during startup in the brackets mounted between heat sink heat exchangers. The bracket geometry assumed for this calculation is shown in Figure 3-3. The bracket is in the shape of a rectangular box, 1.5 in. high by 3 in. in the gas flow direction, with a wall thickness of 0.1 in. The bracket baseplate is heated by convection from the gas and by conduction from the heat exchanger header plates and is therefore assumed to have the same temperature as the header plates. The further conservative assumption is made that the header plate film coefficient is equal to the film coefficient of the core matrix.

Shown in Figure 3-4 are the bracket baseplate temperature vs time from startup and the bracket minimum temperature vs time from startup. The minimum temperature occurs at the midpoint of the bracket wall that is parallel to but removed from the gas flow. Also shown in Figure 3-4 is the temperature differential in the bracket, from baseplate to minimum temperature point. It can be seen that a maximum temperature differential of $174^{\circ}F$ is reached at a time of 353 sec after start.

STRUCTURAL DESIGN

This section discusses the various structural aspects related to the detailed design of the BHXU-Alternate. The unit consisted of two separate heat exchangers, a recuperator, and a heat sink heat exchanger, which were rigidly

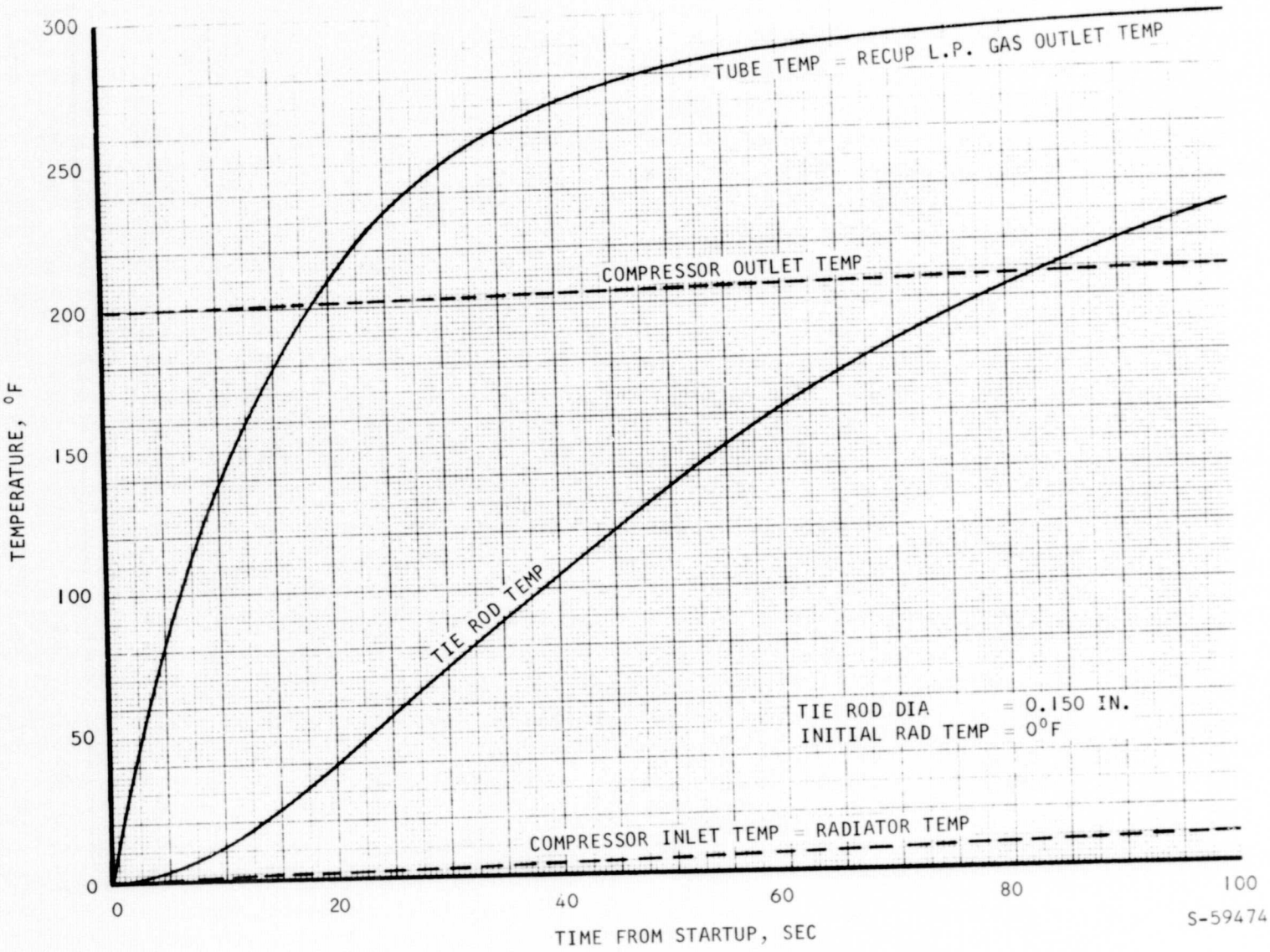

Figure 3-1. Transient Temperatures During Startup

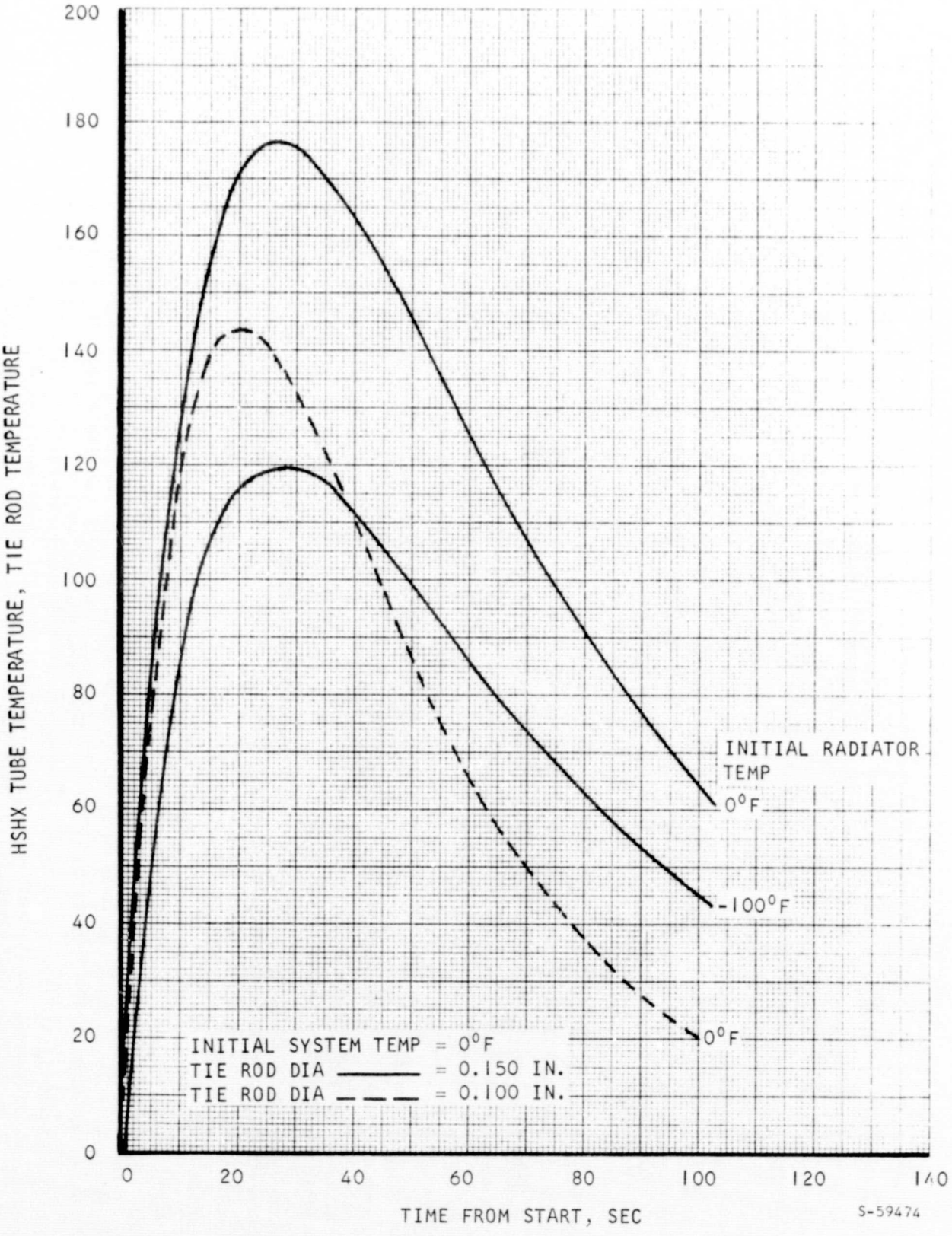

Figure 3-2. BHXU Transients

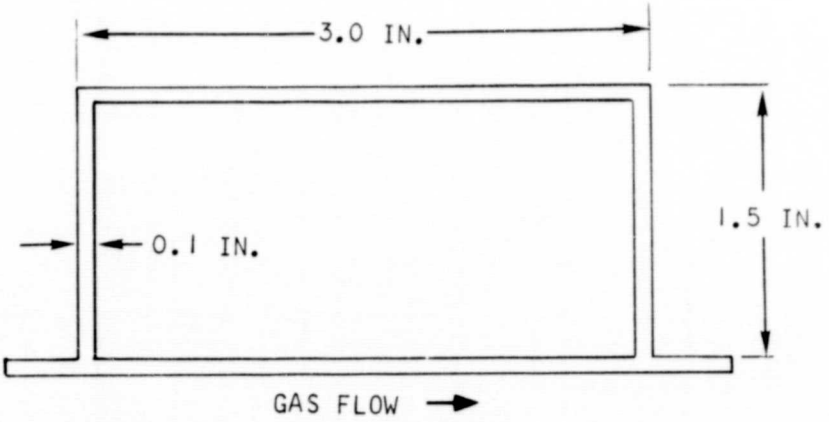

Figure 3-3. Bracket Geometry for Transient Calculations

joined to form an integral structural element with respect to environmental loads, support bracketry, and interconnecting ducts to the BRU and heat source heat exchanger. In addition, the recuperator and heat sink heat exchanger were both designed to provide adequate structural integrity for pressure containment loads and thermal stresses to satisfy the required reliability objectives.

Design Criteria

The operating conditions for the BHXU-Alternate package included a maximum operating temperature of 1701°F (1241°F) in the recuperator for a design life of 5 years (about 44,000 hr). The short-time material properties were used for temperatures below 900°F. For sustained operations at higher temperatures, the one-percent creep and stress properties for 50,000 hr at temperature were used. The design of the heat sink heat exchanger was based on material properties at 440°F (soak conditions).

It was further specified that a 100-cycle life was required for this unit. A typical cycle was defined to be startup of the unit, operation at design temperatures and pressures, and shutdown. This requirement applied primarily to thermal loads due to temperature gradients and differences in the system. Thermal stresses exceeding the material yield strength cannot be completely avoided due to rapid startup conditions.

The basic information for inertial loads was taken from Specification No. P2241-1 dated March 1, 1969; however, the design loads assumed that the BHXU-Alternate would be shock mounted with a 15-Hz isolation system so that resonant amplifications for BHXU-Alternate resonance above 50 Hz would be highly attenuated. The vibratory input at 15 Hz to 0.14 in. double amplitude displacement of critical damping limited the amplification factor of 5.0 at resonance, and this produced 8-g vibratory loading at the mount points. This mounting system also provided shock isolation from the 20-g, half-sine pulse

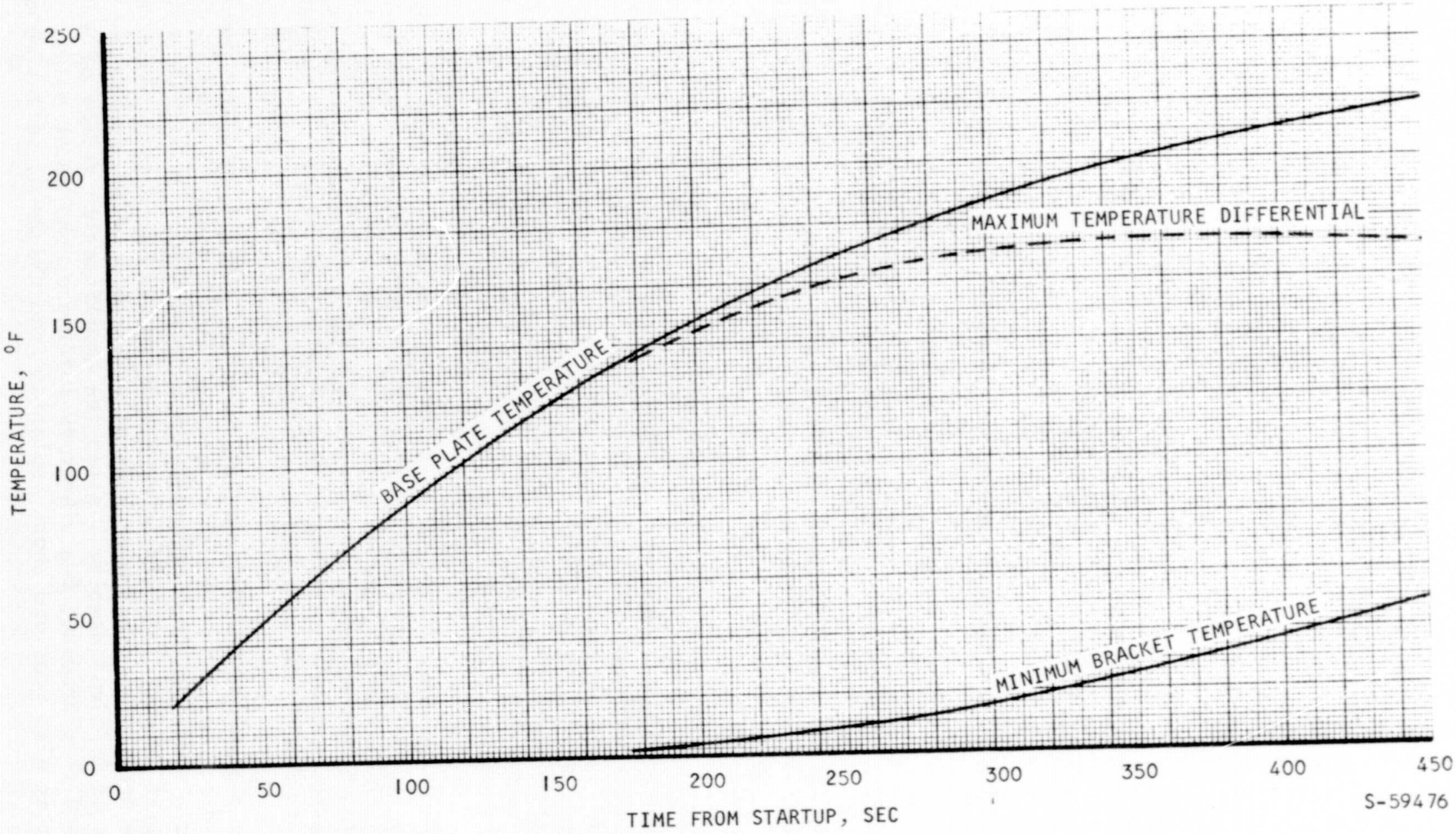

Figure 3-4. Bracket Temperatures During Startup

of 10 msec time duration. The shock isolation factor was 0.5, and the shock factor at the mount brackets was approximately 10 g. These loads combined with the 6-g constant longitudinal and 2-g constant lateral accelerations to produce the following design factors:

Longitudinal = 8 vibration + 10 shock + 6 acceleration = 24 g total

Lateral = 8 vibration + 10 shock + 2 acceleration = 20 g total

It was assumed that the BHXU-Alternate resonance would be sufficiently damped by the isolation system so that the 8-g vibration incurred at a 15-Hz mount system resonance would be the maximum vibration experienced by the BHXU-Alternate.

Material Selection

Hastelloy X was selected for the plate-fin recuperator to provide increased creep strength as compared to Type 347 stainless steel; however, Type 347 stainless steel tubes with copper fins are adequate for the tubular heat sink heat exchanger due to the much lower operating temperatures. The duct and bellows from the BRU to the recuperator are also Hastelloy X since temperatures are equal to the recuperator inlet areas. Other ducting and bellows in the system are 347 or 321 stainless steel where the temperatures are similar to heat sink heat exchanger thermal conditions.

Gold-based braze alloys (Palniro series) were used in brazing the Hastelloy X material in the recuperator to provide an improved high-temperature heat exchanger capability. Standard low-temperature brazing alloys (silver-copper) were used in the heat sink heat exchanger.

The table below shows the materials and the usage in the BHXU-Alternate heat exchanger system.

Location	Item	Material
Recuperator	Tube sheet	Hastelloy X
	Fin	Hastelloy X
	Header bar	Hastelloy X
	Pan	Hastelloy X
	Mounts	Hastelloy X
	Seal plate	Hastelloy X
	Brazing alloy	Gold-based Palniro silver (Palniro 1 and Palniro RE)

Location	Item	Material
Waste heat exchanger	Header plate	CRES 347 (nickel plated)
	Manifold (bar)	CRES 347
	Manifold (liquid)	Nickel 200
	Tubing	CRES 347 (nickel plated)
	Fin	Copper (OFHC)
	Brazing alloy	BAg-8a (71.8 Ag, 28 Cu, 0.2 Li)
Transition section	Side strip	CRES 347, Inconel 718, and Hastelloy X
	Tie rods	Inconel 718
Ducts and bellows	--	Hastelloy X and CRES 347

Recuperator Design

The recuperator is a plate-fin heat exchanger that operates at pressures and temperatures up to 200 psi and 1241°F, respectively. The most severe combinations of temperature and pressure for this Hastelloy X unit are listed in Table 3-4. These conditions included neither the maximum temperature nor pressure experienced by the unit since they were in combination with relatively lower pressures and temperatures. The lower pressure passages were straight-through flow utilizing a rectangular offset fin with 16 fins/in., 0.153 in. high, and 0.004 in. thick. The basic fin in the high-pressure passages was also rectangular offset with 20 fins/in., 0.125 in. high, and 0.004 in. thick. The ends of the high-pressure passages also had plain rectangular fins with 10 fins/in. and the same height and thickness as the basic fin. This is the critical fin in the unit; it has a maximum stress at design conditions (Table 3-4) of 8500 psi compared to an allowable stress of 8800 psi.

Detailed estimates of cycle life of the recuperator were not performed. Operating temperature differences would be required and associated thermal strains would be compared to allowable strain levels for 100-cycle life. The brazed and welded seal plate over the machined header bars and the use of the superalloy, Hastelloy X, in combination with the gold-based brazing alloys were expected to provide considerable improvement over previous designs with the 347 stainless steel material and the nickel-based brazing alloy AMS 4778.

The two recuperator mounts for inertia loads were brazed to the seal plates over the machined header bars. Their location was approximately midway between the inlet and outlet so that temperatures would be less than 1000°F, and material yield and ultimate strength properties rather than creep strength would govern the design.

Heat Sink Heat Exchanger

The heat exchanger was of a tubular design; pressure design conditions are shown in Table 3-4. The unit originally consisted of two banks of tubes; however, one bank was later eliminated as a cost saving. Two tube sizes were used: a basic array of 0.156-in.-OD, 0.008-in.-thick tubes and three rows around the core periphery of 0.188-in.-OD, 0.024-in.-thick tubes. Internal pressure stresses in the tubes were small and the design loads occurred at the periphery where the increased thickness tubes were required to support the possible edge loads due to prospective liquid cover pans (which were not fabricated). The header plate thickness of 0.4 in. also was selected for this loading. Combined pressure, thermal, and inertial loads at the interface were analyzed in detail and stresses were slightly less than the allowable level for the 347 stainless steel.

Several design features were incorporated to accommodate transient temperature difference within the heat exchanger. In particular, thermal loads parallel to the tubes, which could cause excessive tensile stresses or compressive buckling, were avoided. For example, flow guides were used to prevent core bypass on the no-flow sides and tie-rods were included to support the pan edge loads. The flow guides were segmented to avoid tube loads and expansion joints also were provided at the edge of the no-flow pans. Tie rods in parallel with the tubes, particularly for supporting the mounting brackets, required detailed analyses of transient temperatures and the resulting loads and stresses.

The heat sink heat exchanger has two mounting brackets mounted on a box beam located on the gas outlet face. They required detailed analysis since the header plates and tubes had to accommodate their concentrated loads. Loads parallel to the gas flow are supported on the recuperator to obviate the necessity for the excessive reinforcement otherwise required in this tubular heat exchanger.

Manifold and Duct Design

The heat exchanger manifold configurations were selected based on fabricability considerations and the desire to achieve a lightweight design. Recuperator and heat sink gas pans were generally of circular cross-section with an included angle of 180 deg. This design places the greater portion of the shell under direct membrane stress, which produced the lightest weight configuration.

The liquid manifolds on the waste heat exchanger were fabricated from Nickel 200 material in order to minimize the adverse effects of any thermal growth differential between the manifolds and the cover module during the brazing operation.

Bellows Design

Three expansion bellows were required in each of the three ducts connecting the heat exchanger to the BRU. These bellows isolated the BHXU-Alternate thermal movements so that duct loads applied to the BRU scrolls

TABLE 3-4

DESIGN PRESSURE AND TEMPERATURE CONDITIONS

Component	Section	Design Conditions	
		Pressure, psi	Temperature, ^{o}F
Recuperator	Low-pressure side (from BRU turbine)	65	1187
	High-pressure side (from BRU compressor)	120	1142
Heat sink heat exchanger	Gas passages (outside tubes)	200	440
	Liquid passages (inside tubes)	200	440
Ducting and bellows	BRU, turbine to recupterator	65	1187
	BRU, compressor to recuperator	222	440
	Heat sink to BRU compressor	200	440
Transition section	Recuperator to heat sink	200	440

would be within acceptable limits. Preliminary thermal movements at the three bellows were estimated and this information together with other specific design requirements was submitted to several bellows manufacturers to obtain proposed configurations. AiResearch then performed a stress analysis of each candidate bellows configuration. Finally, double-ply, formed bellows manufactured by Aeroquip Corporation were selected for all three ducts, based on the most accurate accommodation of the problem statement. Appendix A discusses the various bellows designs.

Mounting System Design

A four-point mounting system was selected, primarily because it was the most efficient method that avoided placing mounts in the highest temperature areas of the recuperator. The system allowed for free thermal growth of the recuperator and heat sink heat exchanger about a fixed point located on the recuperator. This fixed point was placed on the BRU side of the recuperator to minimize differential expansion differences associated with the separation distance between BRU and BHXU-Alternate system.

The use of pressure-balanced bellows eliminated the need for accommodation of such loads in the mounting system; however, the link system in each duct might be susceptible to vibration. This effect was not analyzed in detail; however, the suggested isolation system might negate the need for separate support of each duct.

SECTION 4

FABRICATION

INTRODUCTION

The fabrication effort on the BHXU-Alternate system is divided into three basic stages for discussion: recuperator fabrication, heat sink heat exchanger fabrication, and final assembly. The basic fabrication sequence in building the BHXU-Alternate heat exchanger assemblies was to fabricate detail parts, braze the parts into an integral assembly, and attach the appropriate pans or ducting. When brazing of the cores was completed, each core module was checked by performing a proof pressure test (1.5 times working pressure) and a helium leak check (the units were Freon cleaned prior to helium leak testing). This evaluation procedure was repeated after the recuperator and heat sink heat exchanger assemblies were completed and also after the ducting and transition sections were welded to the assemblies.

RECUPERATOR FABRICATION

The assembly of the detail parts (fins, tube sheets, header bars) into a plate-fin recuperator is shown in Figure 4-1. This stacking procedure is preceded by chemical cleaning of all detail parts and placement of the 0.001-in. (0.002-cm) Palniro 1 brazing foil on each side of the tube sheets.

Brazing of the modules was accomplished in a vacuum furnace using a graphite brazing fixture with bellows (Figure 4-2) to exert the necessary pressure on the stacked module to ensure the close fin-to-tube-sheet and header-to-tube-sheet contact required for obtaining acceptable brazing joints. After the necessary proof pressure and helium leakage testing, the header bars on the module were end milled to a common plane (Figures 4-3 and 4-4) for the step brazing operation that attached the seal plate assembly (seal plate, mounting bracket (if required), and manifold weld strips to the module. During the milling operation, Braycote 202 was placed in the fin openings to prevent contamination from entering the core module. The brazing alloy, 0.001-in.- (0.002-cm) thick Palniro RE brazing alloy foil, was preplaced at the various brazing joint locations by spot tacking. The brazing of the seal plate assembly was accomplished in a vacuum furnace with graphite fixturing as shown in Figure 4-5; the brazed assembly is shown in Figure 4-6. The two modules with the mounting brackets attached to the seal plates exhibited external leakage from underneath the seal plate in the area of the mounting bracket. The leakage was from the high-pressure circuit at a rate of 2.5 and 44 cc/min with a nitrogen pressure of 100 psig. The seal plate was welded to the side plates and no external or internal leakage was detected from either of the two modules during a 100-psig leak check. Subsequent to welding the seal plate to the side plate, a Stresscoat test was performed on the seal plates of both modules. No indications of highly stressed areas were visible on the seal plates, verifying that no unacceptable unbrazed areas existed in those areas pressurized by the leak. The two modules without the seal plate exhibited no external leakage either before or after welding the seal plates to the side plates.

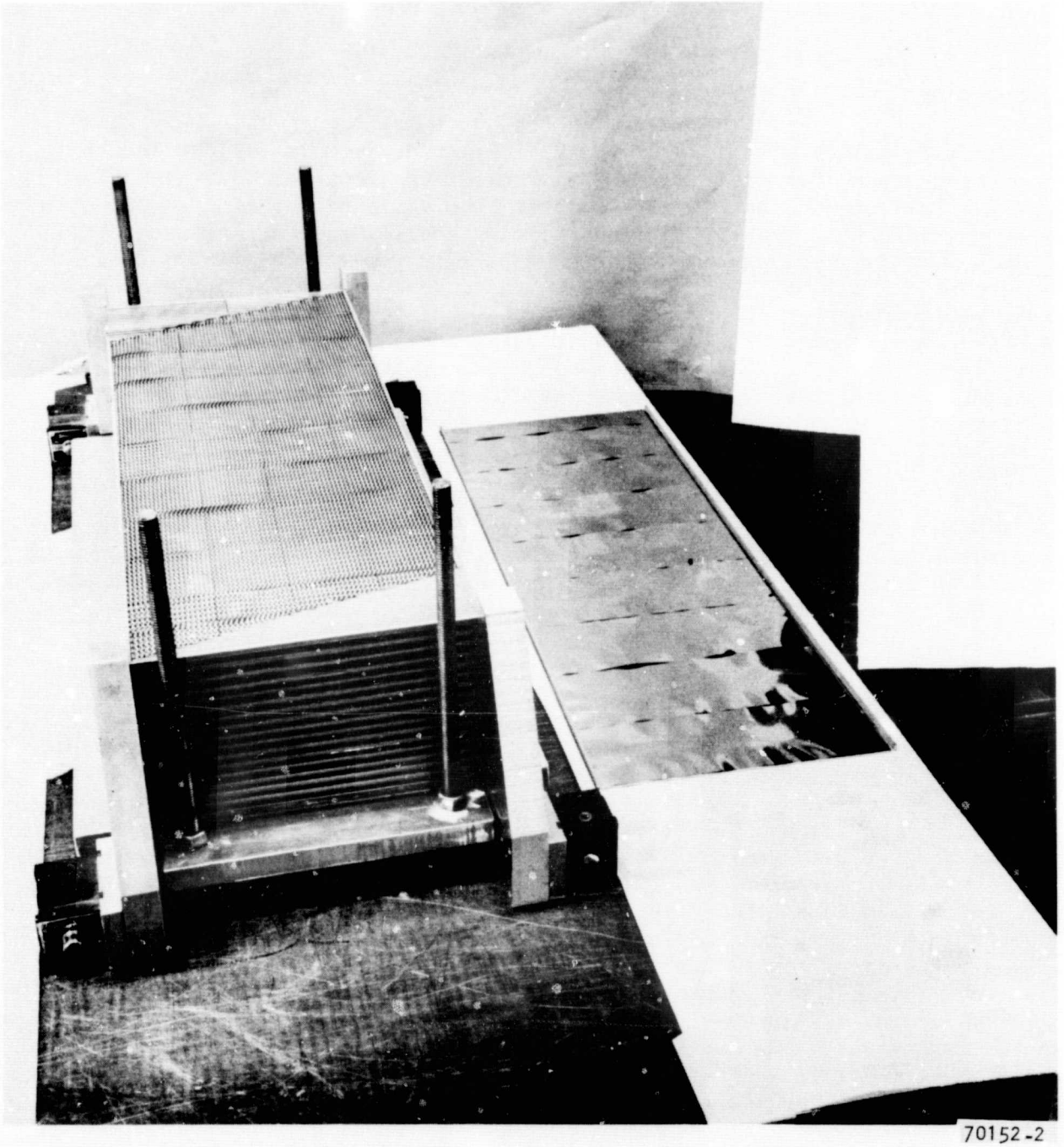

Figure 4-1. Stacking of Plate-Fin Recuperator Module

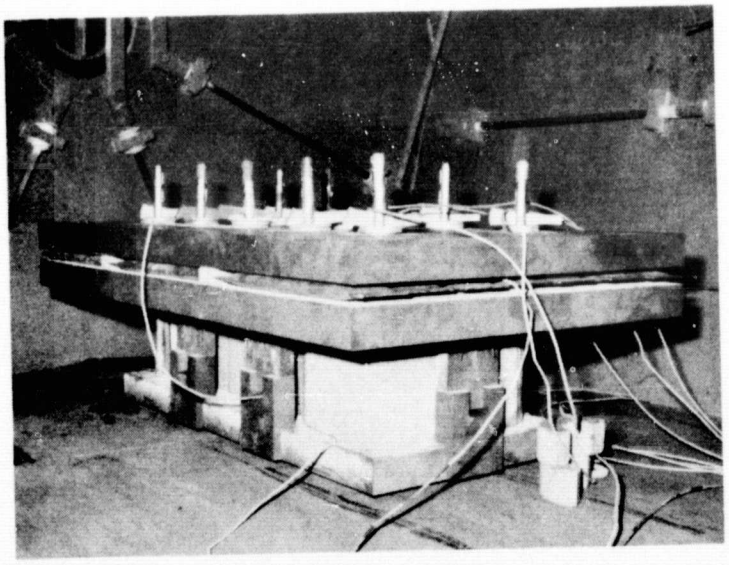

F-13796

Figure 4-2. Core Module 2 Fixtured for the Palniro 1 Brazing Cycle

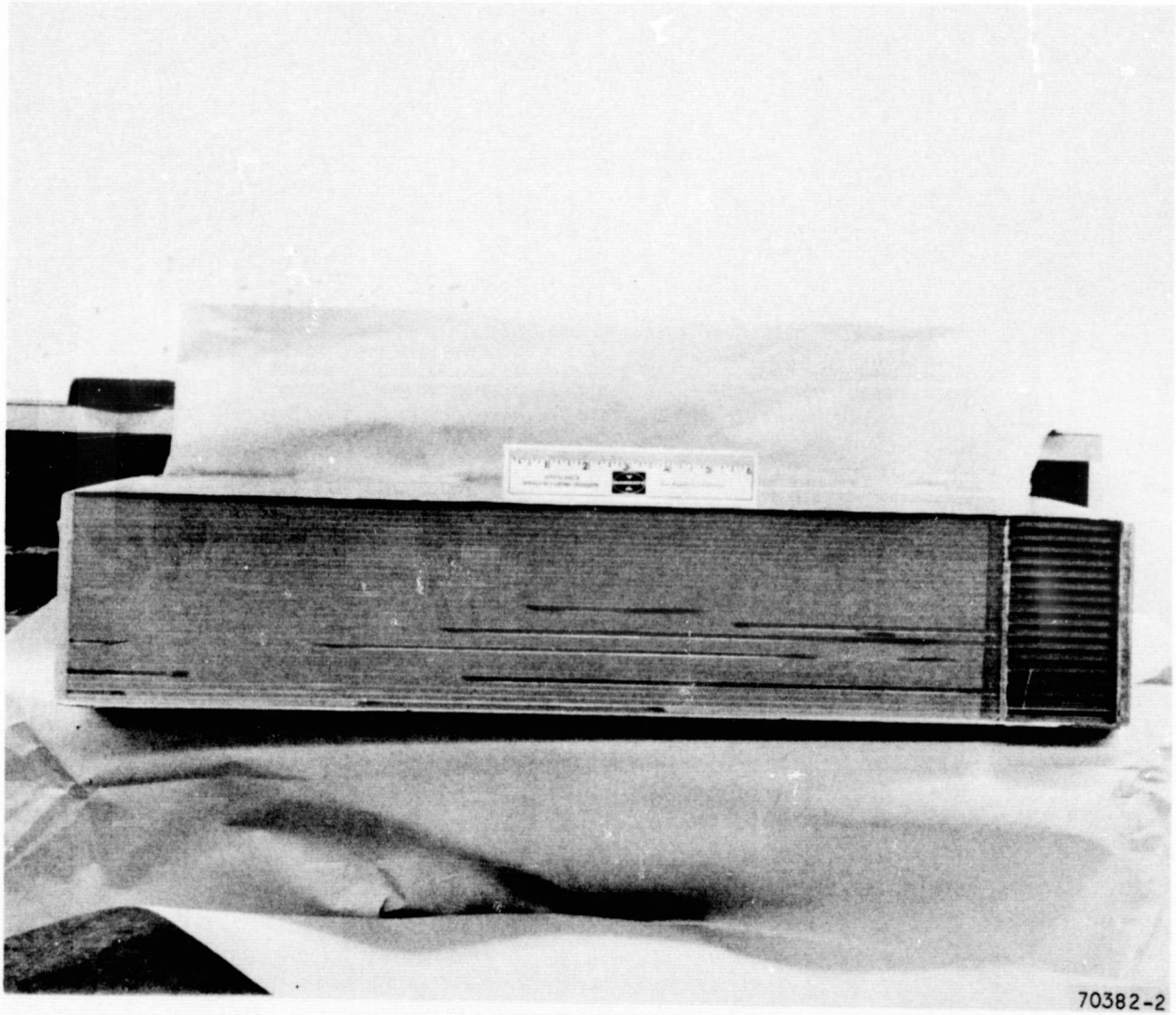

Figure 4-3. Core Module 1 after Machining of Header Bars (Side 1) and the Vacuum Cleaning Cycle

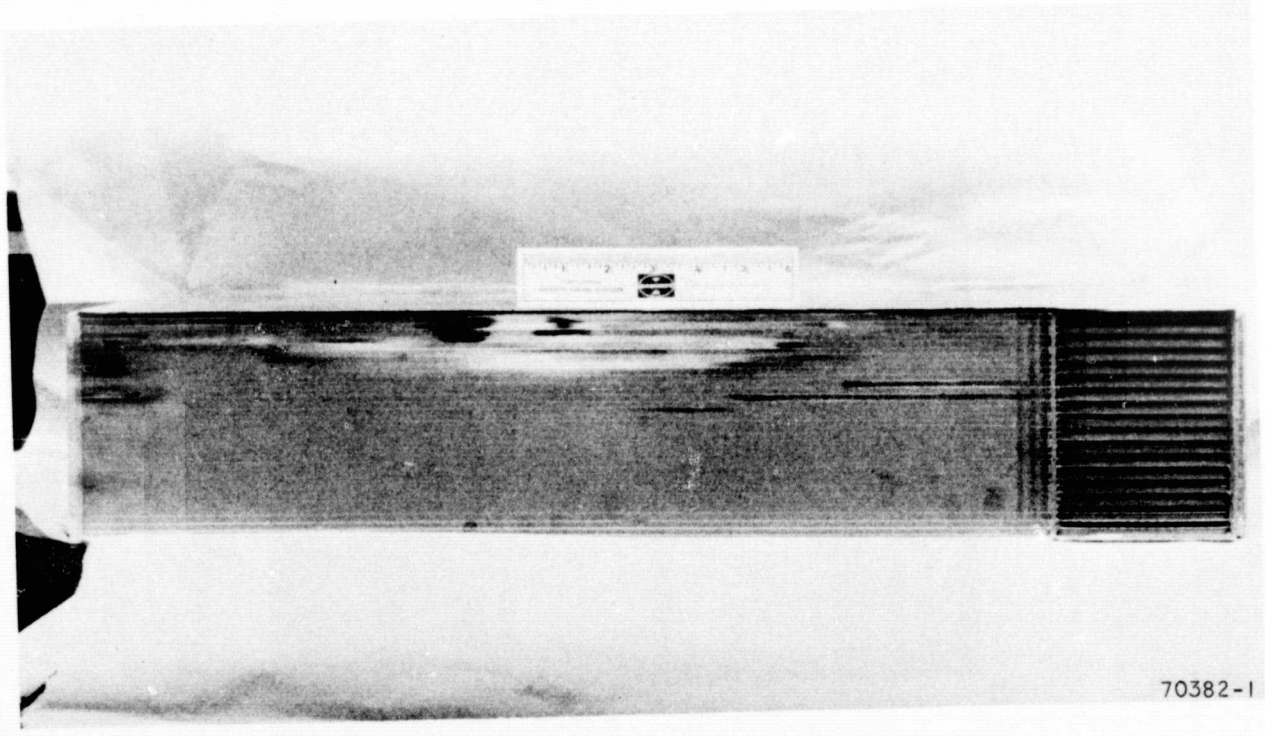

Figure 4-4. Core Module 1 after Machining of Header Bars (Side 2) and the Vacuum Cleaning Cycle

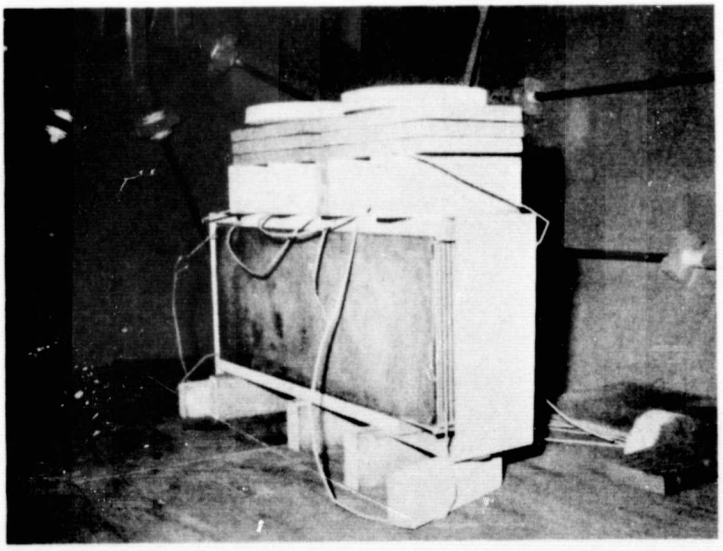

F-13797

Figure 4-5. Core Module 2 Fixtured for the Side Plate Brazing (Palniro RE)

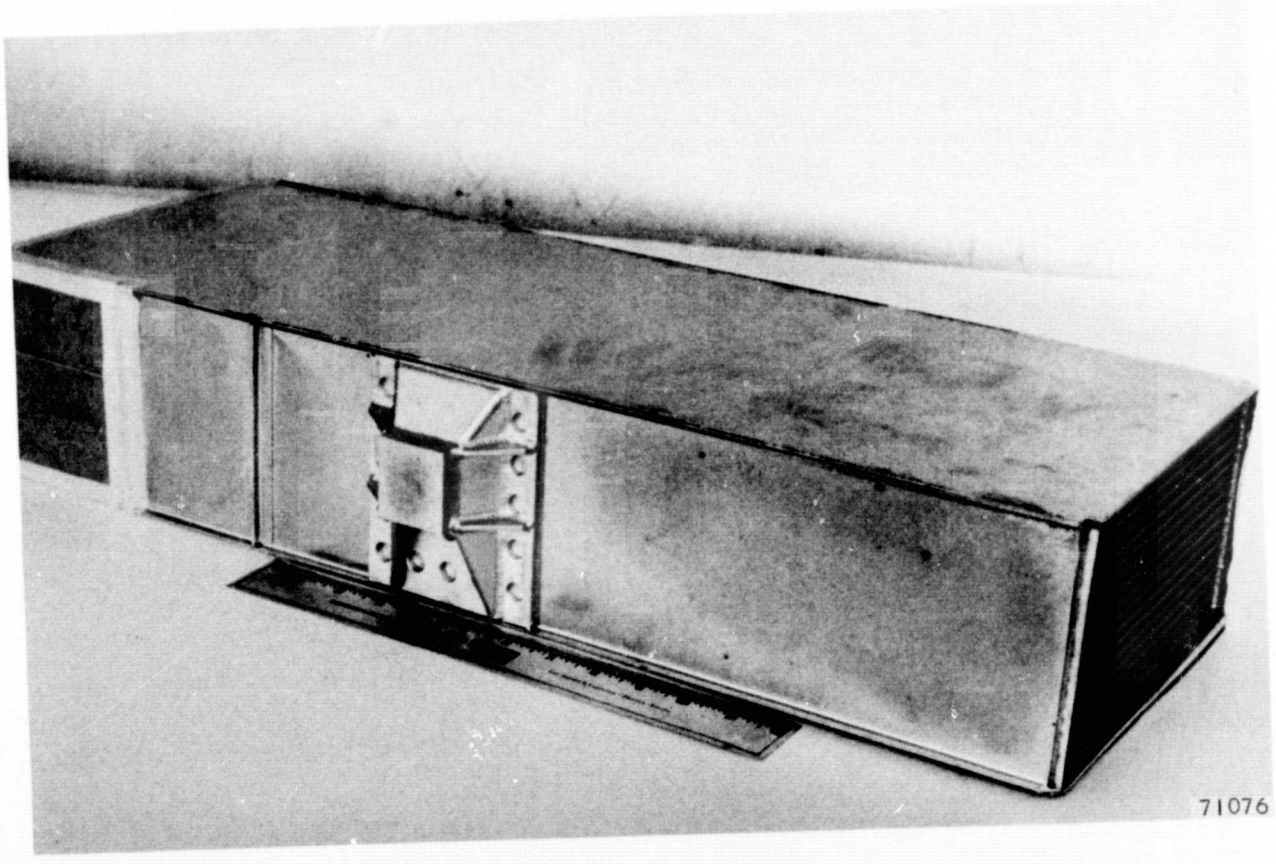

Figure 4-6. Recuperator Module After Palniro RE Step Brazing

The final sequence in fabricating the recuperator modules into an integral assembly was to weld the individual modules together with bleed tubes at the module interfaces, and attach the manifold assemblies. The completed assembly is shown in Figure 4-7. The weight of the completed assembly was 348 lb.

The BHXU-Alternate recuperator fabrication effort was completed successfully. The only major problem encountered was in the second brazing cycle of the first core module, at which time a proof pressure test revealed interpass leakage that was not present prior to this brazing cycle. The core module was sectioned, and it was found that a piece of the silicon carbide from the grinding wheel had entered the core module and lodged in the fin after the first, but prior to the second brazing cycle. The gold from the brazing alloy and the silicon from the grinding wheel formed a low melting point eutectic alloy that was so aggressive at the Palniro RE brazing temperature it eroded the tube sheet. A summary of the metallographic examination of the core module and corrective fabrication procedures is presented in Appendix B.

HEAT SINK HEAT EXCHANGER FABRICATION

The fabrication of the 2016 finned tube heat sink heat exchanger was considered a difficult task because of the exceptionally high quality brazing necessary to meet the helium leakage requirements and the difficult assembly operations required because of the copper-finned tubes. The heat sink heat exchanger fabrication effort was preceded by an investigation into the tolerances needed for brazing the finned tube into the header plates, nickel manifolds, and return bends to satisfy the problem statement. A discussion of this investigation is presented in Appendix C.

Detail Part Fabrication

The detail part fabrication effort basically consisted of forming sheet metal parts, with the exception of the two configurations of copper-finned tubes and the machined header plates. These two items are discussed below.

1. Copper-Finned Tube Fabrication

The copper-finned tubes purchased from Thermal Transfer, Inc., were fabricated by winding 0.003-in.- (0.008-cm) thick oxygen-free copper strip in a helical pattern on a nickel-plated 347 stainless steel tube to obtain a fin density of 30 fins/in. (76.2 fpc). Several trial runs to establish a brazing cycle were made in a continuous hydrogen brazing furnace. Figures 4-8 and 4-9 show the metallographic examination of the fin-to-tube joint on both sizes of tubing brazed with the 90% Cu-10% Sn brazing alloy at 1800°F (1250K). The metallographic examination showed that the fin-to-tube and the turbulator-to-tube joints were adequate, and that some liquid passage blockage by the brazing alloy could occur. Since the heat sink heat exchanger is a series circuit, each of the brazed tube assemblies was subjected to a flow test (Figure 4-10). The criterion for acceptance of a tube from flow consideration was to take the nominal flow rate through each tube, accepting a minimum of 30 percent less than nominal flow at a given inlet pressure. To minimize unit pressure drop, the tubes in the flow range of nominal to 80 percent of

Figure 4-7. BHXU-Alternate Modularized Recuperator

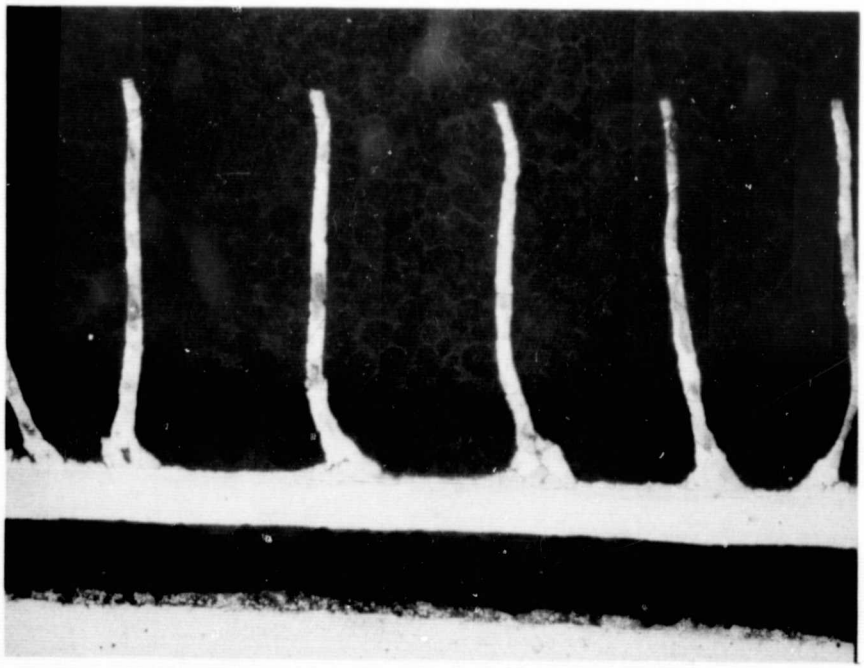

(a) OVERALL VIEW 25 x MAGNIFICATION

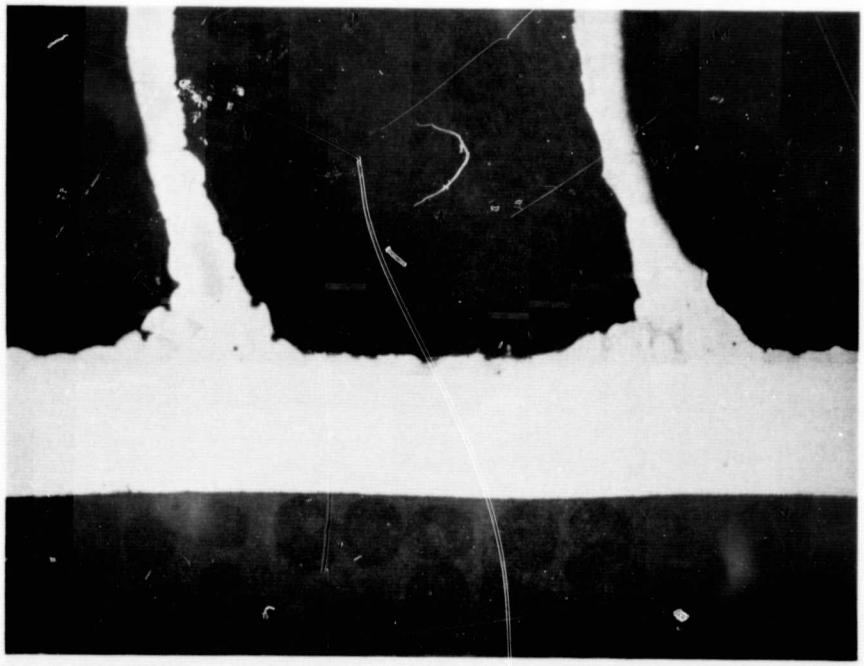

75 x MAGNIFICATION

(b) CLOSEUP VIEW OF COPPER FIN-TO-TUBE BRAZE JOINT F-14501

Figure 4-8. Photomicrographs of the Small-Diameter (5/32-in. OD) Chopper-Finned Tube Showing the Fin-to-Tube Braze Joint

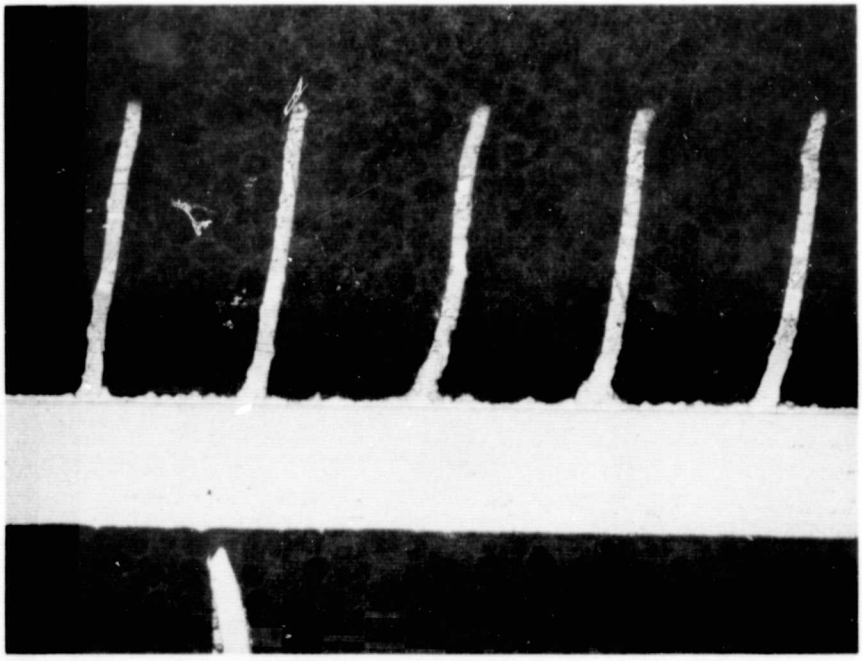

(a) OVERALL VIEW 25 x MAGNIFICATION

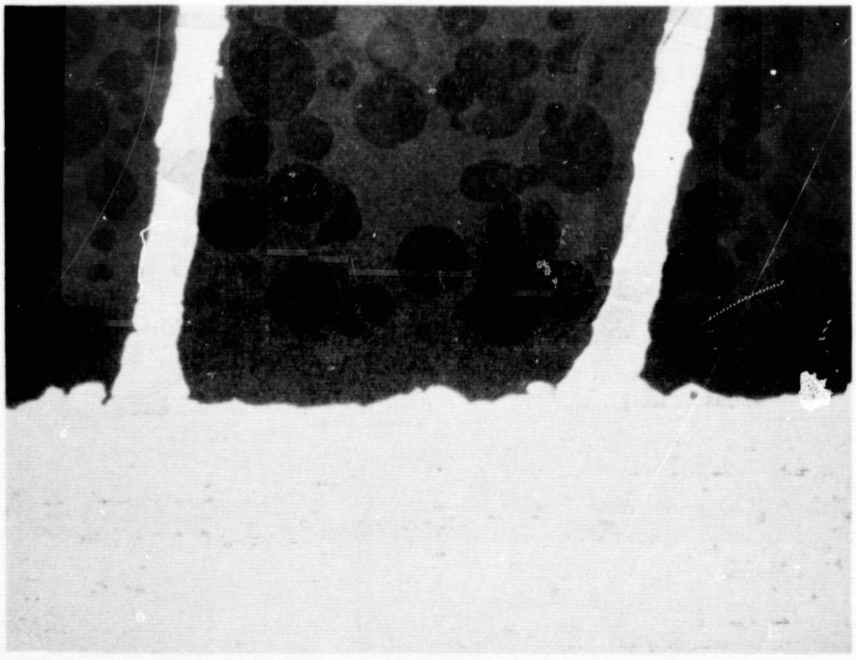

75 x MAGNIFICATION

(b) CLOSEUP VIEW OF COPPER FIN-TO-TUBE BRAZE JOINT

F-14502

Figure 4-9. Photomicrograph of the Large-Diameter (3/16-in. OD) Copper-Finned Tube Showing the Fin-to-Tube Braze Joint

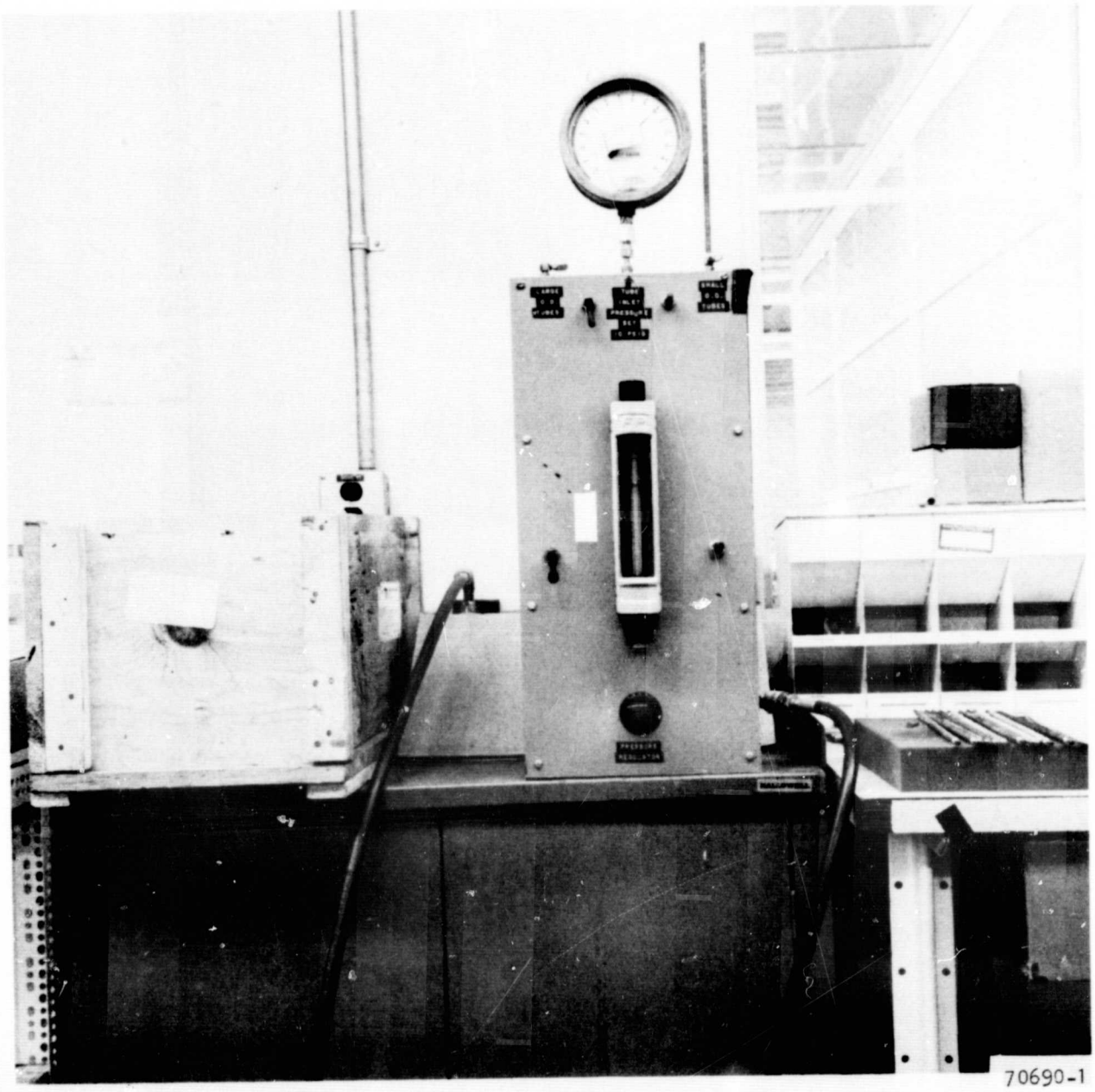

Figure 4-10. Finned Tube Air Flow Isothermal Pressure Drop Test Setup

nominal were used in the assembly, with the tubes in the flow range of 70 to 80 percent of nominal used as backup hardware. Tubes with a flow of less than 70 percent of nominal were rejected. The tubes passing the air flow test were subjected to a helium leakage test (Figure 4-11). The ends of the copper finned tubes were swaged after being accepted in the helium leakage and air flow tests. The 5/32-in.- (0.397-cm) and 3/16-in.- (0.477-cm) diameter tubes were swaged to 0.155/0.154 in. (0.394/0.391 cm) and 0.187/0.186 in. (0.475/0.473 cm), respectively.

2. Header Plate Fabrication

The header plates were fabricated from 347 stainless steel plate stock. The 456 holes 0.189/0.188-in. (0.480/0.478-cm) in diameter and the 1560 holes 0.157/0.156-in. (0.399/0.397-cm) in diameter were drilled undersize and broached to the high end of the final hole diameter in order to account for the 0.0004- to 0.0002-in.- (0.0010- to 0.0005-cm) thick nickel plating placed on the header plate after the broaching of the holes.

Heat Sink Heat Exchanger Assembly

The 2016 finned tube heat sink heat exchanger core assembly detail parts were cleaned by vapor degreasing, and Freon wiped as required on the brazing joint locations. The silver-based brazing alloy BAg-8a was preplaced in wire form in the counter bores of the header plates, return bends, and Nickel 200 manifold assemblies. The top header plate was moved into position simultaneously on all of the 2016 copper finned tubes. An additional preformed brazing alloy ring was placed on the outside of the header plate but on the copper finned tubes as shown in Figure 4-12. The Nickel 200 manifolds and the return bends were then positioned onto the copper finned tubes. Figure 4-13 shows the 2016 copper finned tube core module after completion of the stacking operation.

The heat sink heat exchanger was fired at 1200°F, enclosed within a titanium shield in an argon atmosphere furnace to remove as many contaminants as possible that would impair the brazing operation. The assembly subsequently was heated to 1500°F twice for brazing. A visual examination of the assembly after the first brazing cycle revealed unbrazed tube-to-header joints in one location only. Visual examination of the brazed assembly after the second brazing cycle indicated no braze voids.

A low-pressure nitrogen leak test of the liquid side indicated four return bend-to-finned-tube leaks on only one side of the assembly. These leaks were repaired with AMS 4771 by using a torch brazing technique. The brazed assembly indicated no visible leakage when taken to the full proof pressure of 300 psig with nitrogen while submerged under water. The tube-to-header braze joints were not nitrogen leak checked at this time because there were no pans over the return bends. The liquid side of the 2016 finned tube heat sink heat exchanger was helium leak checked with the helium leakage rate less than 1×10^{-10} scc/sec.

A pan was attached to each of the two header plates to verify the integrity of the tube-to-header joint. The tube-to-header joints on the header plate

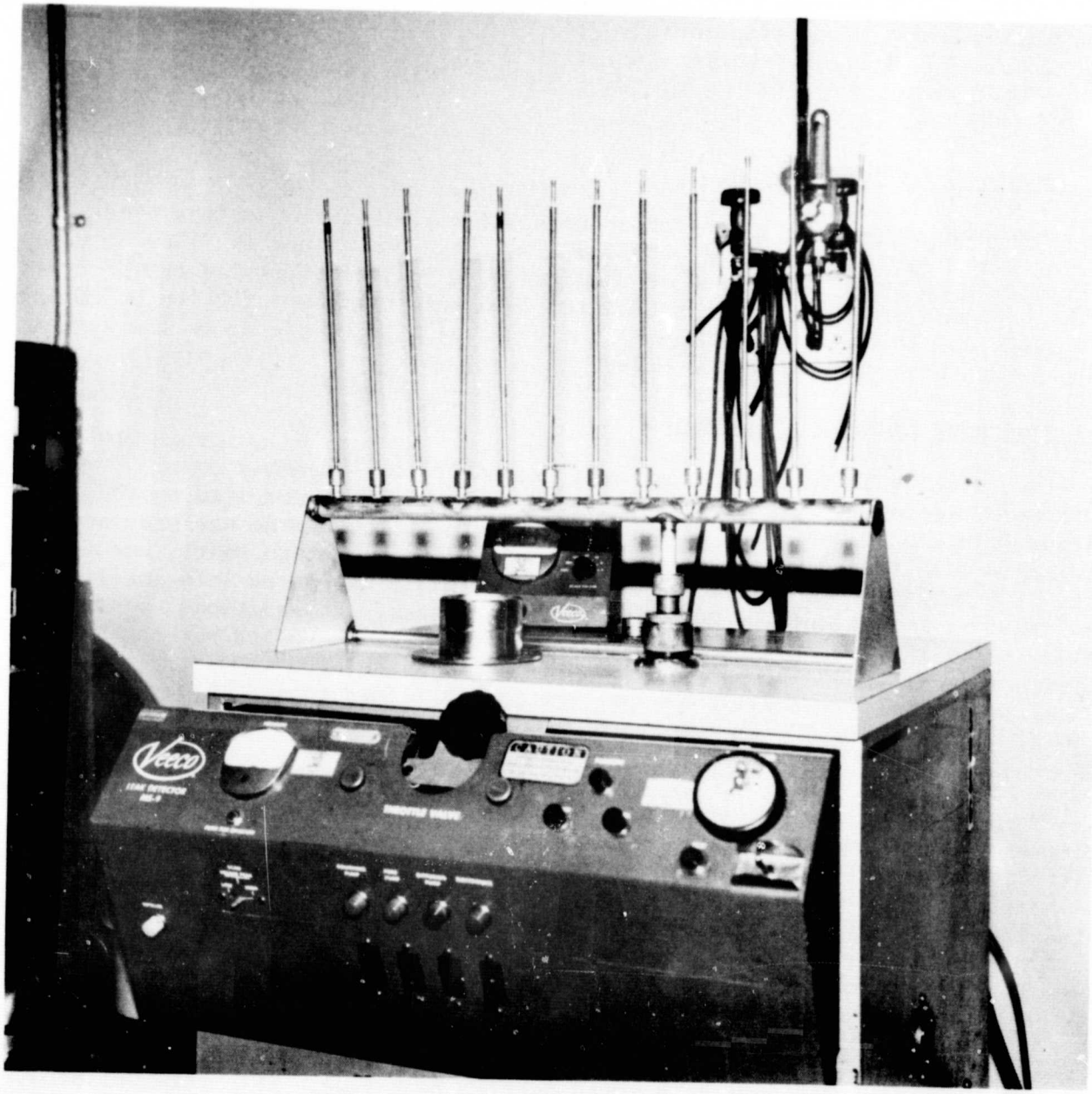

70690-2

Figure 4-11. Finned Tube Helium Leakage Test Setup

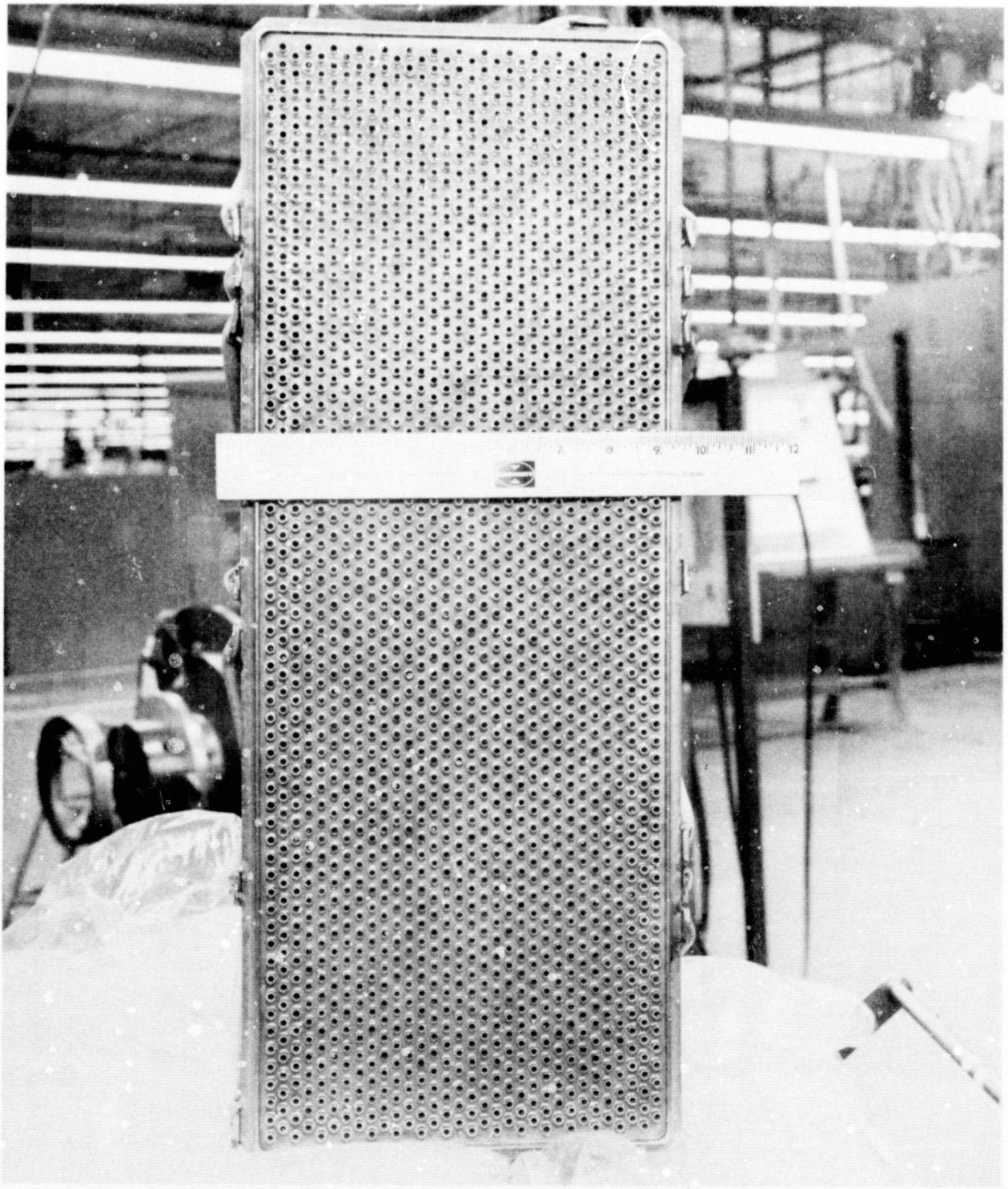

71715-3

Figure 4-12. View of 2016 Finned Tube Stacked Heat Sink Heat Exchanger Core Showing Preplaced Wire Brazing Alloy (BAg-8a) Preformed Rings

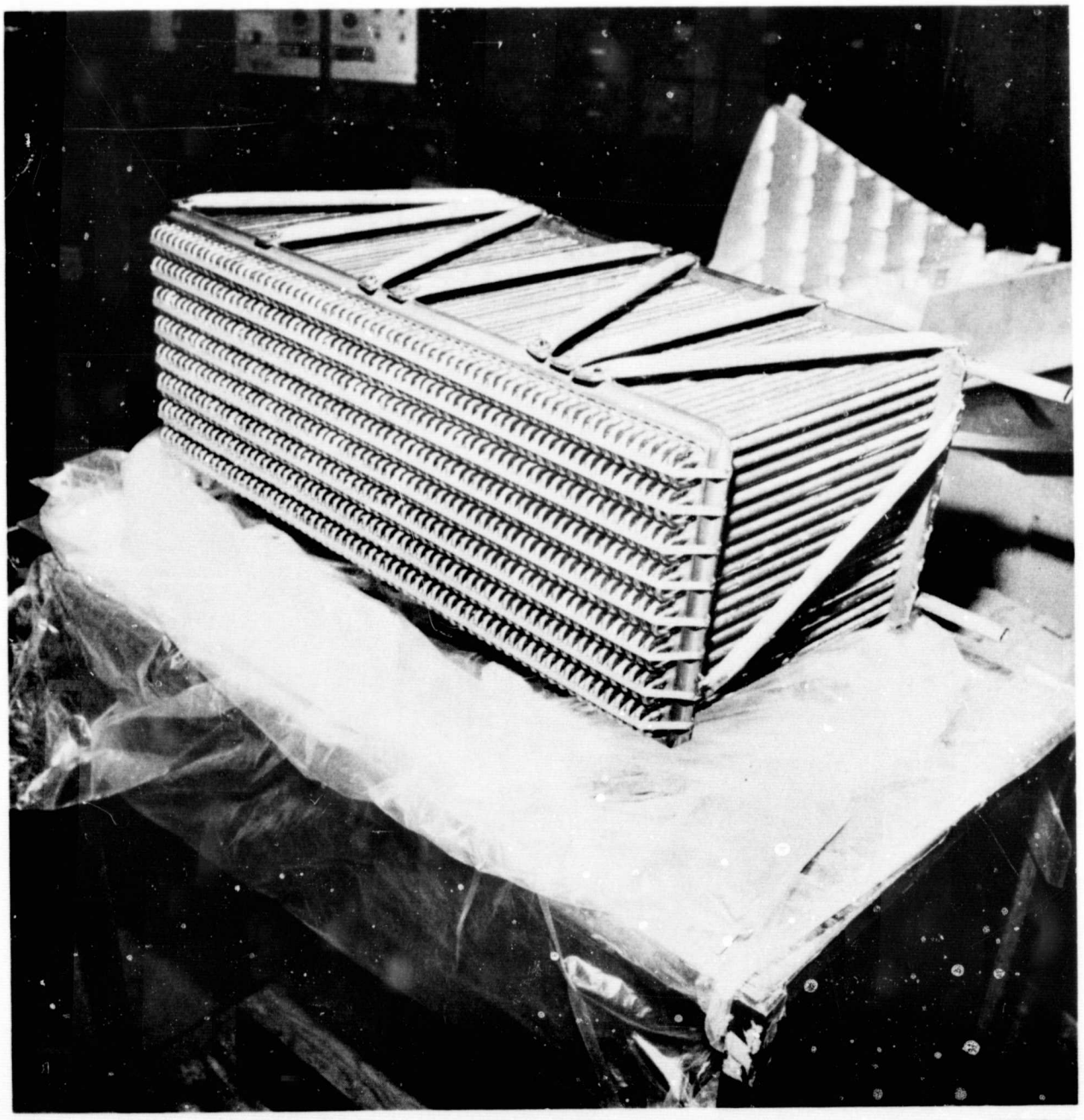

72038-3

Figure 4-13. Heat Sink Heat Exchanger Assembly Stacked for Brazing

opposite the manifolds had a helium leakage rate less than 1×10^{-10} scc/sec, while the tube-to-header joints on the other header plate had leakage. The leakage area was located by pressurizing the pan to 30 psig and placing the assembly under water. A section of the pan was removed and visual examination revealed one questionable tube-to-header braze joint. This joint was alloyed with ASTM 1.5S (1.5% Ag, 97.5% Pb, 1.0% Sn) solder and Lloyd's stainless steel solder flux, and heated to 650°F in an argon retort. After completion of the repair procedure, no visual leakage was observed when a 30-psig nitrogen underwater leak check was performed on the tube-to-header joints. A subsequent helium leakage test indicated the helium leakage rate to be less than 1×10^{-10} scc/sec.

In summary, the 2016 finned tube heat sink heat exchanger was brazed with a very high degree of success. Only 4 out of 4032 return bend-to-tube joints required repair with AMS 4771 braze alloy, and only 1 out of 4032 tube-to-header plate joints required repair with ASTM 1.5S solder. The fabrication of the heat sink heat exchanger was completed with pans and the welded tie rod assembly attached to the finned tube assembly.

BHXU-Alternate System Final Assembly

The completed recuperator and heat sink heat exchanger were placed in the assembly fixture for final fabrication. The heat exchanger assembly was pressure tested after the two assemblies were welded into an integral heat exchanger package with the transition sections and pan assemblies as shown in Figure 4-14. The recuperator high-pressure passages were hydrostatically proof pressure tested at 335 psig and then leak checked under water at a nitrogen pressure of 100 psig. No leakage was observed during either test. The liquid side of the heat sink heat exchanger was proof pressure tested at 300 psig and also leak checked under water with nitrogen at 100 psig. No leakage was observed during either test.

The low-pressure side of the heat exchanger system was hydrostatically proof pressure tested at 300 psig. Leaks were observed on the liquid manifold side of the heat sink heat exchanger. The manufacturing leak test pan covering the return bends was removed in order that the tube-to-header braze joint leaks could be located. The unit was pressurized to 100 psig with nitrogen and ten tube-to-header brazing joint leaks were located underneath the liquid manifold on the downstream (gas) end of the assembly. Subsequently, the leak test pan covering the return bends on the opposite side of the heat sink heat exchanger was removed (Figure 4-15) and a 100-psig nitrogen leak test showed five tube-to-header brazing joint leaks in the outer downstream (gas) tube row.

The tube-to-header brazing joint leaks in the heat sink heat exchanger occurred due to welding the transition section to the heat sink heat exchanger. In addition to the heat effect during the attachment of the transition section to the heat sink heat exchanger, it was found that gussets located inside the manufacturing leak test pans had been bearing on the downstream (gas) liquid circuit manifold and some return bends. The gussets caused one 0.050-in. indentation (Figures 4-16 and 4-17) in the downstream (gas) liquid manifold and 0.015- to 0.005-in. indentations at seven other locations in both

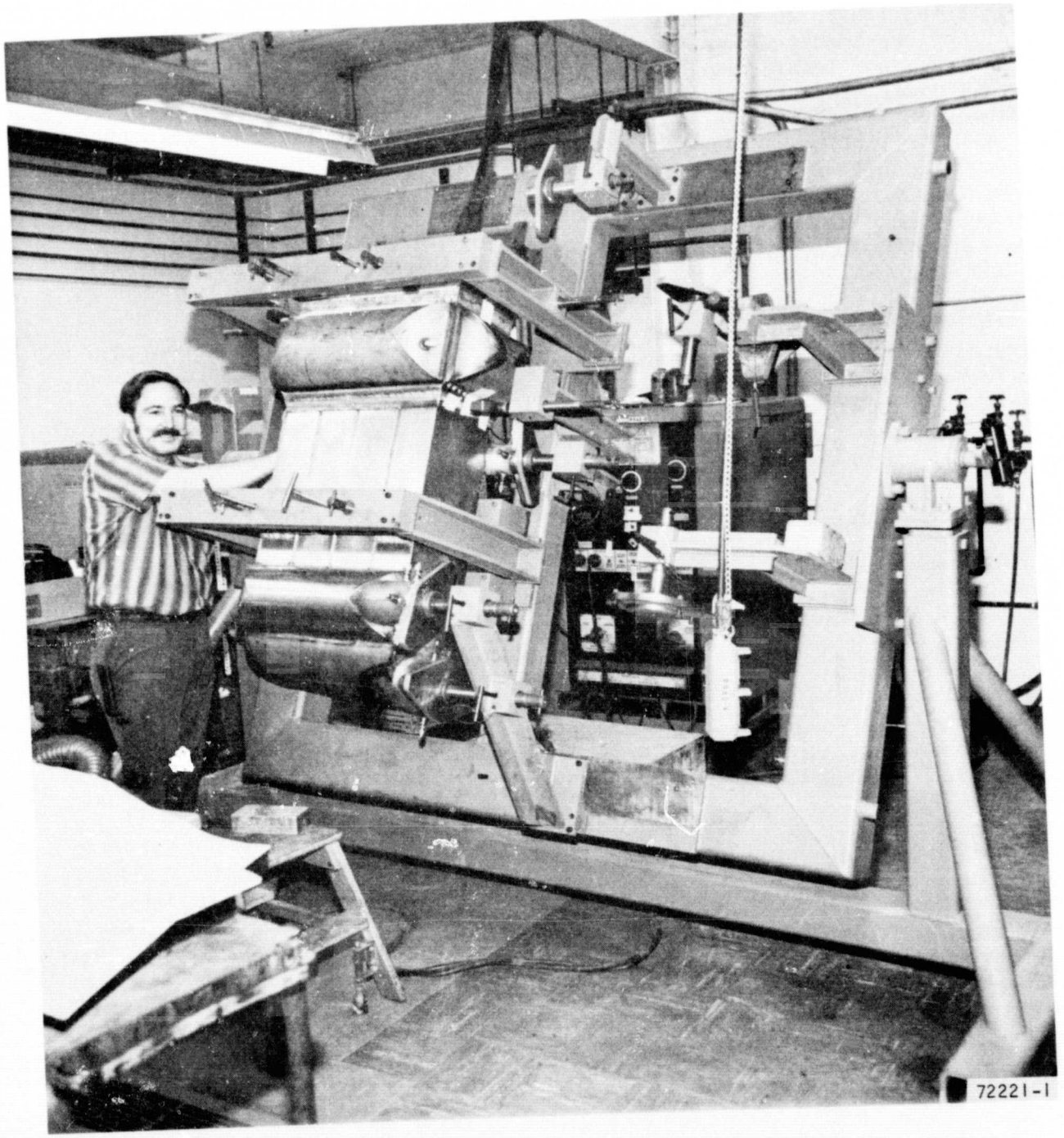

Figure 4-14. BHXU-Alternate Heat Exchanger and Ducting Assembly during Final Assembly

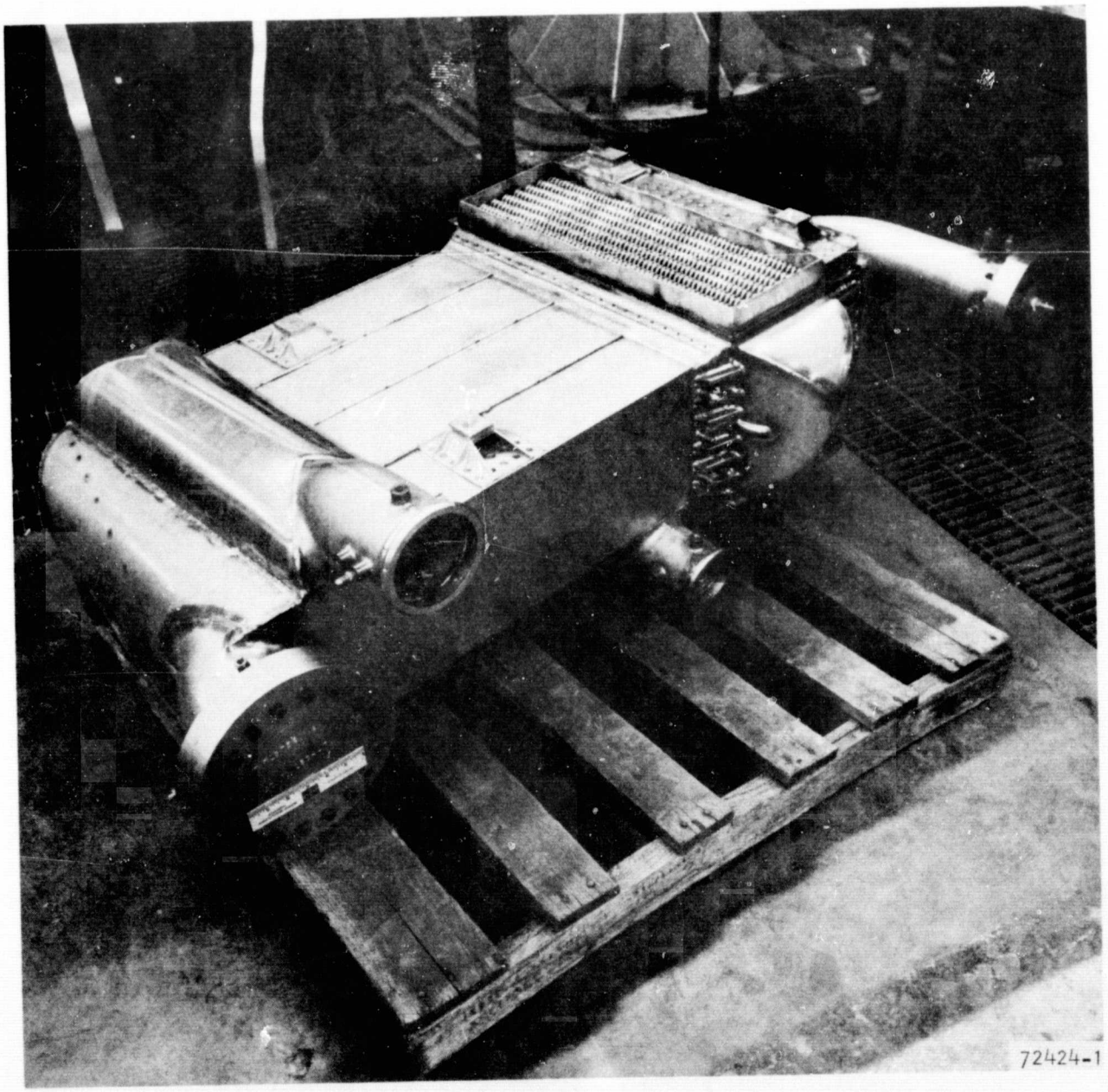

Figure 4-15. BHXU-Alternate Heat Exchanger Assemblies

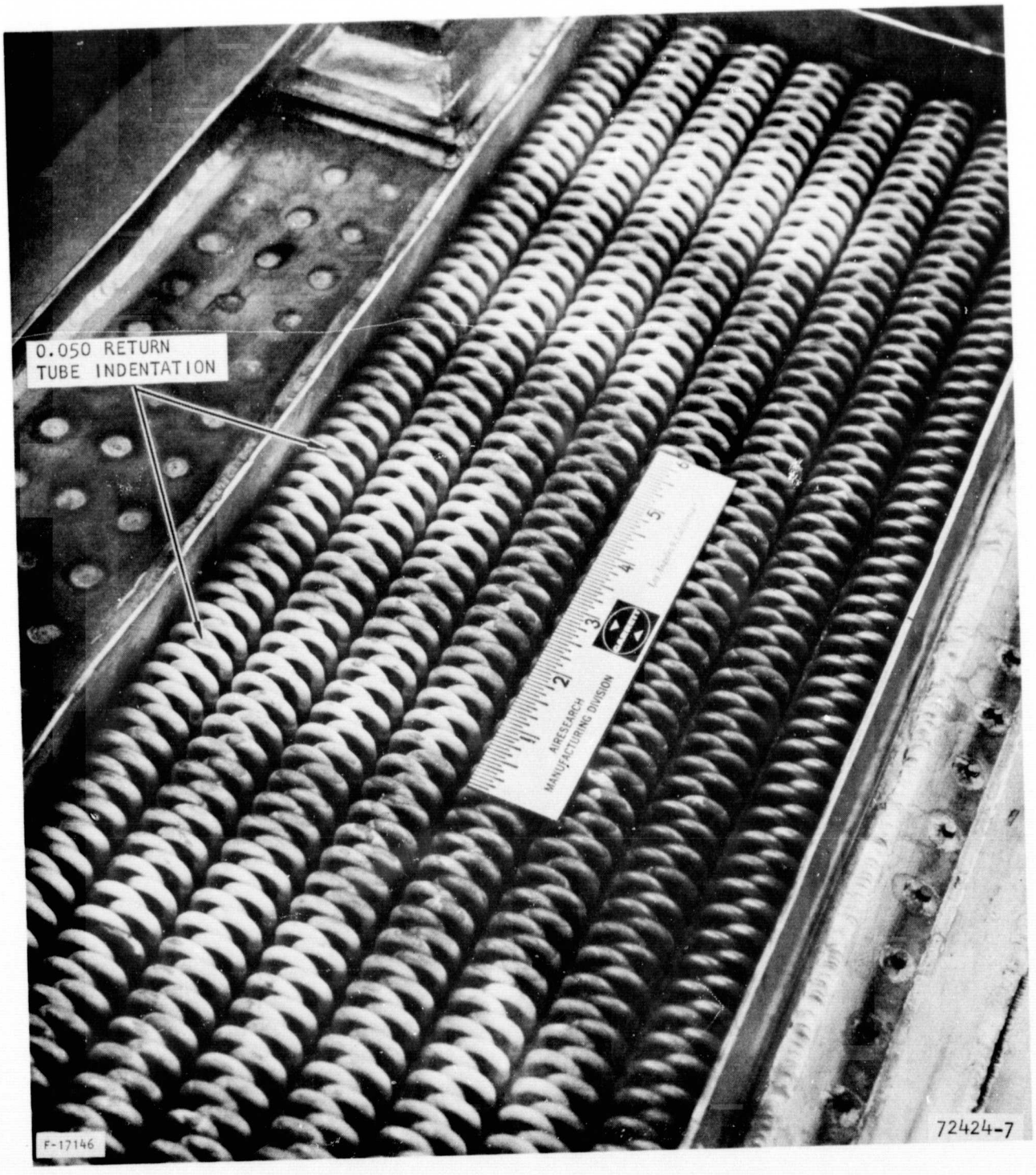

Figure 4-16. Indentations in the Liquid Circuit Manifolds

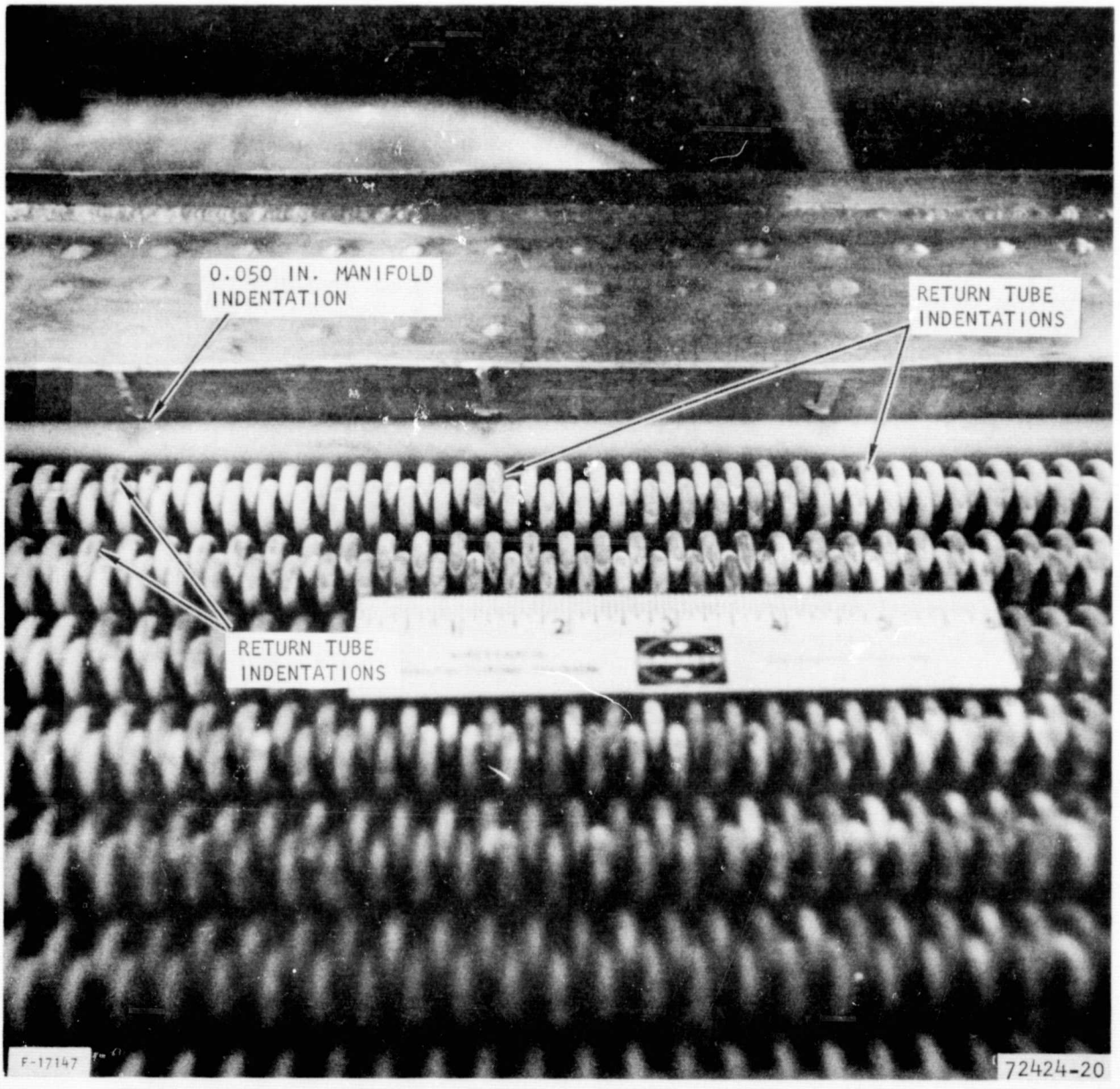

Figure 4-17. Closeup of Indented Return Bends on the Heat Sink Heat Exchanger

of the liquid circuit manifolds. The leak test pan gussets on the side opposite the liquid circuit manifolds caused a 0.050-in. indentation in two return bends and 0.015- to 0.005-in. indentations in eight other return bends.

An ASTM 1.5S solder repair cycle on the heat exchanger assembly was used to repair the tube-to-header brazing joint leaks. The procedure for repair was basically the same as for the repair of the one tube-to-header brazing joint leak found previously on the heat sink heat exchanger assembly. The welded heat exchanger assembly was brazed in an inclined position because of space restraints inside the atmosphere furnace. The ASTM 1.5S (600°F) solder was placed adjacent to the ends of the finned tubes in a horseshoe type shape.

The assembly was cleaned, alloyed, and soldered at 650°F in an argon atmosphere. The joints under the nickel manifold showed no visible leakage under water when pressurized to 100 psig (nitrogen). The tube-to-header joint leaks on the side opposite the nickel manifold (downward gravity side) still showed five leaks when pressurized to 100 psig (nitrogen) and observed under water. The five remaining leak areas were cleaned, alloyed (SN 63), and soldered at 425°F in an atmosphere (argon) retort. The fixture for holding the assembly during the soldering cycle appears in Figure 4-18, which shows the assembly during leak testing.

The unit was subjected to a 100-psig nitrogen leak test and then hydrostatically proof pressure tested (all flow circuits). No visible leakage or deformation was observed during these pressure test operations. The assembly was Freon cleaned prior to helium leak testing, with the following leak test results:

(a) External leakage (bagged): 6.7×10^{-7} scc/sec

(b) Internal leakage recuperator (30 psi ΔP): less than 1×10^{-10} scc/sec

(c) Internal leakage heat sink heat exchanger (30 psi ΔP): less than 1×10^{-10} scc/sec.

The machining of the mounting pads and installation of the bellows and ducting subsequently was completed, and the unit hydrostatically proof pressure tested and helium leak tested. The completed heat exchanger and ducting assembly is presented in Figure 4-19.

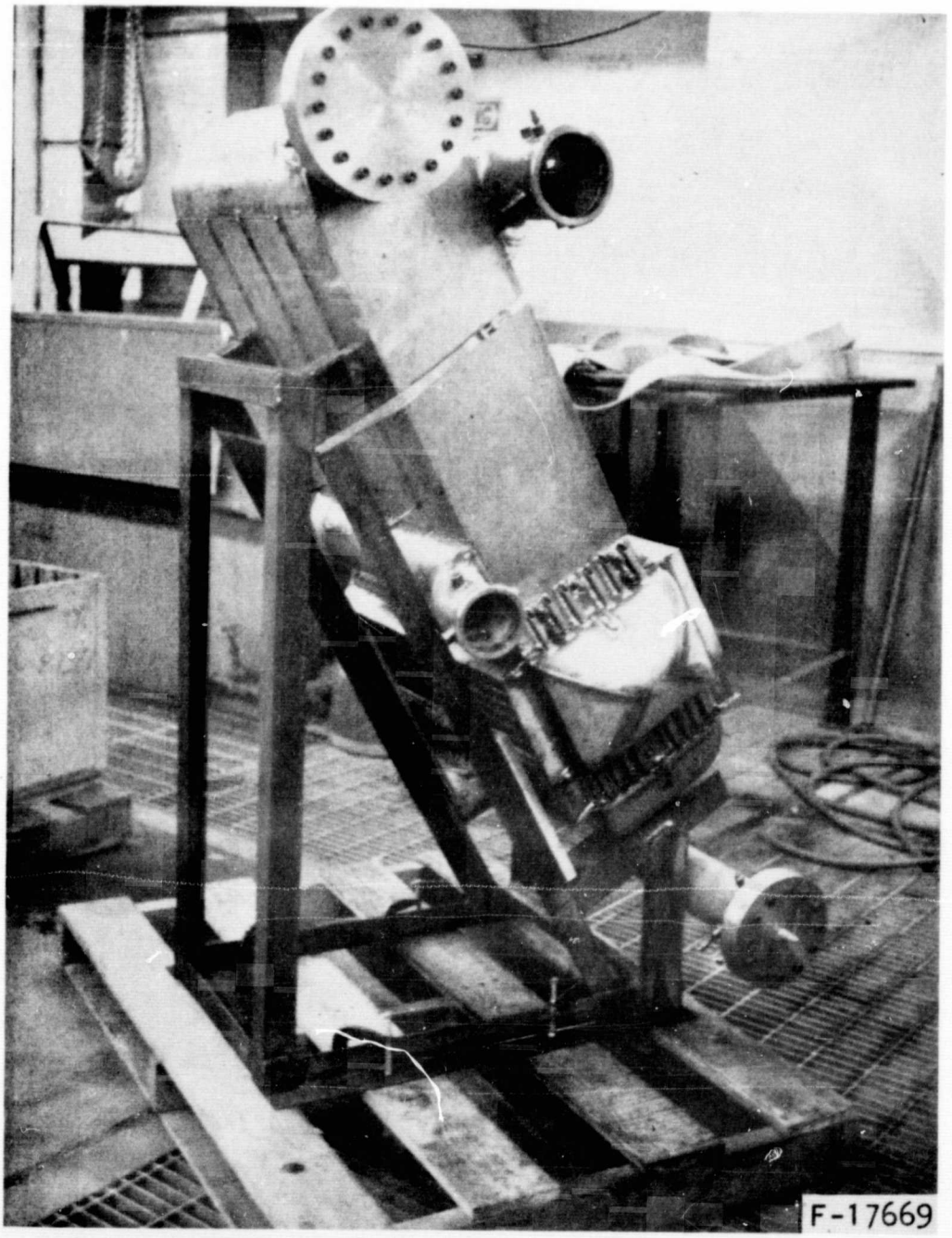

Figure 4-18. Leak Testing of the BHXU-Alternate Assembly. (The assembly is installed in the fixture used for the retort solder repair cycles).

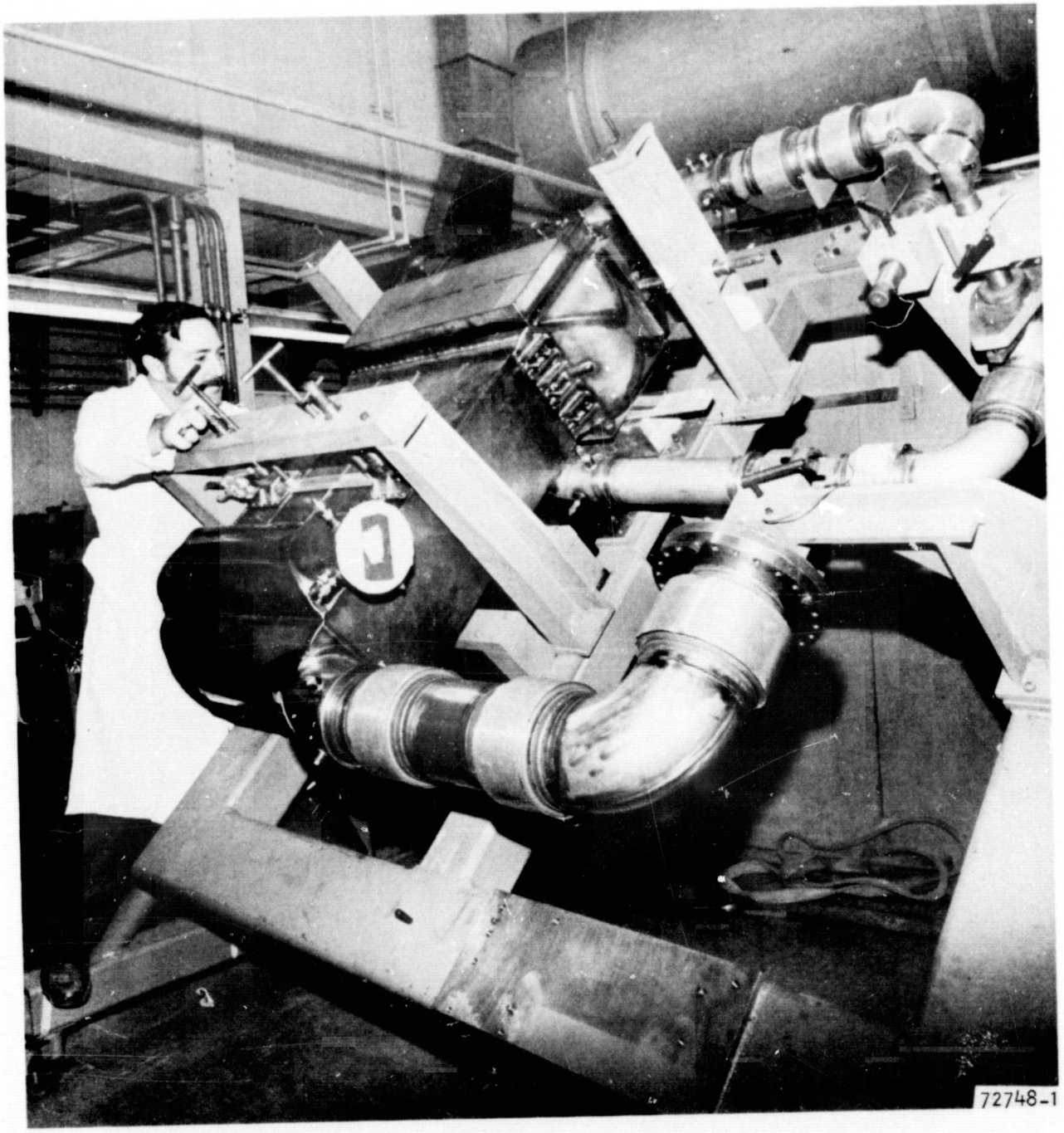

Figure 4-19. BHXU-Alternate Heat Exchanger Assembly

APPENDIX A

BELLOWS DESIGN AND VENDOR SELECTION FOR THE BHXU-ALTERNATE SYSTEM

INTRODUCTION

In the BHXU-Alternate recuperator, the operating pressures for each duct are considerably higher than in the original BHXU Engine B. This required the bellows convolutes to be substantially thicker for the BHXU-Alternate than the BHXU and the utilization of a single bellows for each duct would have led to excessive stresses due to thermal movements and excessive stiffness in the bellows. A successful design solution was effected by using three hinged bellows in each of the three duct connections. In this way the ducting was made to operate as a linkage system, where each bellows provided a rotational hinge point. The internal hinge connection in the bellows made the bellows self-sufficient for absorbing the pressure thrust loads. By use of this design, the effective thermal movement on each bellows unit was reduced to acceptable limits, and the effective stiffness of the linkage system was kept well below the maximum acceptable values.

STRUCTURAL DESIGN

Bellows Design

A bellows design was established and specifications were determined for a nine-bellows system, three bellows in each of the ducts connecting the BHXU-Alternate and the BRU. The bellows were of the link type that provide rotation about any axis. The link was inside the bellows and, in addition to providing rotation capability, it supported the axial internal pressure forces.

The pressure-balanced, link-type bellows were selected for the duct system because (1) a single, unbalanced, shear, and deflection type could not be used in the high-temperature section between the turbine and the recuperator, and (2) use of pressure-balanced bellows in all ducts eliminates the heat exchanger pressure unbalance loads and simplifies the support system for the package. The 6-in. bellows pressure containment design of 65 psi at 1187^{o}F requires a convolute height and thickness that precludes satisfying both buckling and thermal load requirements with a single bellows. The buckling pressure that determines maximum allowable bellows length for a given geometry is the 200-psi shutdown pressure following 800^{o}F maximum turbine outlet temperature conditions. Alternate bellows design incorporating two bellows of various configurations in the 6-in. duct required at least one shear-type bellows. Designs incorporating the shear type experienced limitations similar to the single shear and deflection type and did not lead to a reduced package compared to the selected system. Furthermore, the use of identical sets of bellows in each duct (or for use in more than one duct) permitted use of three designs as opposed to selecting several types and geometries tailored to each duct requirement and bellows location.

A summary of thermal deflections and resultant bellows rotations is provided in Table A-1 for a nine-unit system with the layout shown in drawing SK 51738. The bellows are lettered consecutively starting from the heat exchanger end of each of the three ducts. The link of bellows G, not shown in the layout, was placed 6 in. from the link of bellows H, which is shown in the straight duct section at the low-pressure gas outlet of the heat sink heat exchanger. The operating conditions that determine movements for each bellows system are also listed in Table A-1. The geometrical relations between the input deflections and the bellows rotations are shown in Figure A-1, as well as the general case for a three-point link system with the link at one end constrained and thermal deflections applied to the other end. Figure A-2 shows the geometry of the 6-in. turbine outlet duct from SK 51738 with the X and Z thermal deflection inputs listed in Table A-1. Bellows B has the highest rotation so it will govern the thermal stress design if three identical bellows are used. Thermal motions in the Y-direction will generally be accommodated by the pair of bellows in each duct closest to the heat exchanger. This permits location of a support strut on the movable duct section adjacent to the BRU (L_1 section in Figure A-1) if required to support inertia loads in the Y-axis. The Y-axis thermal motions have a minor influence on maximum bellows rotation since they are smaller rotations, and they are 90 deg to motions resulting from X and Z deflections. The combined equations for the turbine outlet duct with the Y-movements causing a rotation, θ_y are

$$\theta_A = \sqrt{(\Delta\theta)^2 + \theta^2_y}$$

$$\theta_B = \sqrt{(-\Delta\theta_1 + \Delta\theta_2)^2 + \theta^2_y}$$

$$\theta_c = \Delta\theta_1$$

A summary of the design conditions for each of the three bellows is provided in Table A-2. Material properties and the design criteria for pressure containment are based on AiResearch Report 69-5938. For the Hastelloy X bellows, calculations were required to determine which of the operating conditions would be most severe. The most severe pressure conditions occur at 65 psi and 1187°F for 50,000-hr life whereas maximum thermal stresses, limited by 1.5 times the material yield strength, are determined for the 1241°F turbine outlet temperature. The criterion that combined pressure and thermal stresses be less than twice the material yield strength is shown for the Hastelloy X bellows but does not affect the design since maximum pressure and thermal stresses at 1187°F are 12,000 and 59,000 psi, respectively, when the separate conditions are satisfied. The 347 steel units are governed by the maximum operating pressures of 222 and 200 psi at shutdown and the estimated maximum operating temperature of 440°F resulting from soak conditions after 1241°F turbine outlet operations. Design (minimum) buckling pressure is based on the maximum operating pressure times a safety factor of 3. Allowable bending stresses are listed in Table A-2, since in bellows design they are more critical than tensile stresses. BRU

TABLE A-1

BELLOWS MOVEMENT SUMMARY

Pipe System Section	Thermal Movements					Material	Bellows Rotation		
	Design Condition	Bellows Location	Relative Thermal Movement, in.				Bellows	Inside Diameter, in.	Angle, RAD
			ΔX	ΔY	ΔZ				
Recuperator LP inlet (turbine outlet)	1241°F turbine outlet operations	A	-0.282	-0.038	0.100	Hastelloy X	A	6.0	0.045
							B	6.0	0.064
							C	6.0	-0.019
Recuperator HP inlet (compressor outlet)	440°F soak after 1241°F turbine outlet operations	D	-0.087	-0.011	0.046	347 steel	D	3.5	0.030
							E	3.5	0.046
							F	3.5	-0.016
Heat sink LP outlet (compressor inlet)	440°F soak after 1241°F turbine outlet operations	G	-0.080	-0.026	0.052	347 steel	G	4.0	-0.007
							H	4.0	-0.015
							I	3.5	0.010

NOTE:

1. The Z-axis is parallel to the BRU axis of rotation, the X-axis is parallel to duct sections perpendicular to the BRU axis and parallel to ducts connecting the BRU and heat exchangers, and the Y-axis is mutually perpendicular to the other two axes.
2. Thermal movement reference temperature is 70°F. i.e., deflections are zero at 70°F.

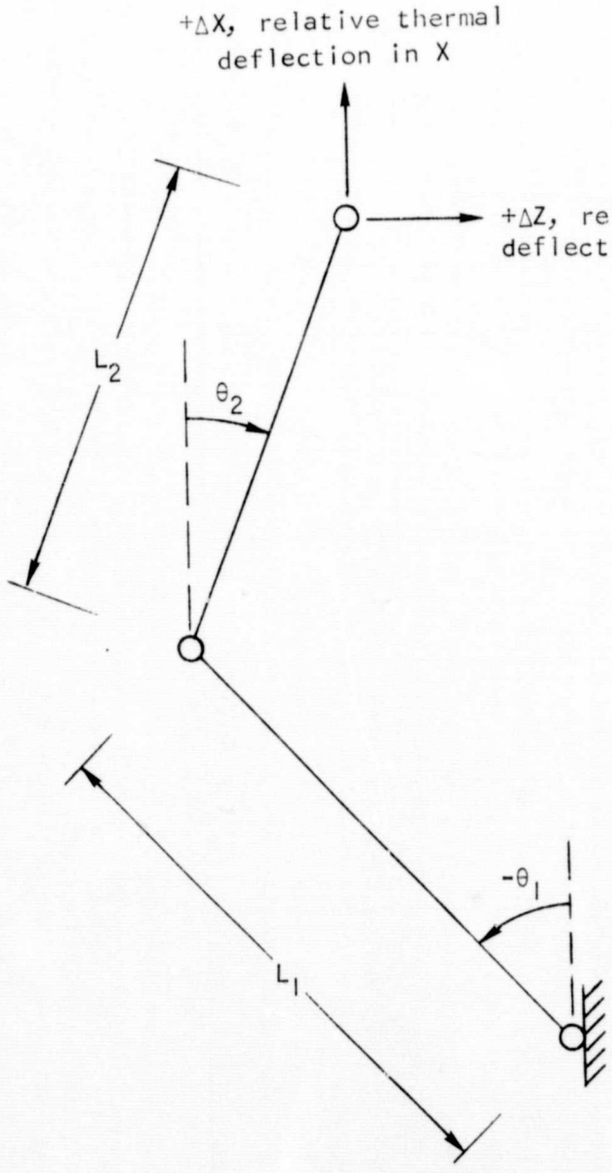

$$\Delta\theta_1 = \frac{\Delta X \cos \theta_2 + \Delta Z \sin \theta_2}{L_1 \sin (-\theta_1 + \theta_2)}$$

$$\Delta\theta_2 = \frac{-\Delta X \cos \theta_1 - \Delta Z \sin \theta_1}{L_2 \sin (-\theta_1 + \theta_2)}$$

Figure A-1. General Geometrical Motions of Three-Link Bellows Systems in the X-Z Plane

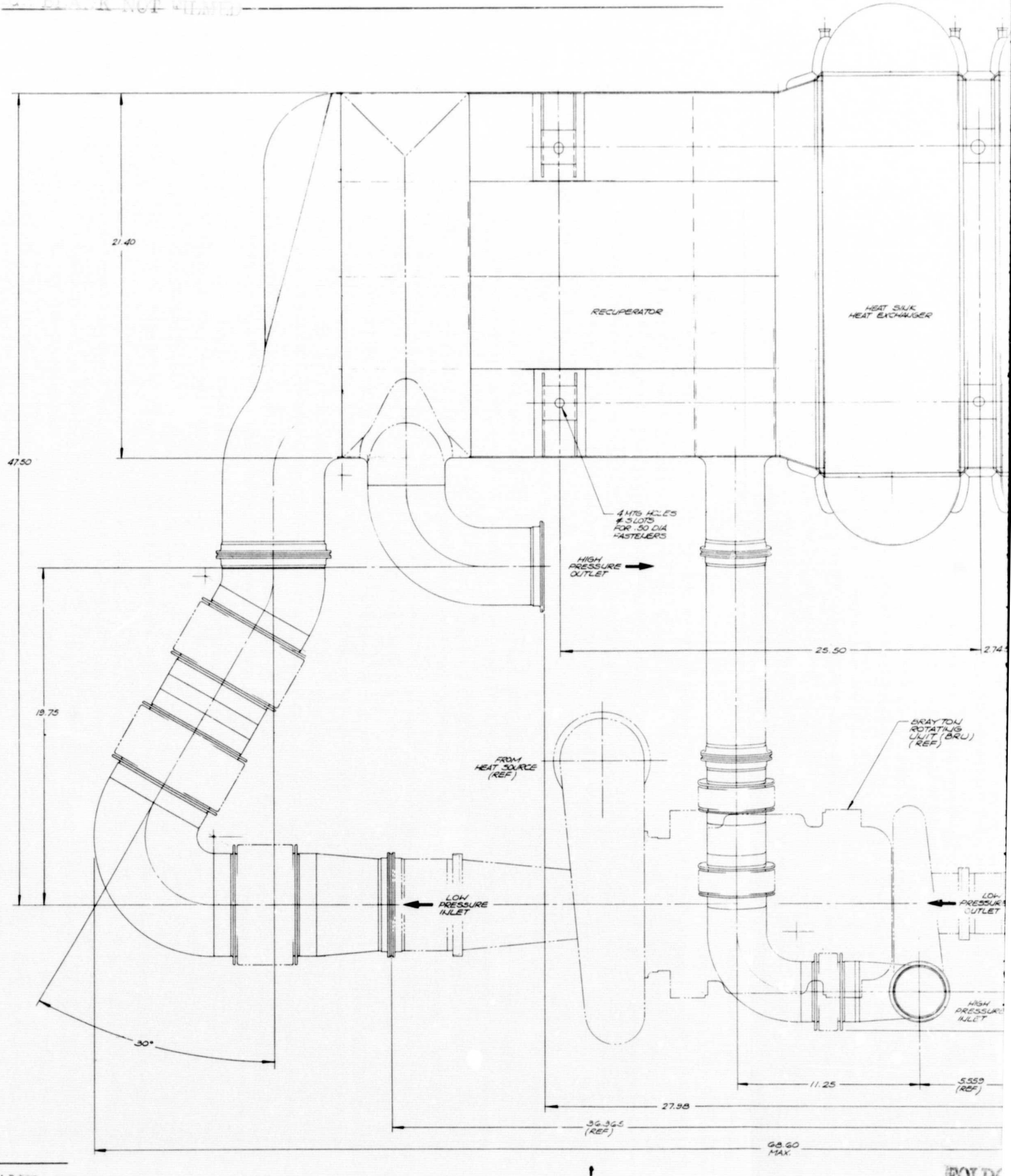

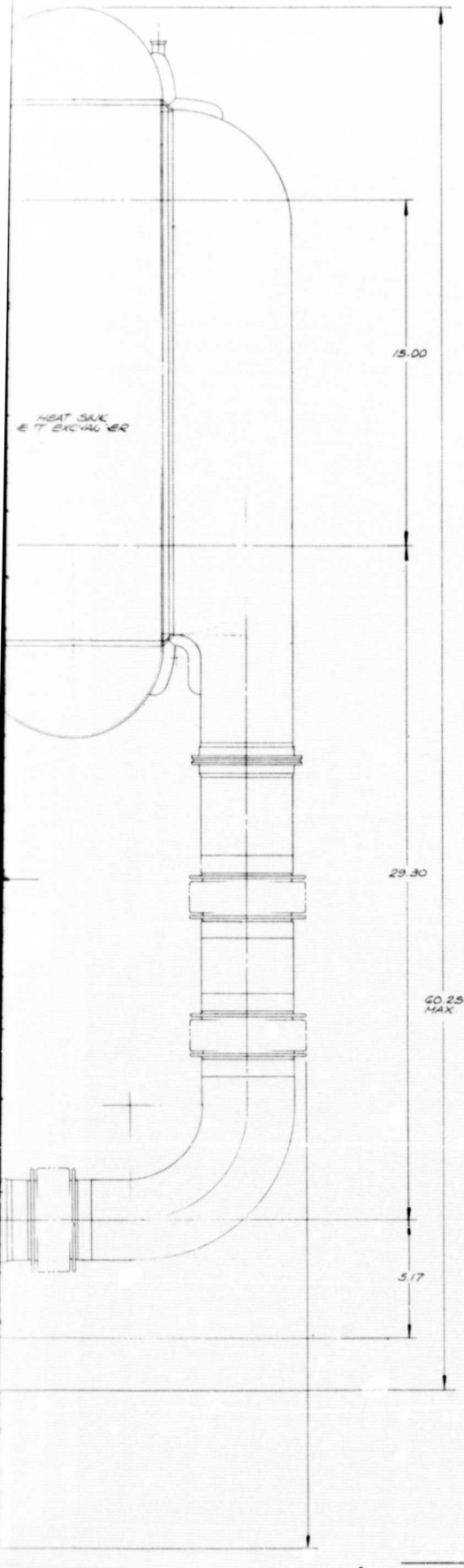

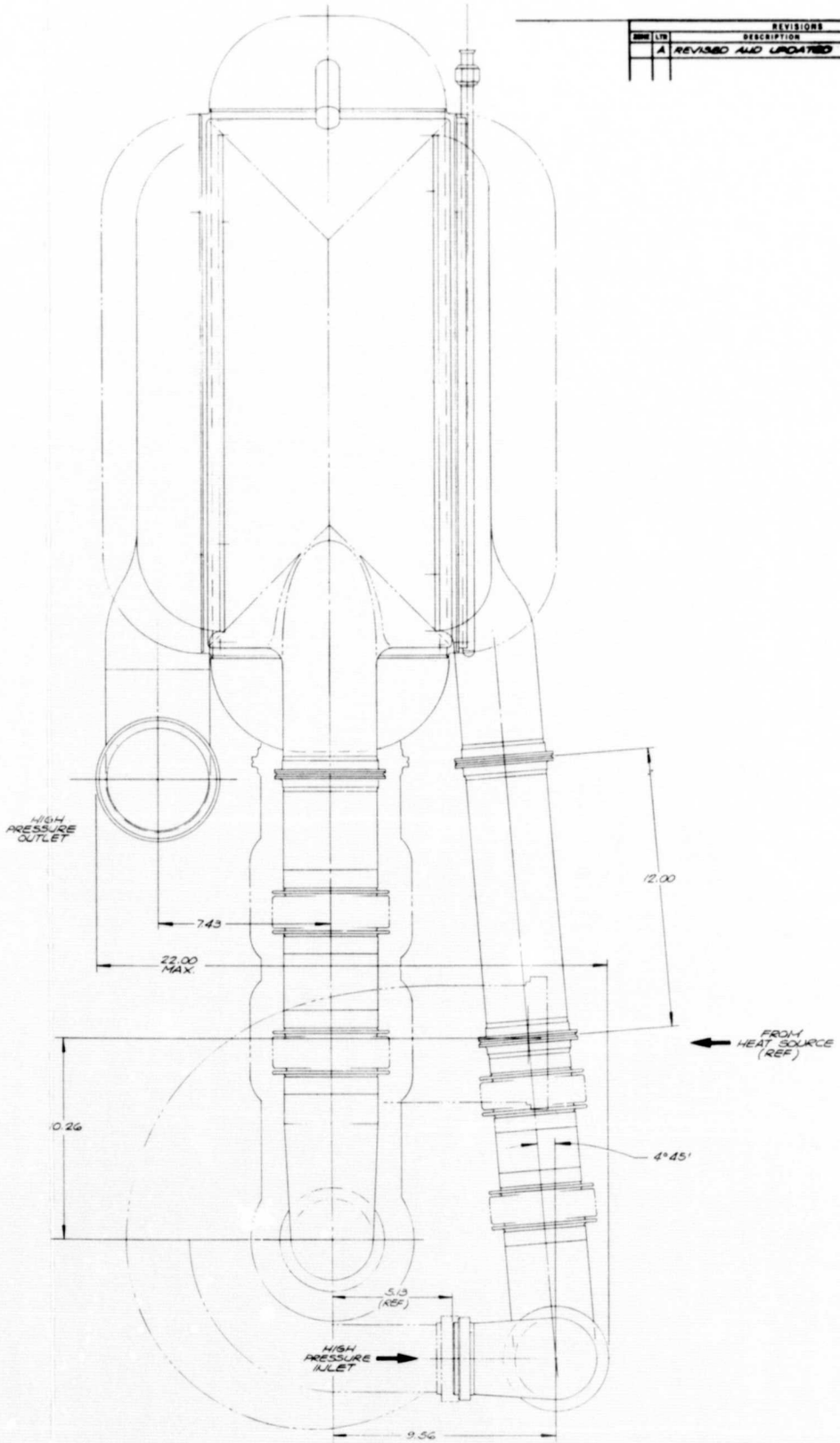

REVISIONS

ZONE	LTR	DESCRIPTION	DATE	APPROVED
	A	REVISED AND UPDATED	2-6-70	

PROPRIETARY NOTICE

THIS LAYOUT DRAWING EMBODIES A PROPRIETARY DESIGN OWNED BY THE GARRETT CORPORATION, AND IS SUBMITTED UNDER A CONFIDENTIAL RELATIONSHIP EXCEPT FOR USES EXPRESSLY GRANTED IN WRITING. ALL RIGHTS ARE RESERVED BY THE GARRETT CORPORATION. THIS DRAWING SHALL BE RETURNED WHEN THE NEED FOR IT HAS BEEN CONCLUDED.

SIGNATURES	DATES	DATE STARTED	WITNESSED BY
DRAWN			
TECH		DATE COMPLETED	WITNESSED BY
ENGR			
ENGR		WORK ORDER NO.	
APPD			
FEATURES			

AIRESEARCH MANUFACTURING COMPANY
A DIVISION OF THE GARRETT CORPORATION
LOS ANGELES, CALIFORNIA

LAYOUT

HEAT EXCHANGER, BRAYTON CYCLE

SIZE	CODE IDENT NO.	DWG NO.
	70210	SK 51738

SCALE 1/2 WT SHEET 1 OF 1

T FRAME

NOTES:

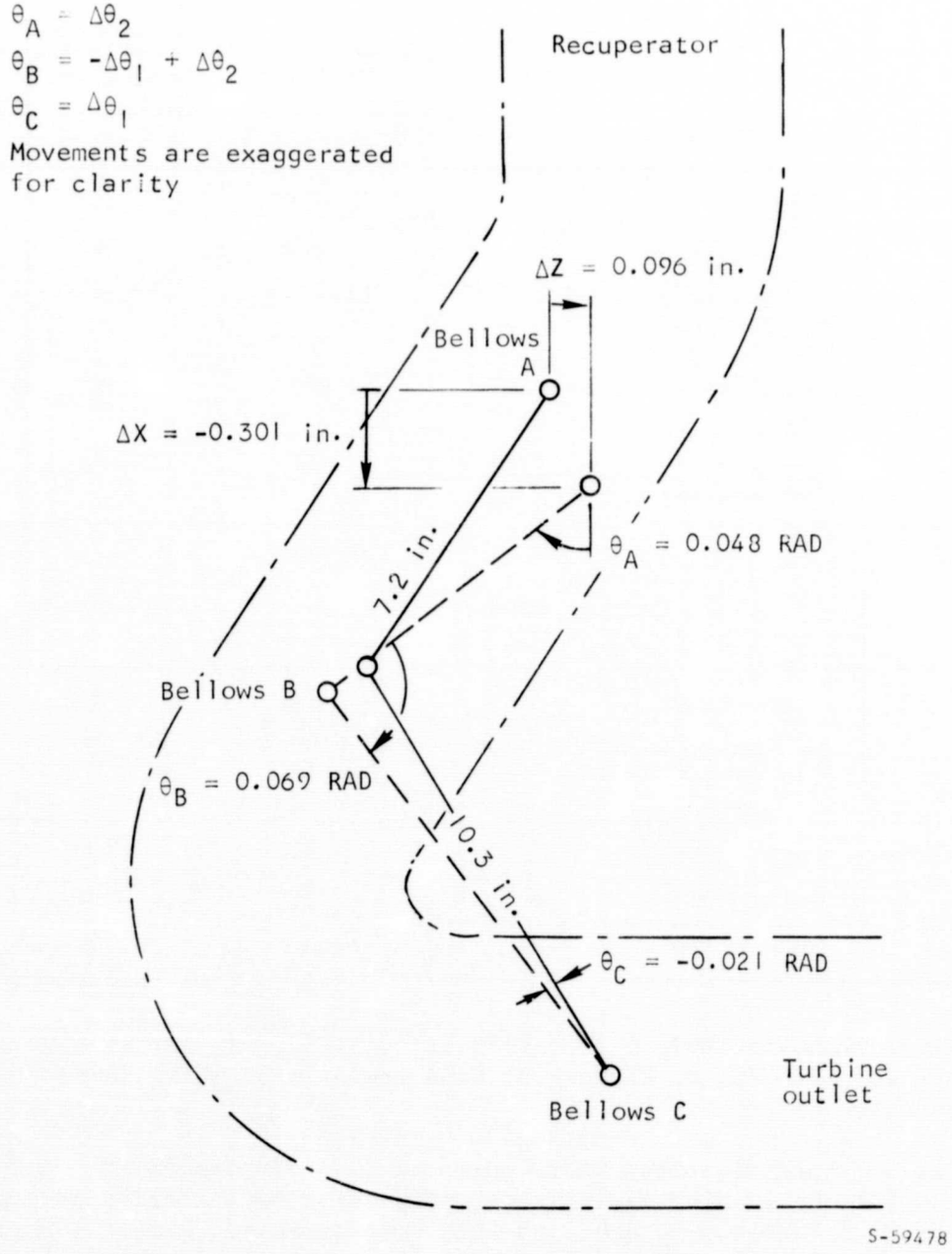

Figure A-2. Turbine Outlet Duct Movements in the X-Z Plane Based on SK 51738 for 1241°F Operating Conditions

TABLE A-2

BELLOWS DESIGN CONDITIONS

	Design Conditions	Pipe Section		
		Turbine Outlet, Hastelloy X	Compressor Outlet, 347 Steel	Compressor Inlet, 347 Steel
Pressure	Temperature, °F	1,187	440	440
	Pressure, psi	65	222	200
	Allowable bending stress, psi	12,000	32,500	32,500
	Buckling temperature, °F	800	440	440
	Buckling pressure, psi (safety factor of 3)	600	666	600
Thermal	Temperature, °F	1,241	440	440
	Allowable thermal bending stress, psi	59,000	65,000	65,000
Combined pressure and thermal	Temperature, °F	1,187	440	440
	Allowable combined bending stress, psi	79,000	65,000	65,000
BRU flange load limitations	Shear, lb	150	300	300
	Axial, lb	150	200	200
	Moment, in.-lb	1,000	2,000	2,000

load limitations in Table A-2 are listed in NASA Lewis letter 5221 of February 20, 1970 (G. N. Kaykaty of NASA Lewis to E. W. Gellersen of AiResearch).

Bellows specifications based on the data in Tables A-1 and A-2 are provided for the turbine outlet duct, compressor outlet duct, and compressor inlet duct in Tables A-3, A-4, and A-5, respectively. Required rotations noted in the specifications include a 1.25 factor on the maximum rotations for each bellows type in Table A-1. The limits on moment to rotate the bellows may exceed the allowable moments in Table A-2 since the maximum bellows rotation does not occur on the bellows adjacent to the BRU. Allowable stresses are tabulated for the turbine outlet duct (Table A-3); however, they are noted for 1290°F rather than making the more accurate distinction in Table A-2.

TABLE A-3

TURBINE OUTLET DUCT (6-IN.-DIA BELLOWS)

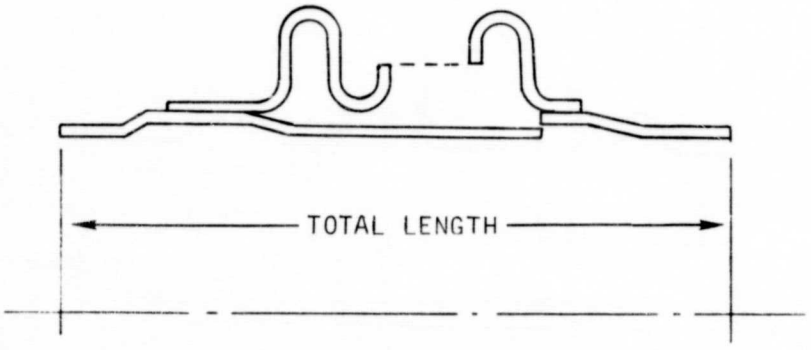

MATERIAL	= HASTELLOY X
BELLOWS TO BE AT LEAST 2-PLY CONSTRUCTION	
BELLOWS MUST HAVE INTERNAL LINK TO REACT INTERNAL PRESSURE FORCE	
MATCHING DUCT DIAMETER	= 6.00 IN. OD X 0.035 IN.-WALL
TOTAL LENGTH	= 6.00 IN. MAXIMUM, ACTIVE LENGTH = 4.0 IN.
LINER REQUIRED, ID	= 5.70 IN.
OPERATING TEMPERATURE	= 1290°F
DESIGN LIFE	= 5 YEARS
WORKING PRESSURE	= 65 PSI AT 1290°F, 200 PSI AT 800°F
REQUIRED ROTATION	= 0.072 RADIANS
MOMENT TO ROTATE BELLOWS (USE HIGH TEMPERATURE MODULUS OF ELASTICITY)	≤ 1000 IN.-LB
ALLOWABLE STRESSES AT 1290°F	
MAXIMUM HOOP STRESS DUE TO INTERNAL PRESSURE	= 8000 PSI
MAXIMUM PRESSURE-BENDING STRESS	= 12,000 PSI
THERMAL STRESS DUE TO APPLIED ROTATION	≤ 59,000 PSI
HELIUM LEAKAGE	= 200 PSI TO BE LESS THAN 1×10^{-8} ATMOSPHERIC CC/SEC (ROOM TEMPERATURE)
REFERENCE	= AIRESEARCH SOURCE CONTROL DRAWING 185692

TABLE A-4

COMPRESSOR OUTLET DUCT (3-1/2-IN.-DIA BELLOWS)

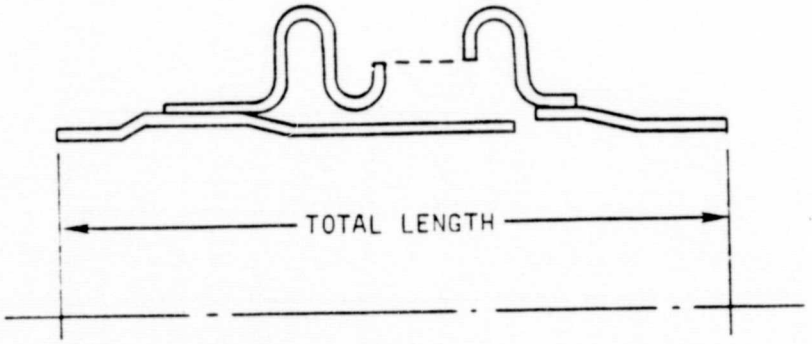

MATERIAL	= TYPE 347 STAINLESS STEEL
BELLOWS TO BE AT LEAST 2-PLY CONSTRUCTION	
BELLOWS MUST HAVE INTERNAL LINK TO REACT INTERNAL PRESSURE FORCE	
MATCHING DUCT SIZE	= 3.50 IN. OD X 0.035-IN. WALL
TOTAL LENGTH	= 4.00 IN. MAXIMUM" ACTIVE LENGTH = 2.50 IN. MAXIMUM
LINER REQUIRED, ID	= 3.30 IN.
OPERATING TEMPERATURE	= 440°F
WORKING PRESSURE	= 222 PSI
REQUIRED ROTATION	= 0.056 RADIANS
MOMENT-TO-ROTATE BELLOWS	$\leq$ 2000 IN.-LB
CYCLE LIFE	$\geq$ 1000
PROOF PRESSURE	= 333 PSI
BURST PRESSURE	= 555 PSI
HELIUM LEAKAGE AT	= 222 PSI TO BE LESS THAN 1×10^{-8} ATMOSPHERIC CC/SEC
REFERENCE	= AIRESEARCH SOURCE CONTROL DRAWING 185694

TABLE A-5

COMPRESSOR INLET DUCT (4-IN.-DIA BELLOWS)

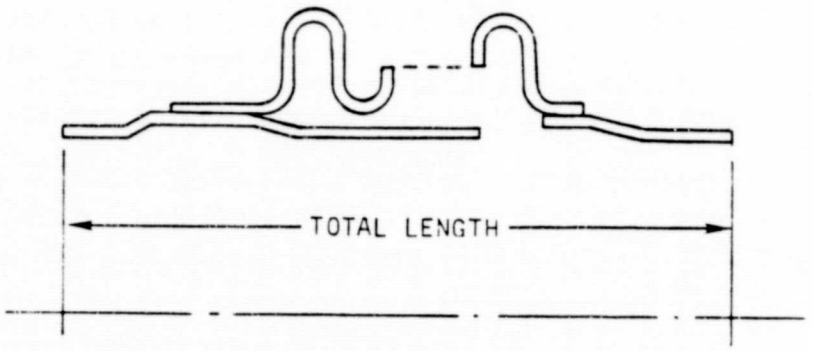

MATERIAL	= TYPE 347 STAINLESS STEEL
BELLOWS MUST BE AT LEAST 2-PLY CONSTRUCTION	
BELLOWS MUST HAVE INTERNAL LINK TO REACT INTERNAL PRESSURE FORCE	
MATCHING DUCT SIZE	= 4.00 IN. OD X 0.035-IN. WALL
TOTAL LENGTH	= 4.00 IN. MAXIMUM, ACTIVE LENGTH = 2.5 IN.
LINER REQUIRED, ID	= 3.75 IN.
OPERATING TEMPERATURE	= 440°F
REQUIRED ROTATION	= 0.019 RADIANS
MOMENT-TO-ROTATE BELLOWS	$\leq$ 2000 LB-IN.
CYCLE LIFE	$\geq$ 1000
WORKING PRESSURE	= 200 PSI
PROOF PRESSURE	= 300 PSI
BURST PRESSURE	= 500 PSI
HELIUM LEAKAGE AT	= 200 PSI TO BE LESS THAN 1×10^{-8} ATMOSPHERIC CC/SEC
REFERENCE	= AIRESEARCH SOURCE CONTROL DRAWING 185693

After presentation of the package layout drawing SK 51738 at the coordination meeting, it was requested that alternate packages be investigated that would (1) simplify the low-pressure inlet duct, and (2) make the overall package more compact. The following discussion presents some alternates considered; however, the maximum benefit achieved is removal of the turning vanes and multiple bends in the low-pressure inlet duct. Use of a right-angle turn rather than the multiple bends would require the following alterations to the package: (1) elimination of the turbine outlet spool piece, and (2) incorporation of the turbine outlet duct transition into the liner of the bellows adjacent to the turbine. With these two changes, approximately a -45-deg angle occurs for the link between bellows B and C (-31.5 deg in SK 51738) and a 0-deg angle is obtained between bellows A and B (33.6 deg in SK 51738). With L_1 = 9.9 in. and L_2 = 11.6 in., all conditions are satisfied with the bellows design in Table A-6, and the distance between the BRU and heat exchangers is reduced by about 2 in.

A further reduction in package size could be achieved with the use of a duct and bellows material with a lower coefficient of thermal expansion and/or a higher strength. Candidate materials with lower thermal expansion coefficients than Hastelloy X are Hastelloy C and Inconel 625, with reduction in movement of about 9 and 4 percent, respectively. Use of Hastelloy C in place of Hastelloy X in the 90-deg turn, using only the change in thermal expansion coefficient, results in a required L_2 of 10.1 in., which is 1.5 in. shorter than in SK 51737. A reduction in the package also would be realized if the pressure stress allowable could be increased from the 12,000-psi value for Hastelloy X. Creep data was obtained for Hastelloy C, Hastelloy C276 (modified Hastelloy C), Inconel 625, and Haynes 188 that indicated all four alloys were stronger than Hastelloy X (up to about 25 percent with Hastelloy C and Inconel 625). The 1-percent creep data available for the alternate alloys is inadequate for a valid comparison for the 50,000-hr life, however, because no extended duration test data has been obtained. (Extended duration in this case is about 1000 hr in the case of Hastelloy X.) The effect on the package for a 25-percent increase in allowable stress can be estimated with no change in thermal expansion or yield strength properties (both of which also are favorably changed). A bellows with a convolution height of 0.26 in. can be used with the same thickness (0.01 in. per ply). The minimum thermal stress will be a 216,000-psi/unit deflection with a maximum of 16 convolutes allowed to satisfy buckling requirements. A length L_2 of 9.6 in. can be used, which is a 2-in reduction from the SK 51738 package. While these reductions would be desirable, a material change recommendation is not warranted due to the uncertainty in material strength.

Structural Analysis

The bellows design stress criteria incorporated improved creep damage estimates based on recent work by Spera on combined creep and fatigue damage for the elevated temperature bellows design. The design criteria considered fatigue damage based on current prediction methods that relate life to plastic strain range; however, creep damage was indirectly considered by avoiding repeating cycles with creep relaxation and, hence, the associated accumulated

TABLE A-6

HASTELLOY X BELLOWS DESIGN
FOR TURBINE OUTLET DUCT

Item	Design Factors		Allowable or Required
Bellows geometry	Inside diameter, in.	5.9	--
	Convolute height, in.	0.23	--
	Number of convolutes	19	--
	Active length, in.	3.3	--
	Number of ply	3	2
	Thickness per ply, in.	0.01	--
Bellows properties	Axial spring rate, lb/in.	1,520	--
	Rotational spring rate, lb/in.	31,600	--
	Thermal stress per unit deflection, psi/in.	237,000	--
	Buckling pressure, psi (safety factor of 3)	617	600
Maximum bellows stresses	Pressure, psi (bending, 1187°F)	12,000	12,000
	Thermal, psi (bending, 1241°F)	50,000	59,000
	Combined pressure and thermal, psi (bending, 1187°F)	59,000	79,000
Turbine flange loads (X-Z plane)	Shear, lb	6	150
	Axial, lb	55	150
	Moment, lb-in.	600	1,000

creep damage. Hastelloy X creep behavior at 1340°F was estimated, and the results provided a modified design criteria for the 100-cycle and 50,000-hr life requirements.

Operating cycles that include damage during load application and sustained strains were considered. These sustained strains arise from pressure loads and long duration (steady-state) deflection stresses set up by temperature differences between components. The calculations were based on Hastelloy X creep properties at 1340°F and tensile properties at 1240°F. The maximum operating temperature is 1241°F; however, as discussed in Report 68-4215, creep properties include a 100°F overtemperature capability.

The calculations showed that damage during the load cycle was negligible, but that damage due to repeated sustained strains that relax out would generally be unacceptable. Deflection stresses or combined pressure and deflection stresses would relax to approximately the creep rupture stress for 50,000 hr. Since repeated relaxation damage is unacceptable, an operating cycle that results in a repeating stress equal to the maximum pressure stress must be achieved. This can be accomplished by limiting either thermal stresses or combined pressure and thermal stresses to the sum of material yield plus the allowable pressure stress for 50,000 hr as illustrated in Figure A-3. Relaxation occurs on only the first load cycle and the predicted 1- to 2-percent life reduction is not of sufficient magnitude to warrant further modification of the pressure stress criteria.

The resulting design criteria for direct stresses at elevated temperatures where creep is a factor are:

Pressure:

$$\sigma_{all}\Big|_p = \min \begin{cases} \sigma_y/1.5 \\ \sigma_u/2.5 \\ \sigma_{1\% \text{ in } 50{,}000 \text{ hr}}/1.2 \\ \sigma_{50{,}000 \text{ hr rupture}}/1.5 \end{cases}$$

Thermal:

$$\sigma_{all}\Big|_{thermal} = \sigma_y + \sigma_{all}\Big|_p$$

Combined pressure and thermal:

$$\sigma_{all}\Big|_c = \sigma_{all}\Big|_{thermal}$$

An allowance of 100°F is provided for overtemperature capability and when bending stresses are considered, the above stresses are multiplied by a factor of 1.5 (see discussion in report 68-4215).

1241°F HASTELLOY X PROPERTIES

σ_y = 39,100 PSI

E = 22.1 X 10^6 PSI

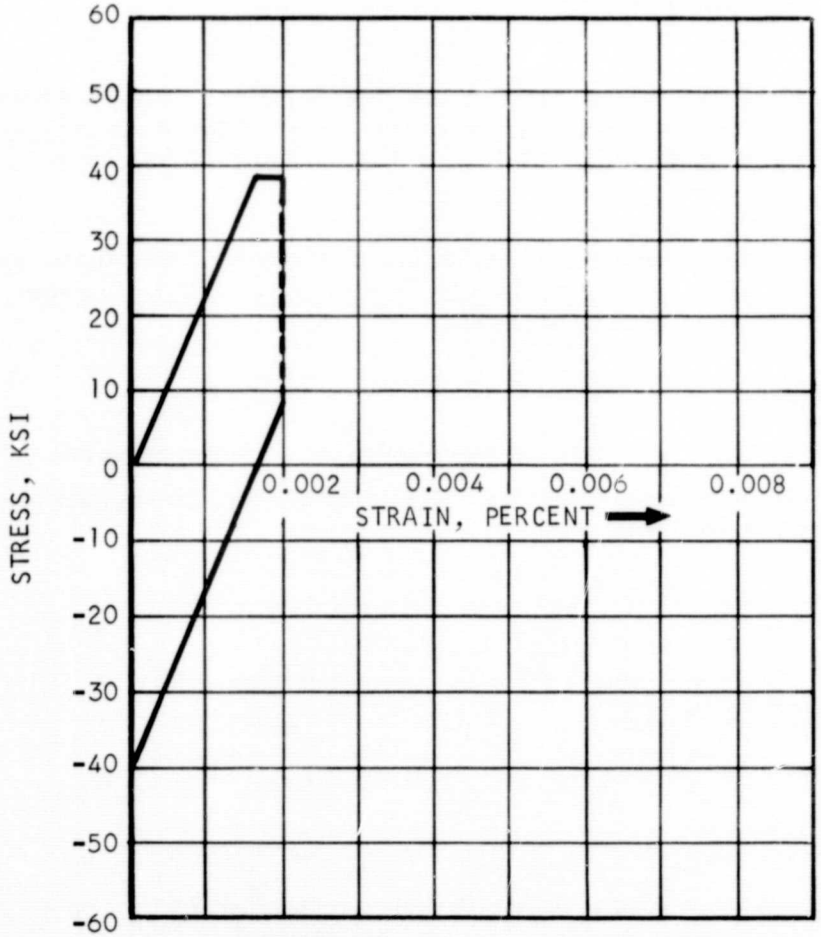

0 TO 1 FIRST LOAD CYCLE, COMBINED PRESSURE AND THERMAL STRESS

1 TO 2 STRESS RELAXATION TO PRESSURE STRESS LEVEL

2 TO 3 FIRST UNLOAD CYCLE AND SUBSEQUENT REPEATING CYCLE WITH COMBINED LOADING

Figure A-3. Maximum Stress Level to Avoid Repeating Thermal Stress Relaxation (Ideal Elastic-Plastic Stress-Strain Behavior)

At room temperatures, where creep is not a factor, the allowable direct pressure stresses are:

$$\sigma_{all}\Big|_p = \min \begin{cases} \sigma_y/1.5 \\ \sigma_u/2.5 \end{cases}$$

and a 1.5 multiple of the above is allowed for bending. For deflection stresses caused by thermal differentials, an acceptable plastic strain range for a computed life of 400 cycles is required to satisfy the 100-cycle design life.

The above room temperature criteria are unchanged from those previously used. The modified elevated temperature criteria result in changes in the allowables that involve thermal stresses.

Calculation Procedure

Material creep rate, $\dot{\epsilon}$, and rupture life, t_r, behavior were related to stress by power law relations using available engineering property data for Hastelloy X. These relations are:

$$\dot{\epsilon} = F\,\sigma^{\ell} \qquad \text{(A-1)}$$

$$t_r = A\,\sigma^{-\ell} \qquad \text{(A-2)}$$

The damage/cycle due to relaxation at constant strain is

$$\Delta\Phi = \sigma_r/AFE \qquad \text{(A-3)}$$

where σ_r is the amount of stress relaxation computed by equation (A-1). The damage per cycle is obtained from equation (A-2), and the Robinson-Tiara expression

$$\Delta\Phi = \int_o^t \frac{dt}{t_r}$$

The product, AF, is about 0.11 and the elastic modulus is 21,500,000 psi, so for a relaxation from a yield of 39 ksi to a pressure stress of 8 ksi (direct stresses, equivalent in bending, 58 ksi and 12 ksi), the damage is 0.013, or 1.3 percent.

Conclusions

The procurement specifications for the four bellows configurations are shown in Table A-7. The data initially was supplied to several vendors and responses were received from three companies. The proposed bellows designs were analyzed using the AiResearch Bellows Stress Analysis Program (X0310); pertinent results are presented in Table A-8. As shown in the table, all bellows were inadequate for pressure containment and most were insufficient for squirm buckling. It should be noted that the stress limitation prescribed for the 3-1/2-in. and the 4-in. bellows was 27,600 psi in the procurement specifications. It was determined that the portion of the bellows exposed to maximum stress was extremely localized and that the Type 347 stainless steel used for these convolutes will undergo cyclic strain-hardening during usage. Accordingly, the allowable stress due to pressure effects was raised to 32,500 psi.

After the first three vendor designs had been reviewed and analyzed with unsatisfactory results, two other companies, the Metal Bellows Corporation and Aeroquip Corporation, were solicited. Neither was among the three vendors indicated in Table A-8. AiResearch has had good success with the products of both companies in the past, and Aeroquip supplied the bellows for the original BHXU Engine B system. At the time of the first procurement effort, Metal Bellows Corporation declined to bid due to a current excess of commitments. Aeroquip inadvertently had submitted only a partial response to the procurement and was declared nonresponsive. Both companies responded promptly with complete designs on this second effort.

Table A-9 presents the results of AiResearch analyses of all the Aeroquip Corporation and Metal Bellows Corporation bellows. All were found to be satisfactory for pressure stresses, thermal stresses, combined pressure plus thermal stresses, and squirm buckling capability; in fact, the computed stresses for the 6-in., 4-in., and 3-1/2-in. bellows are within 10 percent of each other. It was concluded that the designs from both vendors were structurally acceptable for this application.

Aeroquip Corporation was selected as the bellows vendor by competitive bidding. The bellows assemblies received for the BHXU-A system are shown in Figure A-4.

TABLE A-7

BHXU-ALTERNATE BELLOWS PROCUREMENT SPECIFICATIONS

	6-in.-dia Bellows	6-in.-dia Bellows with Reducing Liner	4-in.-dia Bellows	3-1/2-in. dia Bellows
Bellows and end collar material	Hastelloy X (AMS 5536)	Hastelloy X (AMS 5536)	CRES Type 347 (MIL-S-6721)	CRES Type 347 (MIL-S-6721)
Liner, struts, and link material	As required by manufacturer	As required by manufacturer	As required by manufacturer	As required by manufacturer
Bellows construction	2-ply (minimum)	2-ply (minimum)	2-ply (minimum)	2-ply (minimum)
Internal sleeve/link assembly to react internal pressure force	Required	Required	Required	Required
Size (preferable)				
Part full length	Not to exceed 6 in.	Not to exceed 6 in.	Not to exceed 4 in.	Not to exceed 4 in.
Total active bellows length	Not to exceed 4 in.	Not to exceed 4 in.	Not to exceed 2.5 in.	Not to exceed 2.5 in.
Liner internal diameter(s), in.	5.70 min.	5.15 min. on small end; 5.70 min. on large end	3.75 min.	3.30 min.
Collar size, wall thickness, in.	6.00 OD by 0.35	5.56 OD by 0.125 on small end; 6.00 OD by 0.050 on large end	4.00 OD by 0.035	3.50 OD by 0.35
Strut alignment, percent of true position in all planes	±3 deg	±3 deg	±3 deg	±3 deg
Link alignment, percent of true position in all planes	±1 deg	±1 deg	±1 deg	±1 deg
Design conditions				
Maximum pressure stress	12,000 psi at 65 psi internal pressure	12,000 psi at 65 psi internal pressure	27,600 psi at 200 psi internal pressure	27,600 psi at 222 psi internal pressure
Minimum buckling pressure	600 psi at 800°F	600 psi at 800°F	600 psi at 440°F	666 psi at 440°F
Minimum cycling life	-	-	400 cycles for 0.035 rad rotation	400 cycles for 0.020 rad rotation
Maximum thermal stress	59,000 psi at 0.072 rad rotation	59,000 psi at 0.072 rad rotation	-	-
Bellows spring rate	Minimize	Minimize	Minimize	Minimize
Helium leakage	Less than 1×10^{-8} atm cc/sec at 200 psi room temp	Less than 1×10^{-8} atm cc/sec at 200 psi room temp	Less than 1×10^{-8} atm cc at 200 psi room temp	Less than 1×10^{-8} atm cc/sec at 222 psi room temp
Source control drawing	185692	185845	185693	185694

TABLE A-8

VENDOR BELLOWS COMPARISON, FIRST DESIGN ANALYSIS

Bellows Size and Material	Vendor No.	Inside Dia. In.	Convolute Height In.	No. of Convolutes	Active Length In.	No. of Plies	Thickness Each Ply In.	Axial Spring Rate lb/in.	Deflection Stress Per in. Ksi/In.	Pressure Stress Ksi*	Thermal Stress Ksi**	Pressure and Thermal Stress Ksi***	Squirm Buckling Pressure psi
	AiResearch Allowable					2 (Min)				12.0	59.0	59.0	600 (Min)
6.0 in. Dia. Hastelloy X	1	6.0	0.50	16	4.0	2	0.016	794	114.3	15.9	23.8	34.8	348
	2	6.0	0.45	20	4.0	3	0.10	327	73.4	20.2	15.3	32.5	143
	3	6.0	0.50	11	3.98	2	0.012	468	105.8	20.1	22.0	40.4	206
	AiResearch Allowable					2 (Min)				32.5	65.0	65.0	600 (Min)
4.0 in. Dia. 347 CRES	1	4.0	0.50	12	2.50	2	0.016	864	177.0	39.0	6.0	44.1	542
	2	4.0	0.375	14	2.50	3	0.010	621	172.0	41.7	5.8	45.4	390
	3	4.4	0.36	9	2.34	2	0.012	1174	302.5	41.1	10.2	45.2	786
	AiResearch Allowable					2 (Min)				32.5	65.0	65.0	666 (Min)
3-1/2 in. Dia. 347 CRES	1	3.5	0.50	12	2.50	2	0.016	772	176.1	42.3	16.2	58.5	485
	2	3.5	0.44	14	2.50	2	0.010	240	130.2	91.3	12.0	103.3	151
	3	3.5	0.32	10	2.31	2	0.012	1340	355.0	39.0	32.7	59.4	910

*Based on Internal Pressure, of:

6 in. - 65 psi
4 in. - 200 psi
3-1/2 in. - 222 psi

**Based on Axial Defl. of:

6 in. - 0.208 in. at 1241°F
4 in. - 0.0338 in. at 440°F
3-1/2 in. - 0.092 in. at 440°F

***Based on Axial Defl. of:

6 in. - 0.198 in. at 1187°F
4 in. - 0.0338 in. at 440°F
3-1/2 in. - 0.092 in. at 440°F

TABLE A-9

VENDOR BELLOWS COMPARISON, SECOND DESIGN ANALYSIS

Bellows Size and Material	Vendor and Dwg. No.	Inside Dia. in.	Convolute Height in.	No. of Convolutes	Active Length in.	No. of Plies	Thickness Each Ply in.	Axial Spring Rate lb/in.	Deflection Stress Per In. Ksi/in.	Pressure Stress Ksi*	Thermal Stress Ksi**	Pressure and Thermal Stress Ksi***	Squirm Buckling Pressure psi
	AiResearch Allowable					2 (Min)				12.0	59.0	59.0	600 (Min)
6.0 in. Dia. Hastelloy X	Metal Bellows Corp. 65836	6.2	0.4	16	4.0	2	0.016	1540	183.0	9.2	38.1	45.5	605
	Aeroquip MDU L9495	6.16	0.42	16	3.0	2	0.016	1290	163.0	10.2	33.9	42.5	680
	AiResearch Allowable					2 (Min)				32.5	65.0	65.0	600 (Min)
4.0 in. Dia. 347 CRES	Metal Bellows Corp. 65837	4.2	0.4	10	2.5	2	0.016	1830	319.0	27.1	10.8	37.9	1170
	Aeroquip MDU 69496	4.38	0.31	13	2.25	2	0.012	1295	297.0	28.2	10.0	38.3	905
	AiResearch Allowable					2 (Min)				32.5	65.0	65.0	666 (Min)
3-1/2 in. Dia. 347 CRES	Metal Bellows Corp. 65838	3.7	0.4	10	2.5	2	0.016	1600	312.0	31.1	28.6	59.7	1050
	Aeroquip MDU 69497	3.88	0.31	13	2.25	2	0.012	1156	298.0	31.1	27.4	58.5	810

Figure A-4. Bellows Assemblies for the BHXU-Alternate System

APPENDIX B

SUMMARY OF THE METALLURGICAL EXAMINATION OF THE BHXU-ALTERNATE CORE MODULE

INTRODUCTION

The first recuperator core module was brazed with Palniro RE (2025°F) (1380K), to attach the seal plates to the ground header bars. A pressure test showed three areas of interpass leakage in the core at low pressure (10-20 psig). The three areas of leakage had interpass leakages of 2.0, 0.2, and 0.9 liters/min at a pressure of 20 psig. The total equivalent leakage (assuming sonic flow through the leak area) for a helium-xenon operating system would be a bypass leakage of 0.01 percent, which would not seriously degrade system performance; however, since the cause of the interpass leakage was unknown, the leakage rate could increase during long-term operation (50,000 hr) of the recuperator. The core module was sectioned to determine the cause of the leakage. A secondary examination was made of the braze joint quality and the effect of welding over brazing alloy.

INTERPASS LEAKAGE ANALYSIS

The core module was sectioned to determine the cause of the leakage. Figure B-1 illustrates a typical leak area just inside the offset fin in the high-pressure passage of the core. This type of leak was typical at both the inlet and outlet ends. Photomicrographs of the tube plate erosion are seen in Figure B-2. The photomicrographs show the silicon carbide (SiC) particle alloyed with the tube plate and the brazing alloy. An interpass leak area is visible adjacent to the SiC particle. Further testing with Hastelloy X coupons brazed with Palniro 1 and Palniro RE confirmed alloying of the gold and the silicon, which formed a chemically modified Palniro 1 brazing alloy that was aggressive and eroded the Hastelloy X tube sheet. Photomicrographs showed that the microstructure of the test coupons was the same as the sample taken from the core module. This also was substantiated by an electron microprobe analysis. This interaction between the gold braze alloy, Hastelloy X, and SiC was unobserved until the metallurgical analysis revealed the cause of the interpass leakage.

The samples submitted for microprobe analysis identified the elements present in the neighborhood of the particle. Spot scans illustrated that the major constituents were gold, palladium, nickel, iron, chromium, molybdenum, (originating from the Palniro 1 brazing alloy or the Hastelloy X material), silicon, and carbon. Radiographic images were made that showed the metallurgical phases present were a primary gold constituent in a gold-silicon eutectic (see Figures B-3, B-4, and B-5).

Discussion

The presence of silicon and carbon elements adjacent to the particle indicated that the foreign body was a piece of silicon carbide. This silicon carbide had reacted with the gold base brazing alloy to form a gold-silicon

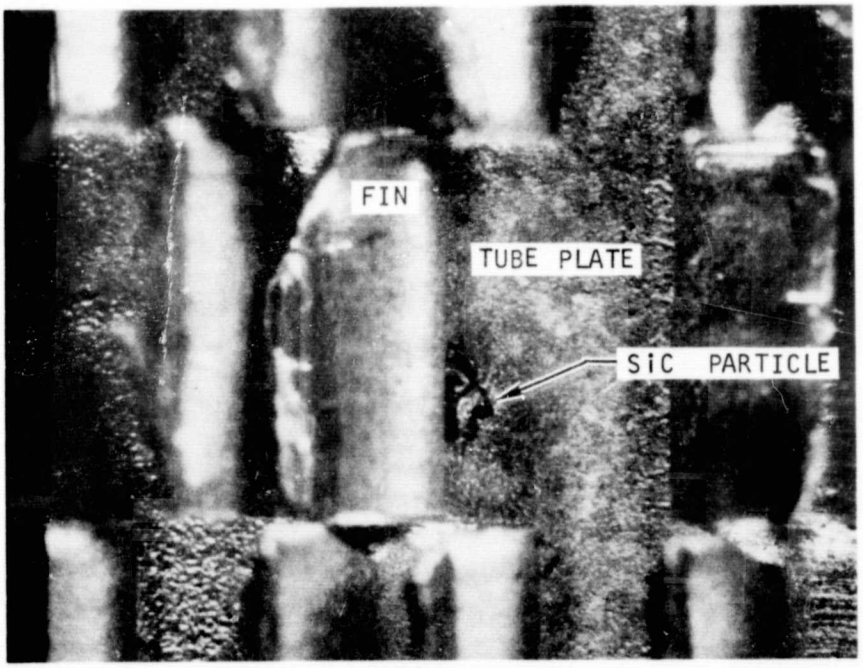

Magnification X16

a. Location: 9th High Pressure Passage

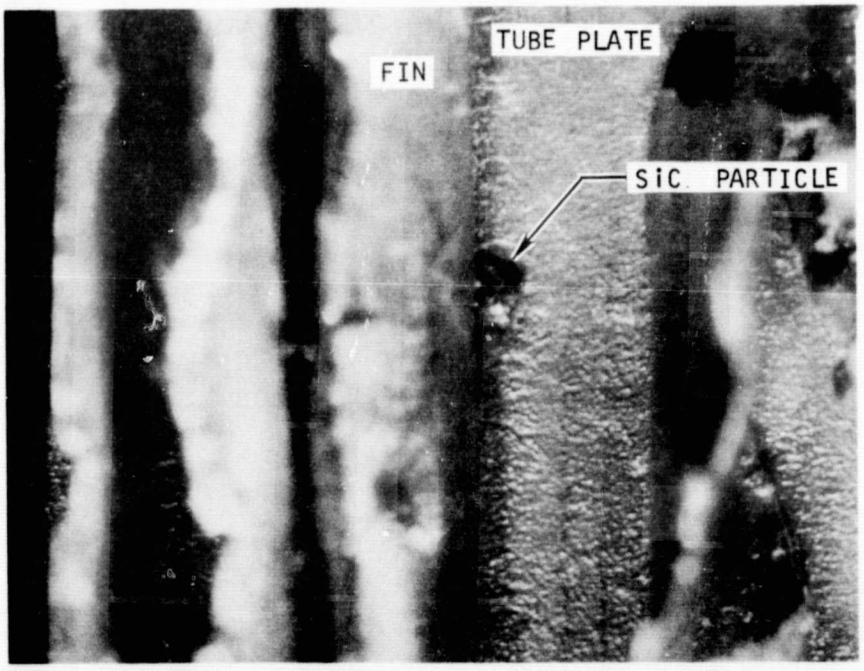

Magnification X16

b. Location: 10th High Pressure Passage

F-13973

Figure B-1. Particle Contamination Shown at Two Locations (Plan View of Tube Plate)

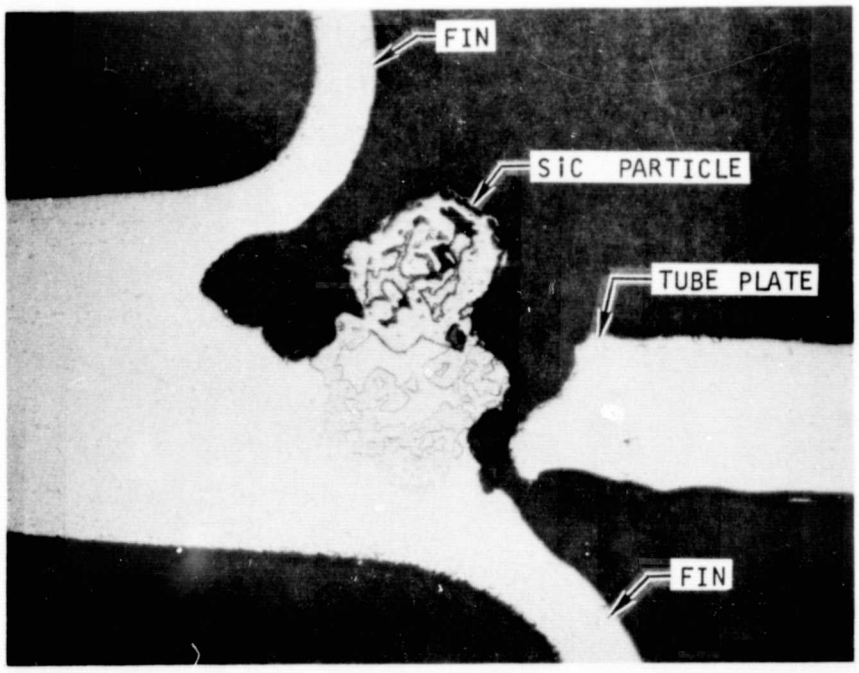

a. Overall View Magnification X100

b. Close-Up of Particle Magnification X180

F-13974

Figure B-2. Photomicrograph of Erosion Area

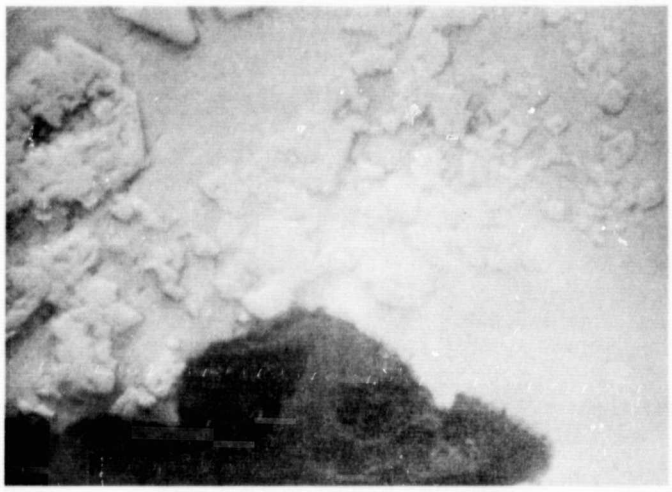

Figure B-3. X400

Photomicrograph Showing Area Examined by Microprobe Analysis

X400

Figure B-4.
X-Ray Image Showing Location of Silicon (White Spots)

X400

Figure B-5
X-Ray Image Showing Location of Gold (White Spots)

F-14198

eutectic, which has a melting point of 665°F (630 K). In turn, the eutectic alloy reacted with the Hastelloy X to cause severe erosion, resulting in complete penetration of the tube sheet.

The silicon carbide particles were introduced during grinding between the two brazing operations. Although the inlet and outlet orifices were masked to prevent ingress of foreign material, such a preventative measure did not prove to be effective.

Conclusions

Silicon carbide particles were responsible for causing the interpass leakage through the Hastelloy-X tube sheets. These particles were introduced into the passes during a grinding operation prior to step brazing with the Palniro RE brazing alloy.

The particles became trapped in the fin-tube sheet joint, and reacted with the Palniro 1 brazing alloy to form a low melting point gold-silicon eutectic. The eutectic in turn severely eroded the Hastelloy-X, resulting in complete penetration of the tube sheet.

The following recommendations are made:

(a) A more effective method of sealing the inlet and outlet orifices should be used so that the ingress of foreign particles is prevented.

(b) Methods other than grinding should be considered for removing the 0.040 in. (0.102 cm) of stock from the header bar.

Subsequent Fabrication Techniques

The header bar machining difficulties were resolved by using the same end mill machining techniques for the entire header bar face of the module that were used to machine the grinding wheel runout areas on core modules 1 and 2. The only difference in the two machining procedures was the use of a 0.75-in.- (1.9-cm) diameter end mill for the machining of the entire surface whereas 0.25-in.- (0.63-cm) diameter end mill was used for the machining of the grinding wheel runout areas.

The Anocut process also was investigated for machining the header bar face. The process attacked the braze alloy more aggressively than the Hastelloy X material and left salt deposits in the core matrix. These results made the process less attractive than end milling and it was eliminated from further consideration.

Braycote 202 grease was packed into the inlet and outlet areas of the core to prevent foreign particles from entering the core during the header bar machining process. The Braycote 202 material was removed first from one end of the core and then the other by using a vapor degreaser. During the removal procedure, the core was oriented at such an attitude as to allow the Braycote 202 and any entrained foreign particles to drain or fall away from and not into the core module.

ANALYSIS OF GOLD BASED BRAZE JOINTS

Sections of the core module were further analyzed to investigate the fin-to-tube plate, header bar-to-tube plate, and the seal plate-to-machined header bar surface brazing joints using the 0.001-in- (0.002-cm) thick gold alloy brazing foil. The effect of welding on a braze joint using a Hastelloy W welding rod also was investigated.

Figure B-6 shows several fin-to-tube sheet joints selected at random from the core module. A close-up view of one of the braze joints illustrates the excellent braze quality obtained using the 0.001-in.- (0.002-cm) thick Palniro 1 braze foil. The brazing joint presented in Figure B-7a indicates some porosity in the braze joint. Figure B-7b shows a local unbrazed area due to a recessed header bar at the seal plate-to-header bar brazing joint.

A metallographic specimen was taken from the high pressure passage showing the header bar-to-tube plate brazing joint. This specimen shown in Figure B-8 was taken from the end of the core, as indicated by the unmachined tube plate.

Welding over a Palniro 1 braze joint was found to have no detrimental effect on the quality of the existing braze joint. Figure B-9 shows a Hastelloy W weld area over a Palniro 1 braze joint. No cracks in the braze joint due to the welding process or contamination of the weld zone by the braze alloy is indicated in the photomicrograph.

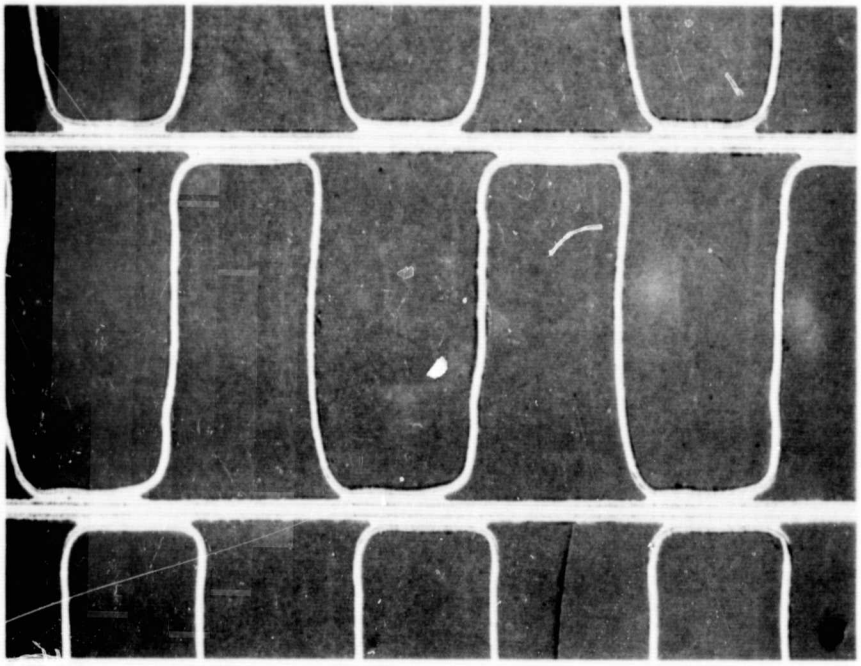

12 x Magnification

a. OVERALL VIEW OF BRAZE JOINTS

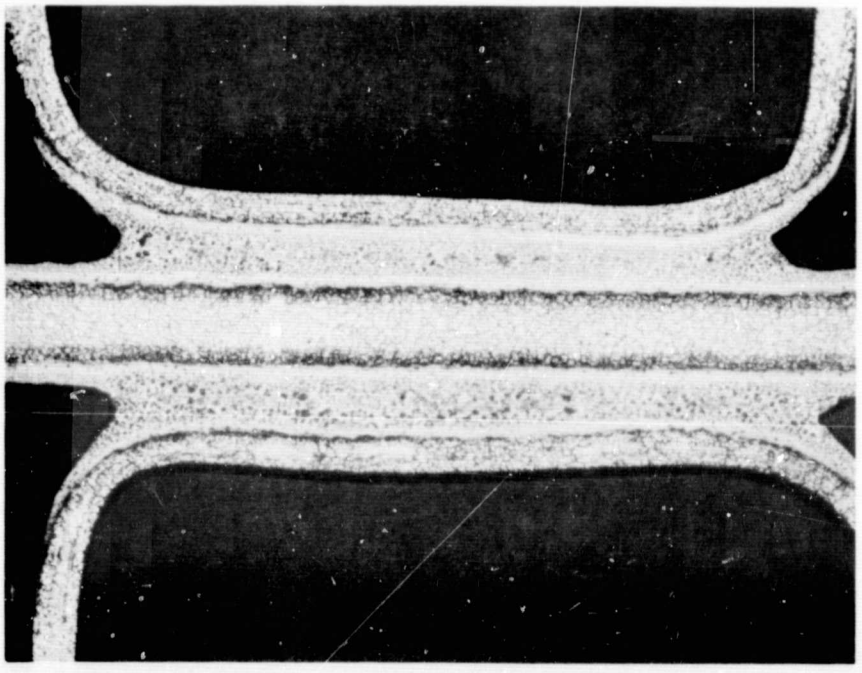

75 x Magnification

b. CLOSEUP OF BRAZE JOINT

F-14397

Figure B-6. Photomicrographs Showing Fin-to-Tube Plate Palniro I Braze Joints In Core Module 1

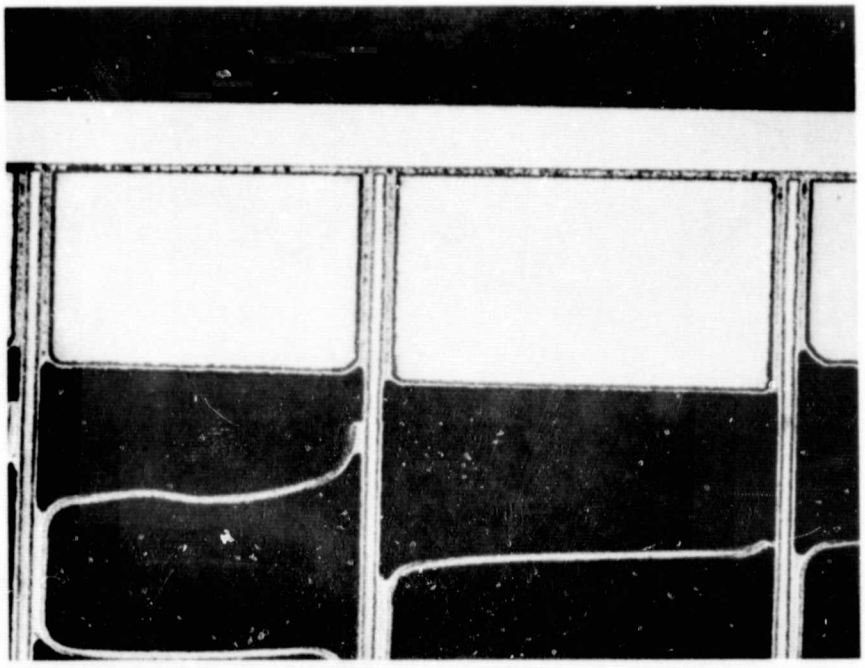

12 x MAGNIFICATION

(a) SEAL PLATE TO HEADER BAR BRAZE JOINT

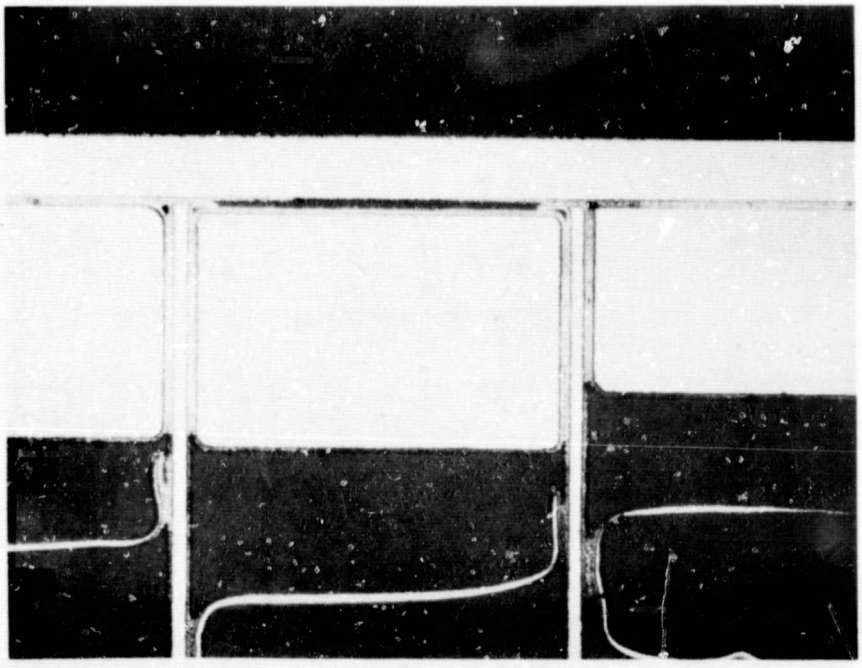

12 x MAGNIFICATION

(b) SEAL PLATE TO HEADER BAR BRAZE JOINT SHOWING UNBRAZED AREA AT A RECESSED HEADER BAR

F-14398

Figure B-7. Photomicrographs of Seal Plate-to-Machined Header Bar Surface on Core Module I

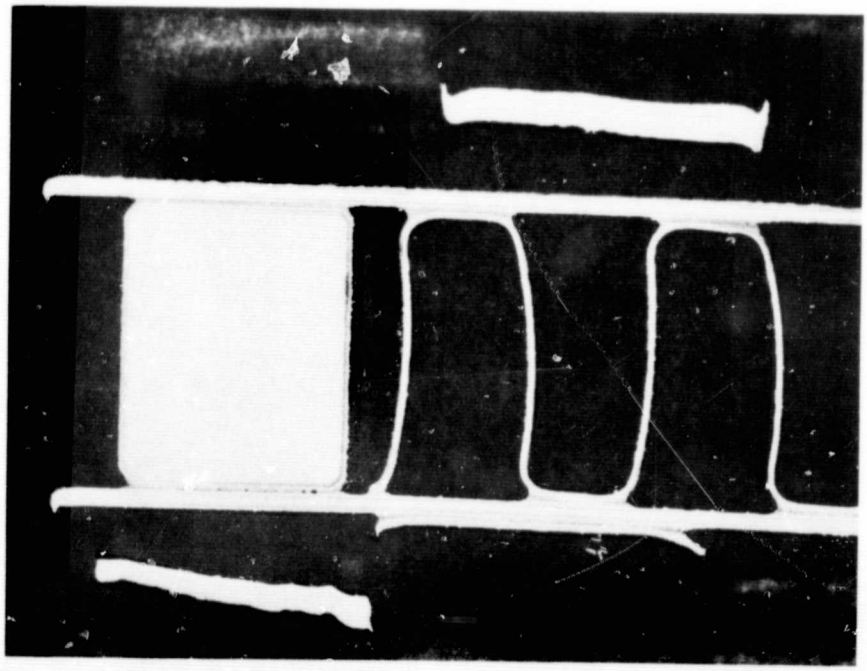

12 x MAGNIFICATION

F-14399

Figure B-8. Photomicrograph Showing High Pressure Header Bar to Tube Plate Braze Joint

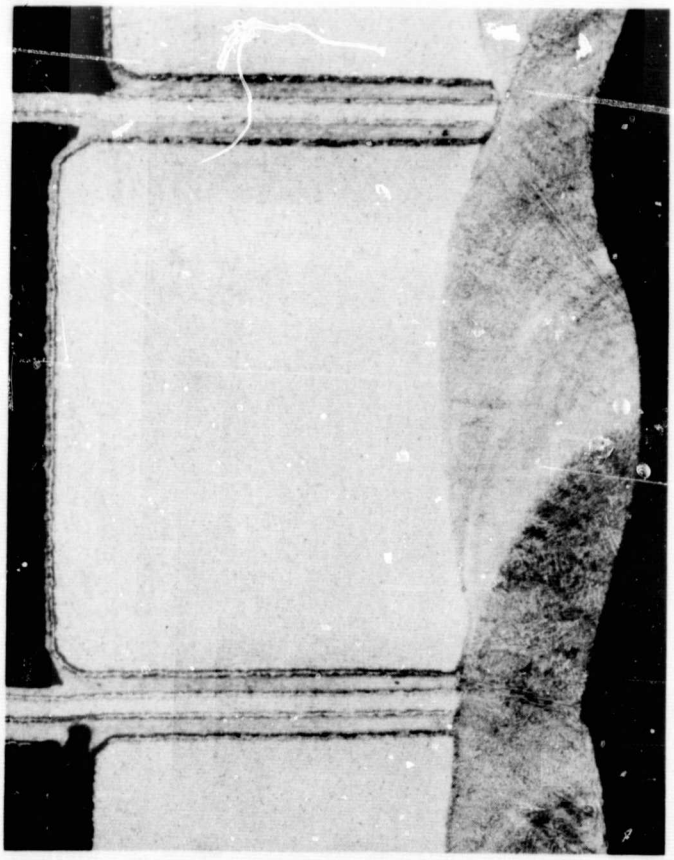

25 x MAGNIFICATION

F-14500

Figure B-9. Photomicrograph Showing Weld Material (Hastelloy W) Over a Palniro I Braze Joint on Core Module 1

APPENDIX C

SUMMARY OF THE FABRICATION EFFORT AND METALLURGICAL EXAMINATION OF THE 1/6-SIZE (378-TUBE) HEAT SINK HEAT EXCHANGER

INTRODUCTION

The 1/6-size (378-tube) test specimen was fabricated to verify the fabrication techniques to be used in assembling of the full-size (2016-tube) heat sink heat exchanger. The areas investigated in the small module were braze joint clearance, assembly techniques for installing the header plates on the finned tubes, and the thermal growth interaction between the Nickel 200 manifold and the finned tubes during the brazing operation.

TUBE-TO-HEADER-JOINT RELATIONSHIP

The tube-to-header brazing joint relationship was investigated using small test specimens as shown in Figure C-1. The specimens illustrated by Figure C-1 consisted of small portions of a spare header with ends of the actual finned tubes and tube return fittings installed.

The first specimen was made up of 5/32-in. dia. finned tubes with the ends swaged to two different diameters, 0.1503 to 0.1507 in. and 0.1537 to 0.1541 in., to produce both an optimum header-finned tube clearance of approximately 0.002 in. and an exaggerated clearance of approximately 0.006 in. Tube return fittings were installed on two pairs of larger diameter and one pair of smaller diameter finned tubes with clearances of approximately 0.004 and 0.008 in., respectively, as detailed in Table C-1. All of the finned tube-header and finned tube-tube return joints were prealloyed with formed wire rings of BAg-8a alloy and brazed with the tube axes and planes of the tube returns horizontal. Figure C-2 illustrates the findings from this specimen; namely, that 0.006-in. clearance was excessive for the quantity of alloy supplied at the tube header joint, but completely adequate joints were obtained from the alloy supplied at the finned tube-tube returns with 0.004-in. clearance.

The second specimen utilized 3/16-in. dia. finned tubes swaged to 0.1857 to 0.1864 in. dia. to provide diametral clearance of 0.0020 to 0.0027 in. as shown in Table C-1. The clearance between finned tube and tube return fittings was much less than on the first specimen (0.005 to 0.001 in.). After prealloying with the same type formed rings as the first specimen, this unit was brazed with the tubes horizontal, but the plane of the tube returns vertical to simulate actual brazing conditions for the larger assemblies. Figure C-3 shows the excellent joint integrity and filleting produced with these parameters.

Based on this experience the 378 tube-header-manifold assembly and the full-size heat sink heat exchanger were fabricated with the following relationships between parts.

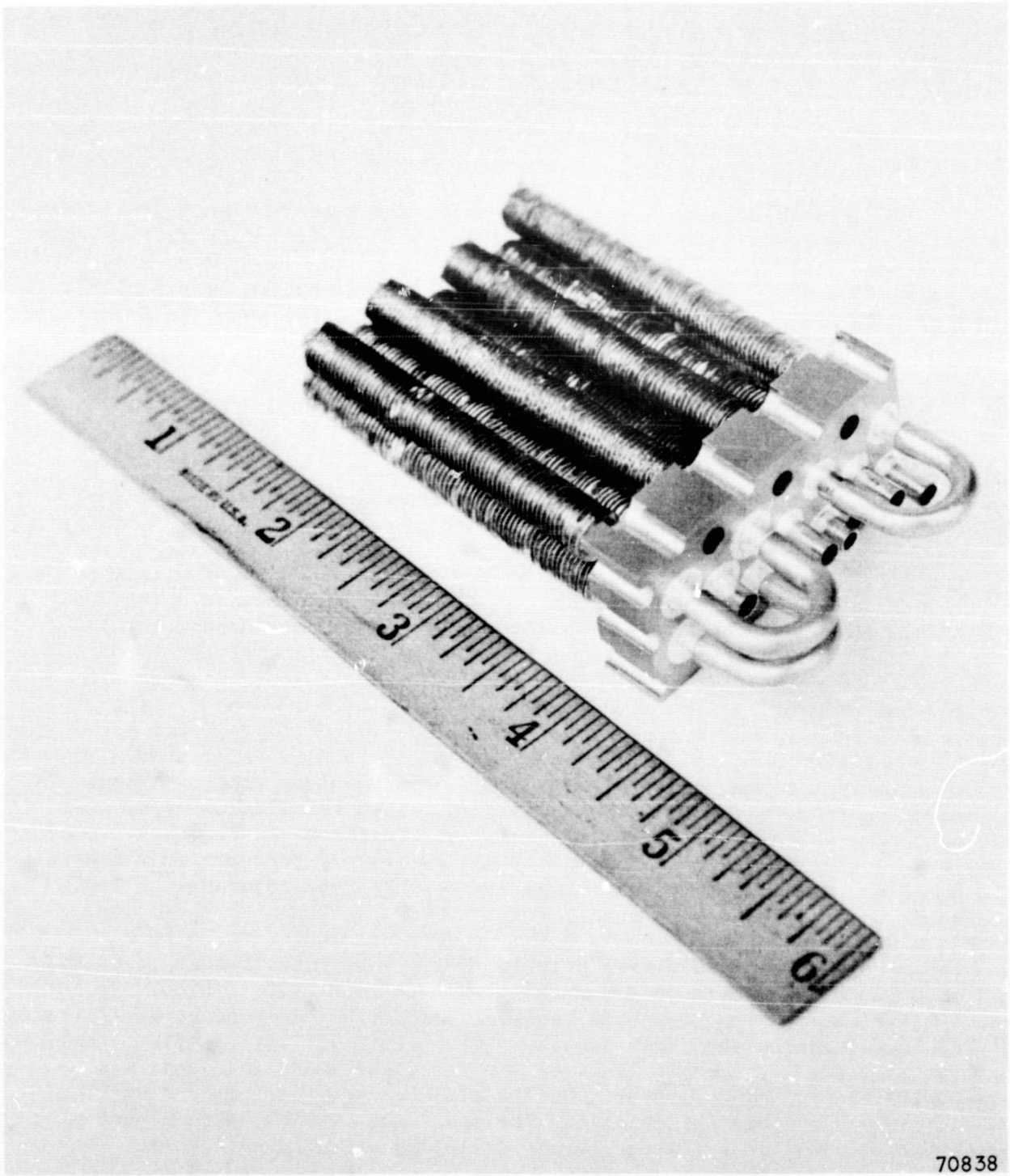

Figure C-1. Typical Finned Tube-to-Header Joint Test Specimen

TABLE C-1

FINNED TUBE-TO-HEADER JOINT RELATIONSHIPS

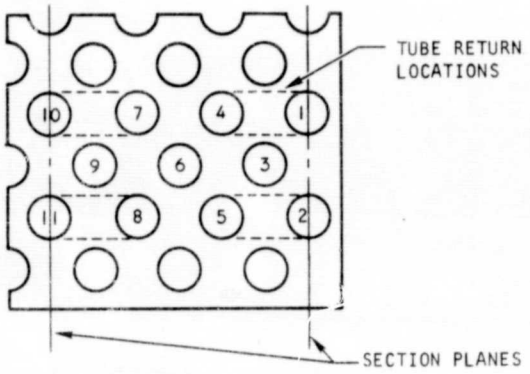

Hole No.	Hdr Hole Size After Plating		Tube Size		Diameter Clearance	Tube Return I.D.		Diameter Clearance
	Min.	Max	Min.	Max	(Mean)	Min.	Max.	(Mean)
1	.1561	.1566	.1505	.1506	.0058	.1580	-	.0074
2	.1560	.1565	.1505	.1507	.0057	-	-	-
3	.1561	.1564	.1505	.1507	.0057	-	-	-
4	.1560	.1564	.1509	.1505	.0058	.1580	-	.0075
5	.1561	.1564	.1509	.1505	.0058	-	-	-
6	.1560	.1564	.1503	.1505	.0058	-	-	-
7	.1559	.1565	.1538	.1540	.0023	.1585	-	.0046
8	.1561	.1564	.1539	.1541	.0023	.1580	-	.0040
9	.1561	.1564	.1539	.1540	.0023	-	-	-
10	.1561	.1564	.1539	.1540	.0023	.1585	-	.0045
11	.1560	.1565	.1537	.1538	.0025	.1585	-	.0047
1	.1883	.1882	.1862	-	.002	.1865	.1870	.0006
2	.1884	.1881	.1862	-	.0021	.1865	.1870	.0006
3	.1884	.1883	.1862	-	.0021	-	-	-
4	.1885	-	.1863	-	.0022	.1865	.1870	.0005
5	.1885	.1884	.1861	-	.0023	.1865	.1870	.0007
6	-	-	-	-	-	-	-	-
7	.1884	-	.1861	-	.0023	.1865	.1870	.0007
8	.1884	.1883	.1857	-	.0027	.1865	.1870	.0010
9	.1884	-	.1863	-	.0021	-	-	-
10	.1884	.1883	.1862	-	.0021	.1865	.1870	.0005
11	.1884	.1883	.1862	-	.0021	.1865	.1870	.0005

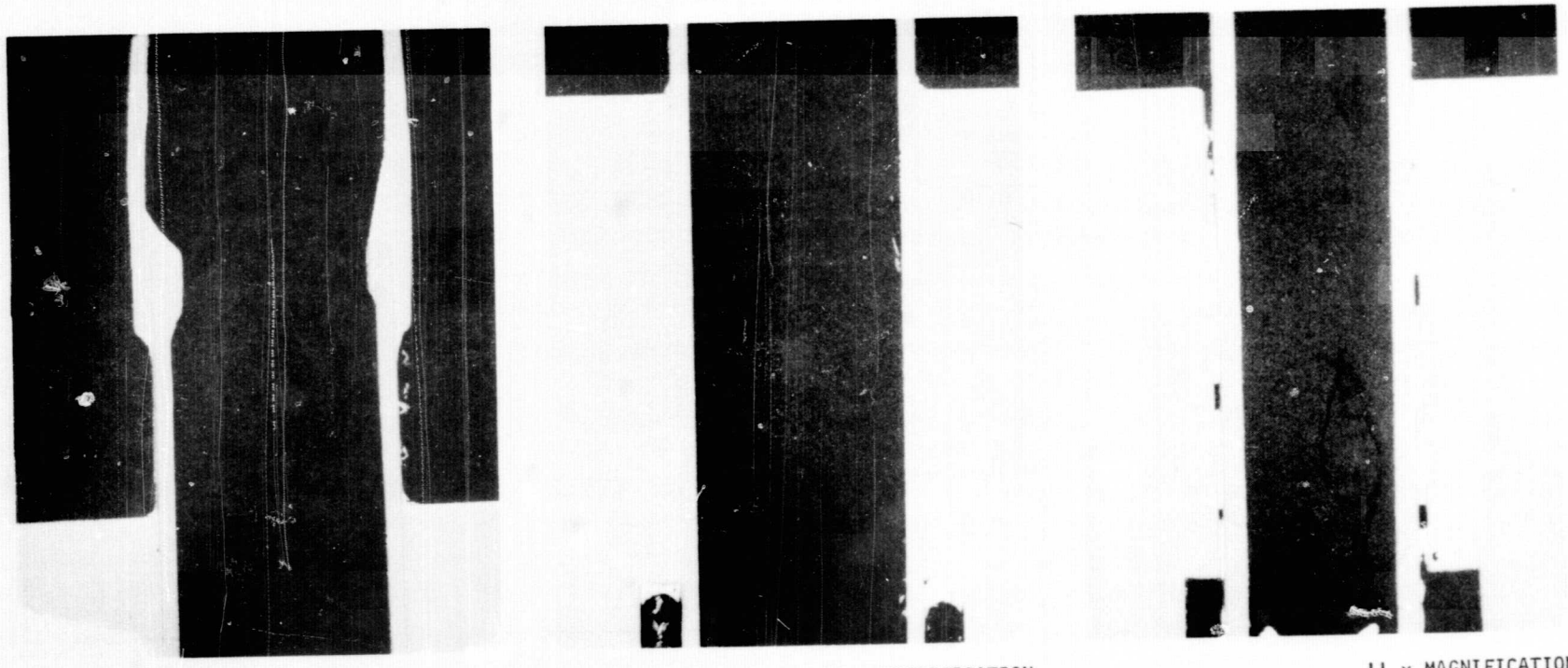

11 x MAGNIFICATION

(a) TUBE RETURN BEND JOINT
0.004 CLEARANCE

11 x MAGNIFICATION

(b) FINNED TUBE TO HEADER JOINT
0.002 CLEARANCE

11 x MAGNIFICATION

(c) FINNED TUBE JOINT
0.006 CLEARANCE

F-14503

Figure C-2. Braze Joint Details, First Finned Tube-to-Header Joint Specimen

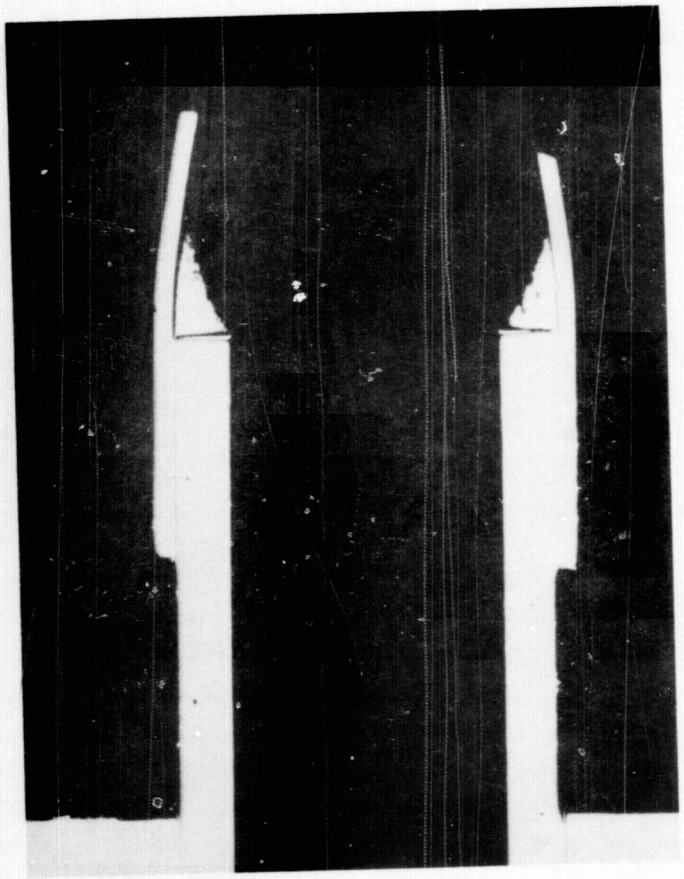

11 x MAGNIFICATION

(a) BRAZE JOINT, FINNED
TUBE-TO-TUBE RETURN

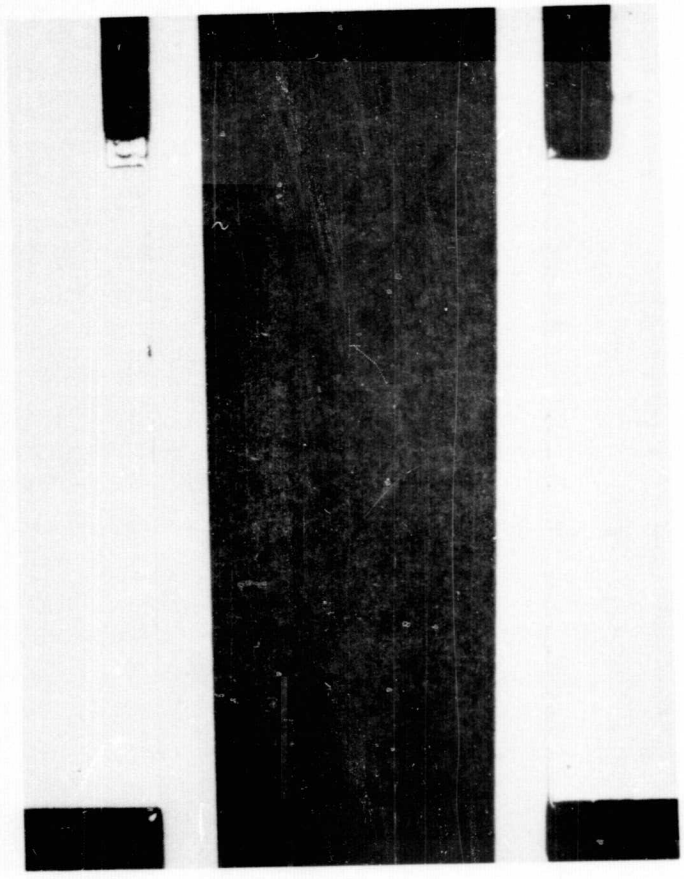

11 x MAGNIFICATION

(b) BRAZE JOINT, FINNED
TUBE-TO-HEADER

F-14504

Figure C-3. Typical Joint Details, Second Finned Tube-to-Header Braze Specimen

Tube Size, In.	Tube OD Swaged, In.	Header ID (Ni Plated), In.	Manifold ID, In.	Tube Return ID, In.
5/32	0.154 to 0.155	0.156 to 0.157	----	0.1555 to 0.1565
3/16	0.186 to 0.187	0.188 to 0.189	0.188 to 0.1885	0.187 to 0.1885

HEAT SINK HEAT EXCHANGER 1/6-SIZE TEST SPECIMEN

The 1/6-size test specimen details were fabricated using the tube-header brazing joint clearances established by the small-scale test specimens.

The diameters of the copper finned tubes were established by a swaging operation, the header plates were broached and nickel plated by electrolysis, and the return bends were expanded to the established internal diameters.

The test specimen was assembled in the stacking fixture for the full-size assembly, brazed in an argon atmosphere, and then pressure and helium leak tested. Figure C-4 shows the initial stage of assembly with the locating pins in the top header plate and tubes. Figures C-5 and C-6 show the test specimen after stacking and fixtured for brazing, respectively. The strapping over the return tubes was installed to prevent return bend-finned tube separation during brazing.

The test specimen was brazed in an argon atmosphere with a titanium shield placed around the assembly to act as a getter. Argon was purged through the liquid manifold to ensure a clean argon atmosphere inside the manifold and finned tubing.

Post-braze inspection and leak testing revealed that one return bend had pulled away from a finned tube and three other return bend-finned tube joints had braze voids. Repair of these areas was made by torch brazing with the silver alloy BAg-3. Pressure testing at 100 psig revealed no finned tube-to-manifold leaks or finned tube-to-return-bend leaks. A helium mass spectrometer test revealed a helium leakage of less than 1×10^{-8} scc/sec. An exact leakage rate was not determined, because the leak detector was calibrated for a leakage rate of 1×10^{-8} scc/sec. Pans were welded to the header plates, (Figure C-7) to leak check the finned tube header plate braze joint. No leakage was observed during a 100-psig nitrogen leak check nor was any helium leakage detected with a mass spectrometer (calibration of 1×10^{-8} scc/sec).

SUMMARY

The fabrication of the 1/6-size heat sink heat exchanger test specimen was successfully completed. There was no adverse thermal growth interaction between the Nickel 200 manifold and the basic core module. The brazing of both the header plates and the Nickel 200 manifold to the tubes was completely successful; the brazing of the return bends to the tubes was not entirely successful since four leaks were found after the initial BAg-8a brazing cycle. It was considered necessary to incorporate two changes into the fabrication effort on

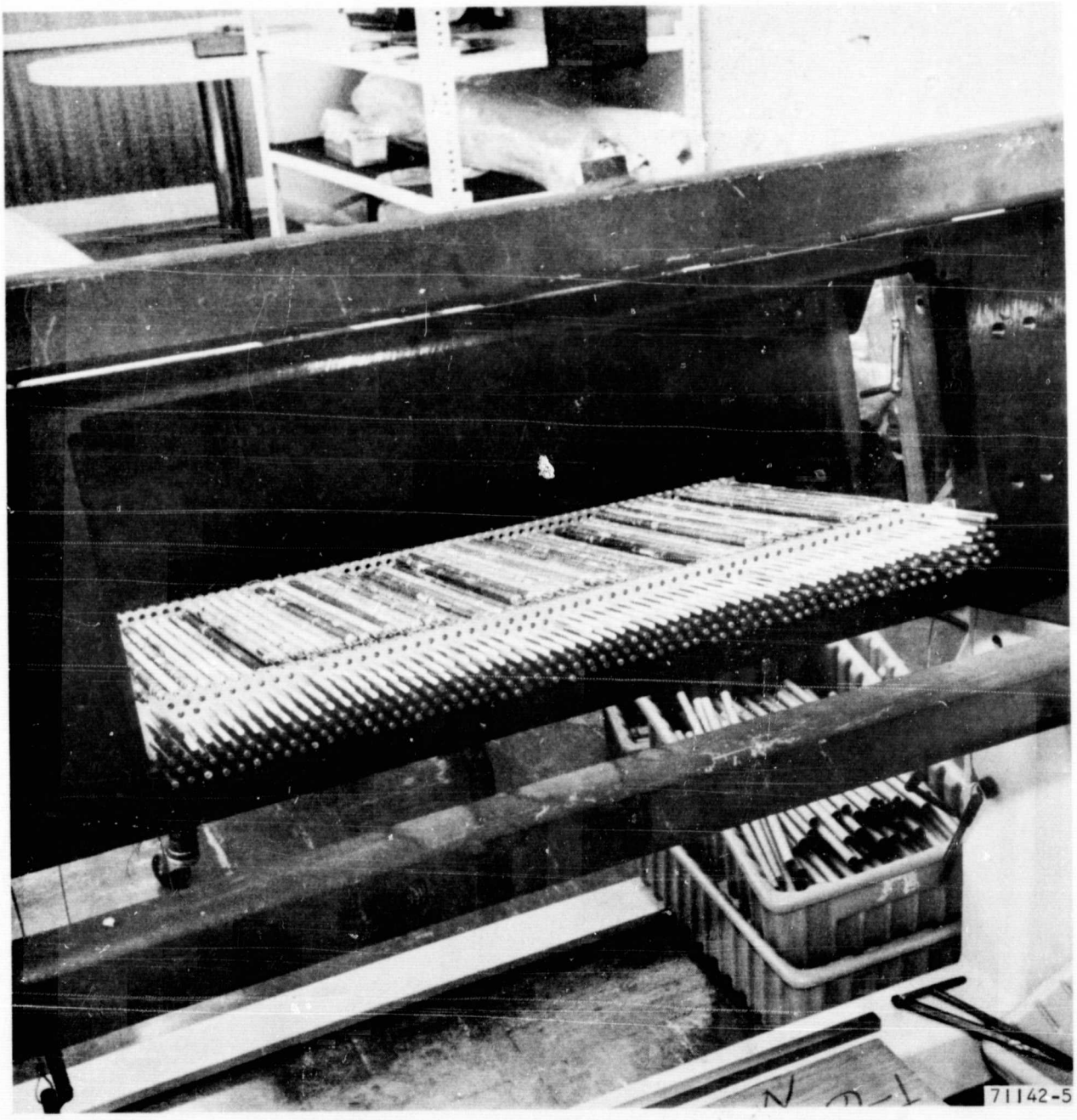

Figure C-4. 378 Finned Tube Test Specimen During Stacking

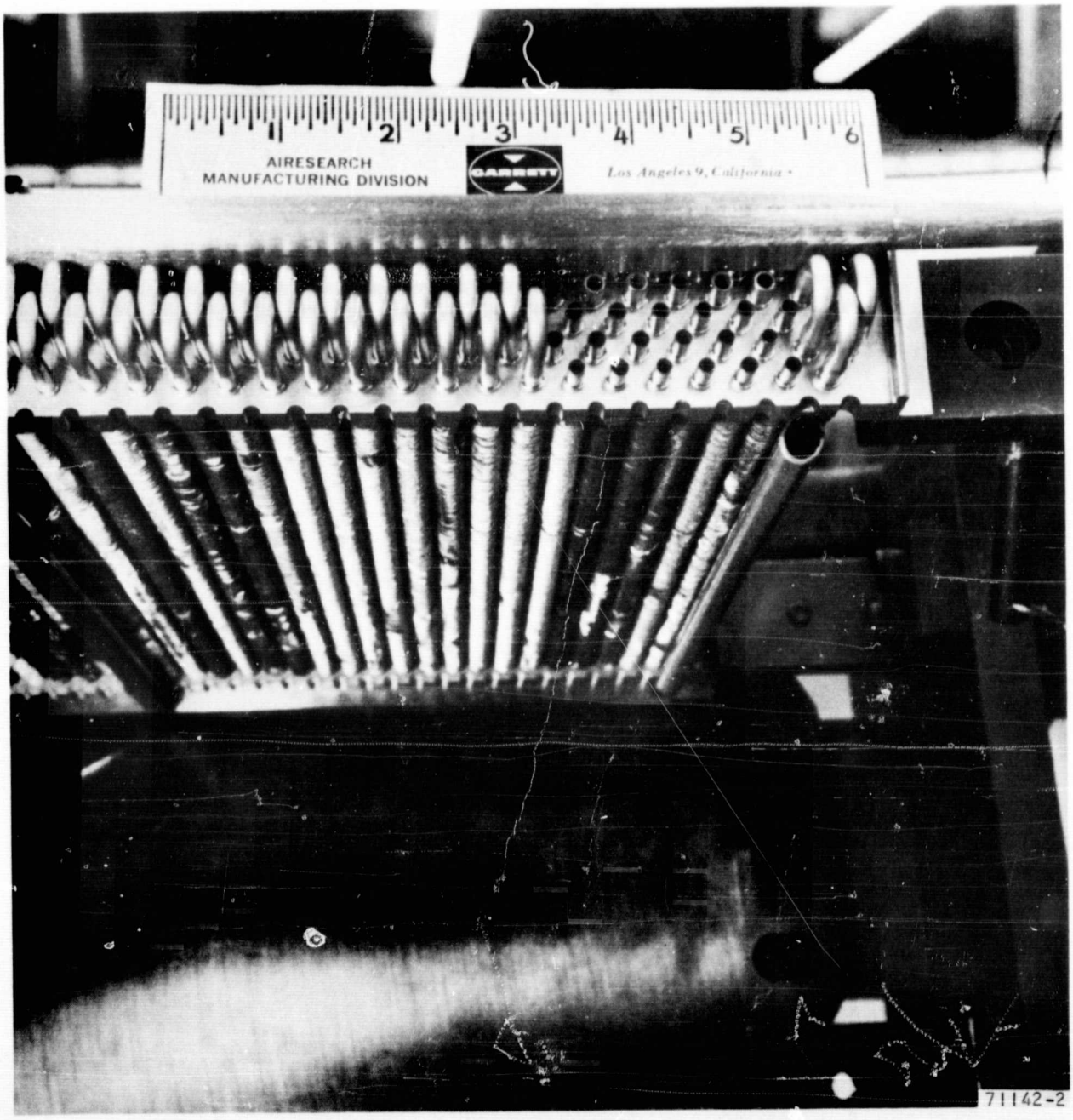

Figure C-5. 378 Finned Tube Test Specimen with Liquid Manifold, Return Tubes and Headers in Position

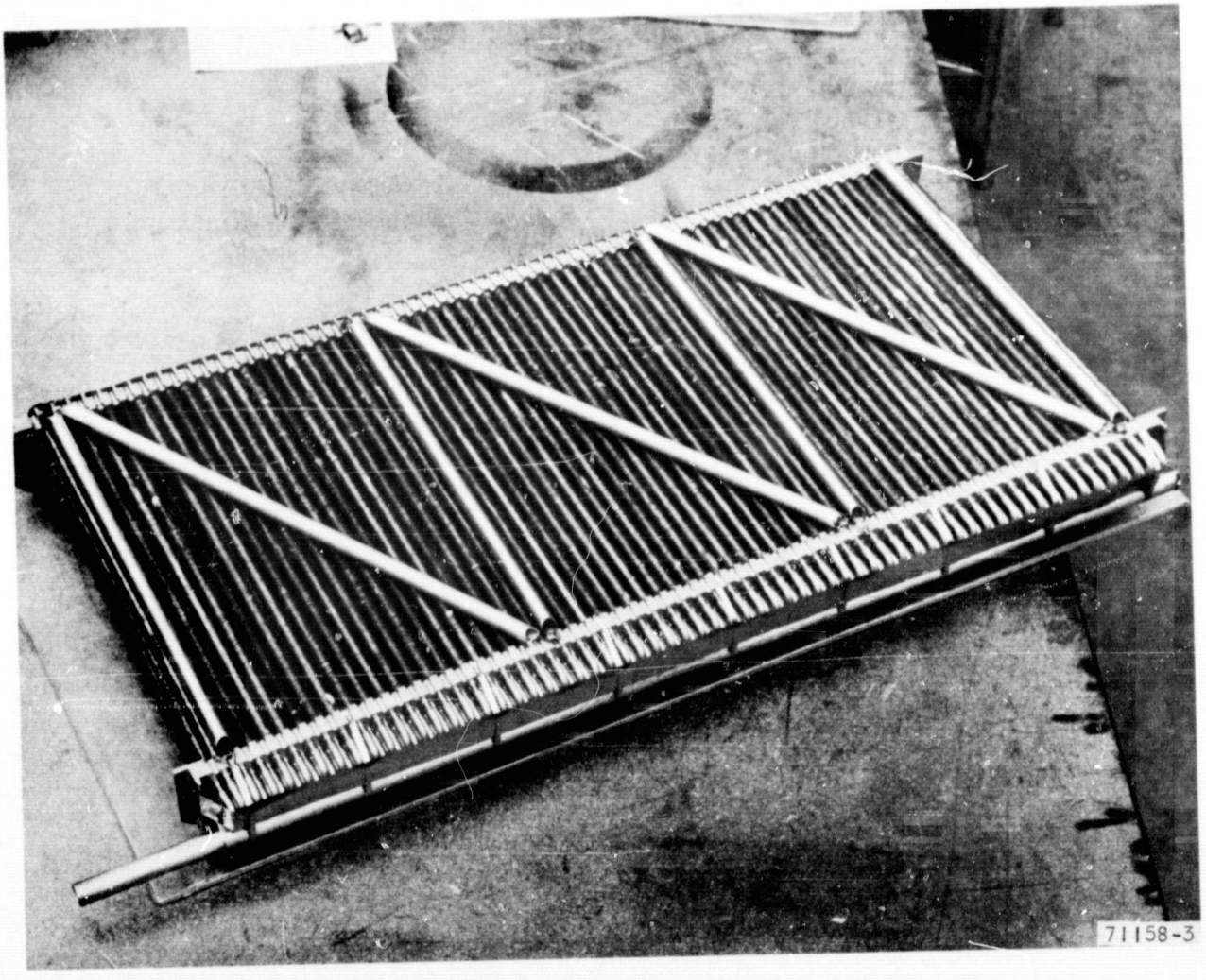

Figure C-6. 378 Finned Tube Test Specimen with Banding Over Return Tubes for Brazing

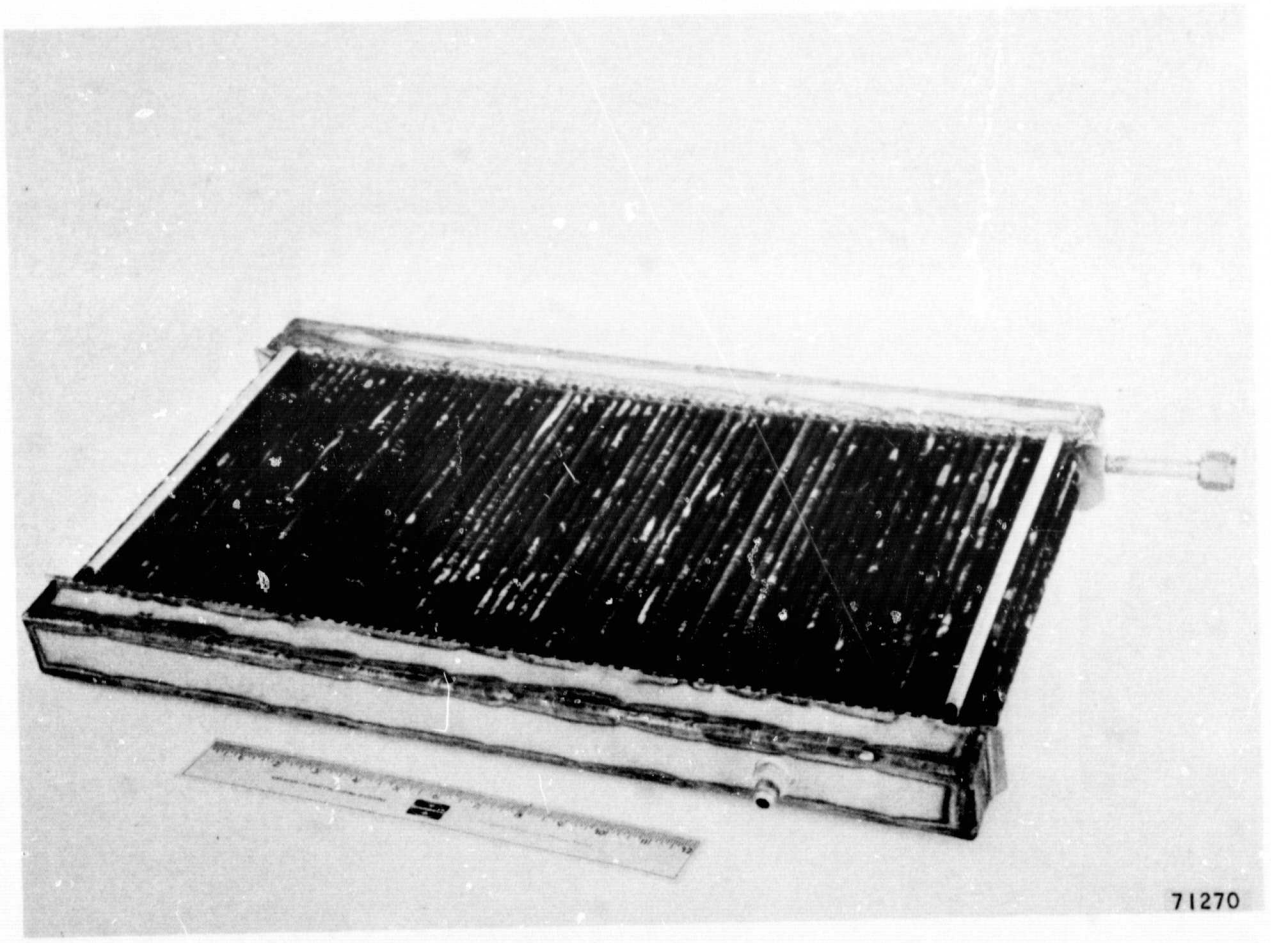

Figure C-7. 37δ Finned Tube Test Specimen with Pans Attached for Pressure and Helium Leakage Testing

the full-size heat sink heat exchanger to minimize potential brazing joint leaks. These changes were (1) to nickel-plate the return bends (the tubes were nickel-plated) in order to increase the wetting and flow characteristics of the brazing alloy on the 347 stainless steel, and (2) to increase the braze land on the return bends in order to achieve more tube-return bend engagement to prevent separation of the return bends from the finned tubes during brazing.